2013

Joining Vacuum High Pressure Die Cast Aluminum Alloy A356 Subjected to Heat Treatment to Wrought Alloy 6061

Meng Wang
University of Windsor

Joining Vacuum High Pressure Die Cast Aluminum Alloy A356 Subjected to Heat Treatment to Wrought Alloy 6061

By

Meng Wang

A Thesis Submitted to the

Faculty of Graduate Studies

through Engineering Materials

in Partial Fulfillment of the Requirements

for the Degree of Master of Applied Science

at the University of Windsor

Windsor, Ontario, Canada

2013

Joining Vacuum High Pressure Die Cast Aluminum Alloy A356 Subjected to Heat Treatment to Wrought Alloy 6061

By Meng Wang

APPROVED BY:

_____

Dr. Henry Hu, Advisor

Department of Mechanical, Automotive and Materials Engineering

_____

Dr. Jerry Sokolowski, Program Reader

Department of Mechanical, Automotive and Materials Engineering

_____

Dr. Behnam Shahrrava, Outside Program Reader

Department of Electrical and Computer Engineering

_____

Dr. Xueyuan Nie, Chair

Department of Mechanical, Automotive and Materials Engineering

August 14, 2013

DECLARATION OF ORIGINALITY

I hereby certify that I am the sole author of this thesis and that no part of this thesis has been published or submitted for publication.

I certify that, to the best of my knowledge, my thesis does not infringe upon anyone's copyright nor violate any proprietary rights and that any ideas, techniques, quotations, or any other material from the work of other people included in my thesis, published or otherwise, are fully acknowledged in accordance with the standard referencing practices. Furthermore, to the extent that I have included copyrighted material that surpasses the bounds of fair dealing within the meaning of the Canada Copyright Act, I certify that I have obtained a written permission from the copyright owner(s) to include such material(s) in my thesis and have included copies of such copyright clearances to my appendix.

I declare that this is a true copy of my thesis, including any final revisions, as approved by my thesis committee and the Graduate Studies office, and that this thesis has not been submitted for a higher degree to any other University or Institution.

ABSTRACT

The objective of the present work was to investigate the feasibility of joining high pressure die cast aluminum alloy A356 for automotive applications. Joining of vacuum high pressure die cast aluminum alloy A356 subjected to different heat treatments with wrought 6061 was carried out by using the Gas Metal Arc Welding (GMAW) process. The results of tensile testing showed that the order of the welded samples with the overall engineering performance combining the strengths and ductility from the highest to the lowest were T5-A356 alloy, as-cast A356 alloy, T6-A356 alloy and T4-A356 alloy. The SEM microstructure analysis indicated the high level of porosity present in heat treated alloys should be responsible for the failure of the filler alloy. The fractographic analyses revealed that the 6061 samples exhibited the highest ductility among the tested alloys, which were consistent with the results of tensile testing.

DEDICATION

I dedicate this thesis to my parents and grandmother. Their love, support and encouragement during my study at University of Windsor has become part of my strength, and enabled me through those difficulties and finally completed this work.

ACKNOWLEDGEMENTS

First of all, I would like to express my sincere gratitude to my supervisor, Dr. Henry Hu, for kind suggestion, excellent guidance and providing me the greatest opportunity to join the engineering group in University of Windsor.

Many thanks to the program reader, Dr. Sokolowski and the outside program reader, Dr. Behnam for taking time on my thesis presentation and great suggestion given to this project.

I am very grateful to the university department technicians, Mr. Andy Jenner for helping me machine tensile samples, and Mr. Gang Li's help of SEM training and sample preparation for the microstructure analysis, and also to the classmates in my group, Xuezhi Zhang and Yanda Zou, for their great help on the experiment and valuable discussion for the research work.

Great thanks to Mr Patrick Cheng (Ryobi Die Casting, USA), for supplying materials and conducting mechanical tensile tests, and Mr Gary Meng (AGS Agreatsun Welding, Mississauga), for technically welding samples.

Most of all, I would like to express my deepest gratitude to my family, especially my parents for the love, encouragement and support they place in me.

TABLE OF CONTENTS

LIST OF TABLES

LIST OF FIGURES

CHAPTER 1.

INTRODUCTION

1.1 Background

Aluminum alloys with silicon as a major alloying element consist of a class of alloys, which provides the most significant part of all shaped castings manufactured, especially in the aerospace and automotive industries. This is mainly due to the outstanding effect of silicon in the improvement of casting characteristics, combined with other physical properties, such as mechanical properties and corrosion resistance. Casting processes are among the oldest methods for manufacturing metal goods. Aluminum based products are successfully cast in any kind of casting process. In general, an optimum range of silicon content can be assigned to casting process. The two types of conventional aluminium alloys (A356 & 6061) contain 6.5-7.5% and 0.4-1.8% silicon [1].

High pressure die casting (HPDC) is a manufacturing process in which molten metal (aluminum) is injected with a die casting machine under force using considerable pressure into a steel mold or die to form products. Because of the excellent dimensional accuracy and the smooth surfaces, most high pressure die castings require no machining except the removal of flash around the edge and possible drilling and tapping holes. High pressure die casting production is fast and inexpensive relative to other casting processes [2]. Although in high pressure die casting process, high velocity allows for the production of thin-walled castings, the associated turbulent conditions remain the major source of interior and surface casting defects, which may have

deleterious effects on the mechanical properties. Because of this, castings usually contain internal pores in which gases, such as air, hydrogen or vapours formed by the decomposition of organic die wall lubricants are entrapped. The formation of porosity may also result from metal shrinkage during solidification. Defect-containing regions in a tensile sample reduce the load-bearing area and, therefore, produce a concentration of the strain.

1.2 Motivation

Currently, there are three major types of aluminum alloys, i.e., Al-Si-Cu, Al-Mg and Al-Si-Mg alloys used for die casting [3]. One of the most widely used conventional high pressure die casting(C-HPDC) aluminum alloys, named A356 is in the Al-Si-Mg group, which possesses excellent die castability, weldability, high ductility and strengths (UTS: 221 MPa, YS: 136 MPa) [4]. Meanwhile, wrought 6061 aluminum alloy has applied in this experiment, which is a precipitation hardening aluminium alloy, containing magnesium and silicon as its major alloying elements. It also has good weldability and strengths (UTS: 190 MPa, YS: 70 MPa) [5]. To improve the mechanical properties, such as UTS and YS, casting are often subjected to a T4, T5 and T6 heat treatment to achieve the required mechanical properties although the application of heat treatments adds extra costs to castings, particularly high for large castings and makes them less competitive despite of property enhancement.

To develop light-weight complex and large-scale chassis and body structures for automobiles, joining of cast Al components with wrought and/or cast similar metals is often considered a good strategy for design engineers, which enables them to take advantages of different manufacturing processes such as casting, extrusion and forming. Up to now, most studies on joining cast Al alloys [6,7] have been focused on friction stirring welding of the Al components made by

relatively costly casting processes such as permanent mold, and squeeze casting, which contains low amount of porosity in materials. Relatively expensive friction stir welding has been attempted on joining C-HPDC Al alloy ADC 12 despite of its high cost. Meanwhile, fusion welding of C-HPDC Al alloys is difficult due to the formation of blowholes by entrapped gases and the presence of brittle intermetallic in the weld metal [7]. V-HPDC as an emerging technology minimizes the entrapment of porosity, which could improve mechanical properties and engineering performance of welded die cast aluminum alloys [8-10].

Gas metal arc welding (GMAW), sometimes referred to by its subtypes metal inert gas (MIG) welding or metal active gas (MAG) welding, is a semi-automatic or automatic arc welding process in which a continuous and consumable wire electrode and a shielding gas are fed through a welding gun [11]. A constant voltage, direct current power source is most commonly used with GMAW, but constant current systems, as well as alternating current, can be used. In order to evaluate their mechanical properties and analyze microstructure, joining of different types of aluminum alloys (A356 & 6061) are identified in this experiment. However, work on applying fusion welding processes to join vacuum high pressure die cast aluminum alloys is very limited in the public domain.

1.3 Objectives & Tasks

The aims of this study were to examine the weldability and tensile properties of wrought and cast aluminum alloys in weld-fusion zone with heat treatments. To achieve the proposed objectives, as-cast A356/6061, T4-A356/6061, T5-A356/6061 and T6-A356/6061 were considered to be joined due to the wide use of wrought alloy 6061 and vacuum high pressure die cast A356. The MIG method was selected to join the different types of aluminum alloys together with desired process parameters due to its capability of continuous operation for mass production.

1.4 Thesis Layout

The thesis is divided into six chapters. Chapter 1 present a general background of the investigation conducted in this study as an introduction to the high pressure die casting process, and subject of the different solution treatment of high pressure vacuum die casting of the A356 alloy. Chapter 2 provides a literature review of vacuum die casting technology, gas metal arc welding and tungsten arc welding, the A380 alloy and work of other researchers performed on solution treatment of 3xx serial aluminum casting alloys. In addition, the fundamentals of the solution treatment on aluminum alloys are presented. In Chapter 3, the experimental procedures are outlined. Chapter 4 presents the effect of various treatment schemes on the microstructure evolution, and the mechanical properties of the welded A356/6061 alloys. The influence of different dendrite arm spacing (DAS) and fractograph are also compared and discussed. Finally, the conclusions of the present study are summarized in Chapter 5, and outlines future work on the present study.

CHAPTER 2.

LITERATURE REVIEW

2.1 Introduction

Aluminium alloys are alloys in which aluminium (Al) is the predominant element. The typical alloying elements are copper, magnesium, manganese, silicon and zinc. There are two principal classifications, namely casting alloys and wrought alloys, both of which are further subdivided into the categories heat-treatable and non-heat-treatable. About 85% of aluminium is used for wrought products, for example rolled plate, foils and extrusions. Casting aluminium alloys produce cost effective components due to the low melting point, although they generally have lower tensile strengths than wrought alloys. The most important cast aluminium alloy system is Al-Si, where the high levels of silicon (4.0% to 13%) contribute to give good casting characteristics [12]. Aluminium alloys are widely used in engineering structures and components where light weight or corrosion resistance is required.

Alloys composed mostly of the two lightweight metals aluminium and magnesium have been very important in aerospace manufacturing since 1940. Aluminium-magnesium alloys are both lighter than other aluminium alloys. Aluminium alloy surfaces keep their apparent shine in a dry environment due to the formation of a clear, protective layer of aluminium oxide. In a wet environment, galvanic corrosion can occur when an aluminium alloy is placed in electrical contact with other metals with more negative corrosion potentials than aluminium.

2.1.1 Characteristics of Aluminum Alloys

Based on the classifications in the Aluminum Association of the United States, there is a distinction between wrought alloys and cast alloys (Table 2-1 and 2-2). Wrought Alloys, which have excellent machining characteristics, are well suited to multiple-operation machining. There are obtained by working on ingots of particular forms. This work can be affected by rolling, extruding, drawing or forging; Cast alloys containing copper, magnesium, or zinc as the principal alloying elements impose few machining problems. There are those for which the ingots are melted and poured into mould having the shape of the final product. The main difference between the two classes of alloys lies in the elements added to the aluminum base.

In the classification used by the Aluminum Association of the United States for cast alloy in the 1××××.× series, the second and third number indicate the purity of the aluminum. Thus 150.× signifies at least 99.5% of aluminum. The last digit, after the decimal point, indicates the form of the product: 0 for a cast part and 1 for an ingot [13].

Heat-treatable alloys are the alloys that can have higher strengths by heat-treatment. Alloys in this group contain one or more elements chosen to give higher strength by precipitation hardening (age hardening). The most commonly used ones use copper, magnesium and silicon, or zinc. Copper is used because of its high strength, relatively low corrosion resistance, and excellent machinability and heat treatability. The combination of magnesium and silicon is the most popular extrusion alloy, due to its good extrudability, strength, corrosion resistance, machinability, weldability, formability, and heat treatability. Zinc is used because of its very high strength, good machinability, and heat treatability.

Table 2-1 Designation of Aluminum Alloys [14]

Major Aluminum Alloys	Wrought Alloys	Cast Alloys
Aluminum	1XXX.1	1XX.0
Aluminum-Copper	2XXX.1	2XX.0
Aluminum-Manganese	3XXX.1	-
Aluminum-Silicon	4XXX.1	4XX.0
Aluminum-Magnesium	5XXX.1	5XX.0
Aluminum-Magnesium & Silicon	6XXX.1	6XX.0
Aluminum-Zinc	7XXX.1	7XX.0
Aluminum-Lithium	8XXX.1	-
Unused	-	9XX.0

Table 2-2 Heat Treatable Aluminum Elements [15]

Major Alloying Element	Wrought Alloys	Cast Alloys	Characteristics
Copper	2XXX	2XX.0	High strength-to-weight ratio, low corrosion resistance, heat treatable
Magnesium & Silicon	6XXX	6XX.0	Medium strength; good formability, machinability and weldability
Zinc	7XXX	7XX.0	Moderate to very high strength, heat treatable, prone to fatigue

2.1.2 Definitions of Welding

Welding is a fabrication or sculptural process that joins materials, usually metals or thermoplastics, by causing coalescence. This is often done by melting the workpieces and adding a filler material to form a pool of molten material (the *weld pool*) that cools to become a strong joint, with pressure sometimes used in conjunction with heat, or by itself, to produce the weld. This is in contrast with soldering and brazing, which involve melting a lower-melting-point material between the workpieces to form a bond between them, without melting the workpieces[4].

Many different energy sources can be used for welding, including a gas flame, an electric arc, a laser, an electron beam, friction, and ultrasound. While often an industrial process, welding may be performed in many different environments, including open air, under water and in outer space. Welding is a potentially hazardous undertaking and precautions are required to avoid burn, electric shock, vision damage, inhalation of poisonous gases and fumes, and exposure to intense ultraviolet radiation.

Aluminum and its alloys can be joined by more methods than any other metals, but aluminum has several chemical and physical properties that need to be understood when using the various joining processes.

2. 2 Welding Design and Processes

Aluminum base metals are classified in two ways: as wrought alloys produced by mechanical working such as rolling, extruding, or forging, or cast alloys produced by pouring into a mold. Wrought alloys are further divided as either heat treatable or non-heat treatable depending on the composition. The welding of aluminium alloys often involves safety consideration and process selection.

2.2.1 Welding Safety

Safety is considered as the most important issue for all the experiments and tests. Arc welders use a powerful electric arc to make and repair plain, coated, or treated metal items. Welders can be stationary, electric powered or portable, diesel/gas powered. There are some points that are need to be known before doing the welding [16].

- To protect your body from burns due to arc welding heat, ultraviolet light (UV), molten metal, and sparks, wear dark colored coveralls with long sleeves and pant legs. The coveralls should be fire retardant, cuffless, and pocketless with no holes, tears, or worn spots. A skull cap protects your head and hair. Leather gauntlet gloves and safety boots protect your hands and feet. Wear hearing protection in noisy environments and to keep sparks out of your ears.
- Goggles or safety glasses and welding helmets/shields protect your eyes from flying sparks, chipped slag, and UV light. Welding helmets and shields should be non-reflective and free of cracks, gaps, and openings. Use the correct filter setting for the power output of the arc welder.

- Arc welders can reach temperatures greater than 10,000 degrees F, posing a fire and explosion hazard [16]. Avoid welding, cutting, or hot work on used drums, barrels, or tanks, where residual fumes can ignite and explode. Weld on a firebrick surface on concrete or other fire-resistant flooring surrounded by spark curtains. Fill cracks in the flooring to prevent sparks and hot metal from entering and smoldering. Keep an ABC fire extinguisher, fire blanket, and first aid kit available at all times. It may be necessary to set a "fire watch" to ensure that a fire does not start.
- To avoid electric shock from arc welding, use an insulating mat when you weld steel or other conductive materials. If you are welding in a wet or damp area or perspiring heavily, wear rubber gloves underneath your leather gloves. Keep welding cables clean and intact and position them so they do not get sparks or hot metal on them [17].

2.2.2 Description of Fusion Welding Processes

The most popular fusion welding processes are Gas Metal Arc Welding (GMAW), sometimes called MIG welding and Gas Tungsten Arc Welding (GTAW) sometimes referred to as TIG welding. A third process, Shielded Metal Arc Welding (SMAW) or stick welding, has limited use on aluminum and is used primarily for small repair jobs on material 1/8" or thicker [17].

GTAW - **G**as **T**ungsten **A**rc **W**elding - *TIG Welding*

TIG Welding is easily performed on a variety of metals. It generally requires little or no post weld finishing. It is an electric welding process in which heat for welding is generated by an electric arc between the end of a non-consumable tungsten electrode & the base metal. Filler

metal may be added, if necessary. An inert shielding gas supplies shielding for the arc. Inert gas creates a protective atmosphere around the welding in process.

GMAW - **G**as **M**etal **A**rc **W**elding - *MIG Welding*

Gas metal arc welding is quick & easy on thin-gauge metal as well as heavy plate. It generally calls for little post weld clean-up. GMAW is an electric arc welding process where heat is produced by an arc between a continuously fed filler metal electrode & the base metal. Shielding is obtained from an externally supplied gas or gas mixture.

2.2.3 Inert Shielding Gas

GTAW- Argon is suggested for thicknesses up to approximately 1/2". For thicker sections, argon-helium mixtures or pure helium may be used. Pure helium may also be employed for deeper penetration[18].

GMAW - Argon is used for most applications. It provides deeper penetration and clean welds. Argon-helium mixtures of 25 – 75% helium are helpful for thicker material (over ½ inch). Helium produces a hotter arc which is sometimes necessary due to the high thermal conductivity of aluminium. It also produces a wider weld fusion shape [18].

2.2.4. Filler Metal Selection

A filler metal is a metal added in the making of a joint through welding, brazing, or soldering. Four types of filler metals exist—covered electrodes, bare electrode wire or rod, tubular electrode wire and welding fluxes. The main force is on bare electrode wires, which is used in both Gas Metal Arc Welding and Gas Tungsten Arc Welding process. Sometimes

non-consumable electrodes are included as well, but since these metals are not consumed by the welding process, they are normally excluded.

Filler metals are generally produced with closer control on chemistry, purity, and quality than base metals. The choice of a filler metal for a given application depends on the suitability for the intended application.

The selection of filler metals is based on several factors. One consideration is the ability to provide suitable mechanical properties for heat treatable and non-heat treatable base metals both wrought and cast. Other important factors are freedom from cracking, service conditions and weld color after anodizing. The tensile strength, impact toughness, electrical conductivity, thermal conductivity, corrosion resistance, and weld appearance needed for a specific weldment are important considerations as well. Deoxidizers are sometimes added to the filler metals to provide better weld soundness [19].

2.3. TIG Welding

2.3.1 Introduction to TIG Welding

Gas Tungsten Arc Welding (GTAW) is frequently referred to as TIG welding. TIG welding is a commonly used high quality welding process. TIG welding has become a popular choice of welding processes when high quality and precision welding are required.

In TIG welding, an arc is formed between a no consumable tungsten electrode and the metal

being welded. Gas is fed through the torch to shield the electrode and molten weld pool. If filler wire is used, it is added to the weld pool separately [20].

2.3.2 Process Principles

The basic equipment for TIG welding comprises a power source, a welding torch, a supply of an inert shield gas, a supply of filler wire and perhaps a water cooling system. A typical assembly of equipment is illustrated in Figure 2-1.

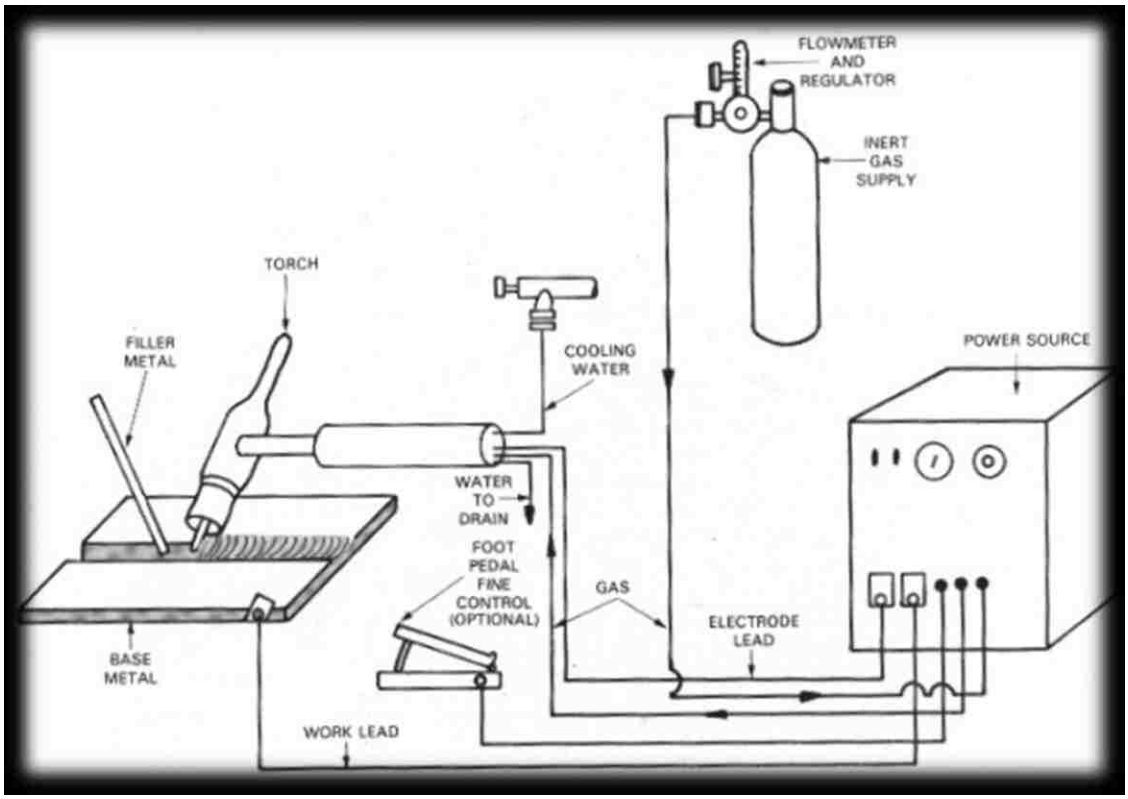

Figure 2-1 Schematic of the TIG welding process [20].

For welding most materials, the TIG process conventionally uses direct current (DC) with the electrode connected to the negative pole of the power source, welding on this polarity does not give efficient oxide removal. A further feature of the gas shielded arc welding processes is that the bulk of the heat is generated at the positive pole. TIG welding with the electrode connected to

the positive pole, results in overheating and melting of the electrode. Manual TIG welding of aluminum is therefore normally performed using alternating current, AC, where oxide film removal takes place on the electrode positive half cycle and electrode cooling and weld bead penetration on the electrode negative half cycle of the AC sine wave. The arc is extinguished and reignited every half cycle as the arc current passes through zero, on a 50Hz power supply requiring this to occur 100 times per second, twice on each power cycle[8]. To achieve instant arc reignition a high-frequency (HF), high-voltage (9–15 000 V) current is applied to the arc, bridging the arc gap with a continuous discharge. This ionises the gas in the arc gap, enabling the welding arc to reignite with a minimum delay (Figure2-2). This is particularly important in the half cycle [21].

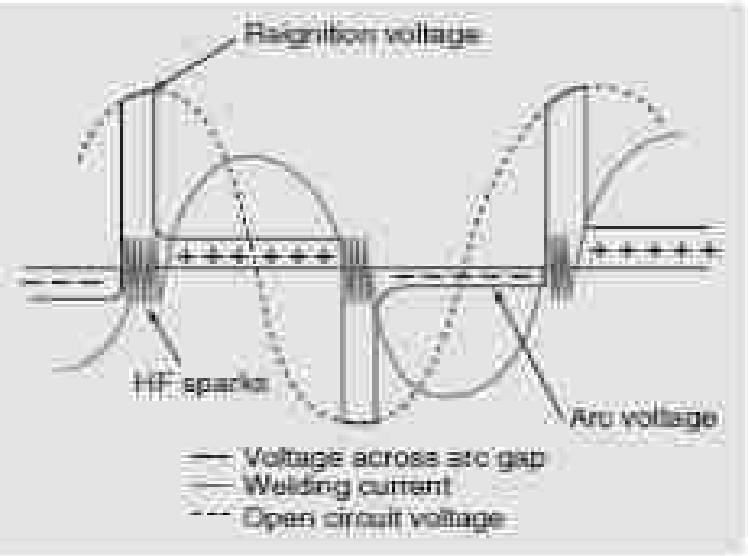

Figure 2-2 HF current and Effect on Voltage and Current [21].

Aluminum is a poor emitter of electrons, meaning that it is more difficult to reignite the arc on the electrode positive half-cycle. If there is any delay in reigniting then less current flows on the positive half cycle than on the negative half cycle. This is termed partial rectification and can eventually lead to full rectification where no current flows on the positive half cycle. The arc

becomes unstable, the cleaning action is lost and a direct current component may be produced in the secondary circuit of the power source, leading to overheating of the transformer. This is prevented on older power sources by providing an opposing current from storage batteries and in more modern equipment by inserting blocking condensers in the power source circuit.

2.3.3 Shielding Gases

The preferred gas for the AC-TIG welding of aluminum is Argon, although helium and argon–helium mixtures may be used. Argon gives a wide, shallow penetration weld bead but leaves the weld bright and silvery in appearance. The easiest arc ignition and most stable arc can also be achieved with argon. Typical butt welds in 3 mm and 6 mm plate are illustrated in Figure 2-3, and a fillet weld in 6 mm thick plate is shown in Figure 2-4. Suggested welding parameters for use with argon as a shield gas are included in Table 2-3.

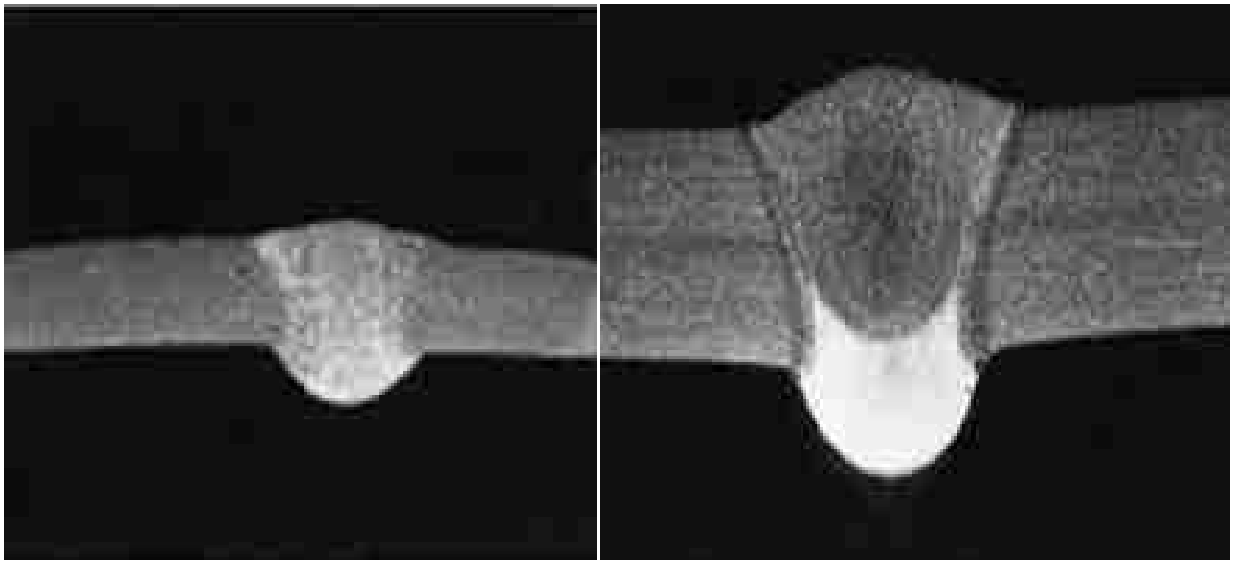

(a) (b)

Figure2-3 AC-TIG argon shielded (a) unbacked 3mm sheet, single pass, flat position;
(b) unbacked 6mm thick plate, two pass, flat position [21].

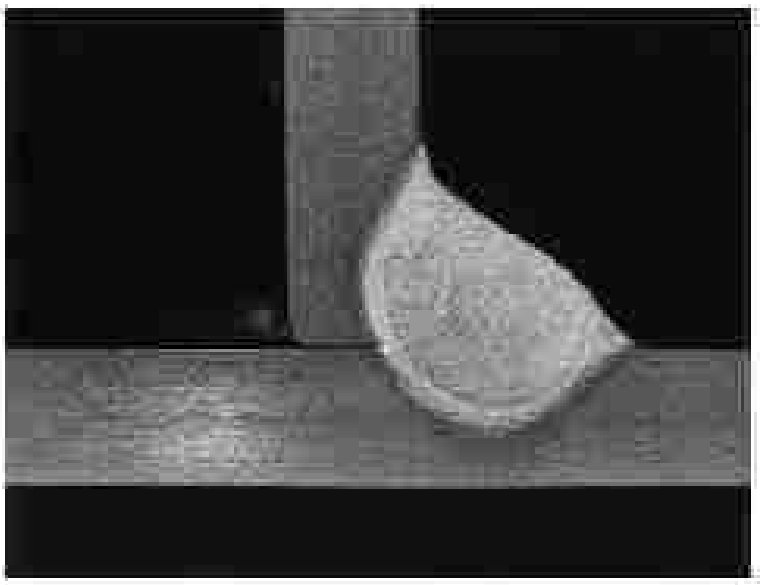

Figure 2-4 AC-TIG argon shielded, 6mm thick plate, single pass, horizontal–vertical [21].

Table 2-3 Suggested welding parameters – argon gas shielding [15]

Thickness (mm)	Joint type	Root gap (mm)	Current (A)	No. of passes	Filler diam. (mm)	Travel speed (mm/min)	Nozzle diam. (mm)
0.8	sq. butt	nil	55	1	1.6	300	9.5
1.2	sq. butt	nil	100	1	2.4	400	9.5
1.5	sq. butt	0.8	130	1	2.4	470	9.5
1.5	fillet		100	1	2.4	250	9.5
2	sq. butt	0.8	160	1	3.2	380	9.5
2.5	sq. butt	0.8	170	1	3.2	300	9.5
2.5	fillet		140	1	3.2	250	9.5
3.2	sq. butt	0.8	160	1	3.2	300	12.7
3.2	fillet		175	1	3.2	300	12.7
5	sq. butt	1.6	250	1	4.8	200	12.7
5	fillet		240	1	4.8	250	12.7
6.5	70 V-butt	nil	320	1	4.8	150	12.7
6.5	fillet		290	1	4.8	250	12.7
8	70 V-butt	nil	340	2	4.8	165	12.7
10	70 V-butt	nil	350	2	6.4	180	12.7
10	fillet		370	2	6.4	250	16

Helium increases arc voltage with the effect of constricting the arc, increasing penetration but making arc ignition more difficult, and adversely affecting arc stability. Some of the modern welding power sources are equipped with a facility to start the weld with argon and, once a stable arc is established, for an automatic change-over to helium to be made.

In the UK, helium is a more expensive as than argon – some five to six times more – and provides little or no arc cleaning action. Indeed, in some circumstances, the use of helium can resulting 'soot' being deposited in the HAZ and although this may normally be removed by wire brushing, it can be difficult to remove. For these reasons, 100% pure helium is rarely used in manual AC-TIG welding.

The addition of argon to helium improves arc striking and arc stability. Travel speeds and penetration will be less than with pure helium but greater than with argon. It is possible to control bead width and penetration by varying the amount of argon in the mixture. The most popular mixture in the UK is 25% helium in argon [23].

2.4 MIG Welding

2.4.1 Definition

The Gas Metal Arc Welding (GMAW) is frequently referred to as MIG welding. MIG welding is a commonly used fusion process with a high deposition and production rates. Wire is continuously fed from a spool. MIG welding is therefore referred to as a semi-automatic welding process.

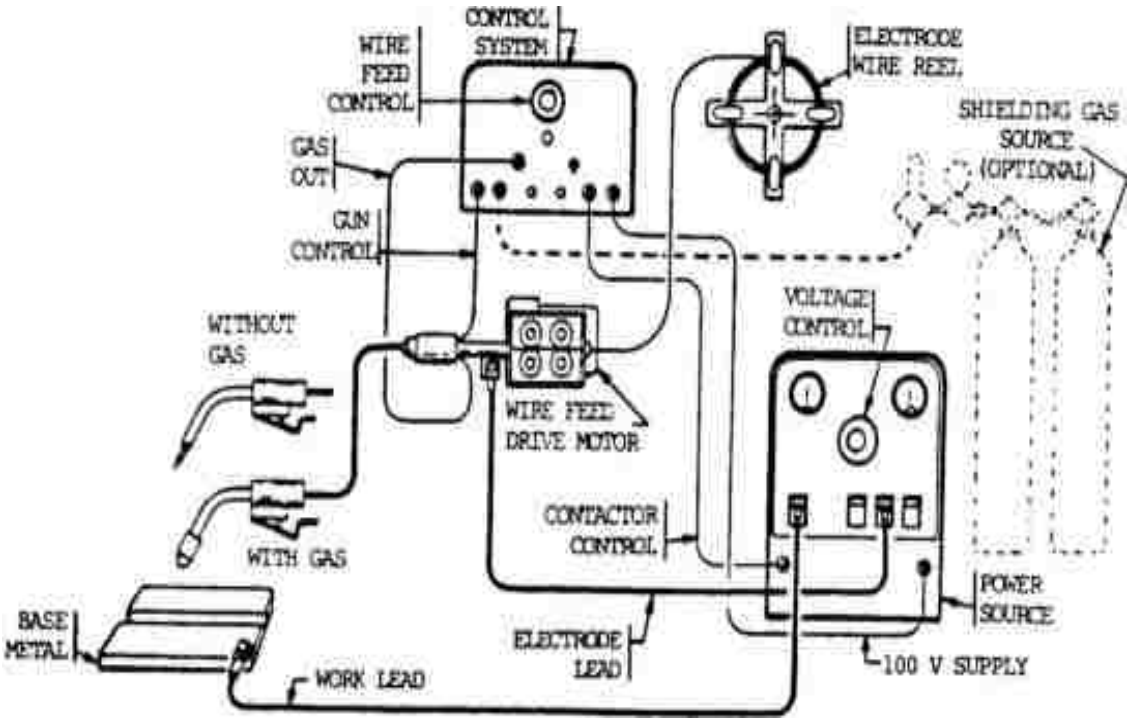

Figure 2-5 Schematic of the MIG Welding Process [24].

2.4.2 Process Principles

The MIG welding process, illustrated in Figure 2-5, as a rule uses direct current with the electrode connected to the positive pole of the power source, DC positive, or reverses polarity in the USA, results in very good oxide film removal. Recent power source developments have been successful in enabling the MIG process to be converted with AC. Most of the heat developed in the arc is generated at the positive pole, in the case of MIG welding the electrode, resulting in high wire burn-off rates and an efficient transfer of this heat into the weld pool by means of the filler wire [24].

When welding at low welding currents, the tip of the continuously fed wire may not melt sufficiently fast to maintain the arc but may dip into the weld pool and short circuit. This short circuit causes the wire to melt somewhat like an electrical fuse and the molten metal is drawn

into the weld pool by surface tension effects [25]. The arc re-establishes itself and the cycle is repeated. This is known as the dip transfer mode of metal transfer. Excessive spatter is produced if the welding parameters are not correctly adjusted and the low heat input may give rise to lack-of-fusion defects. At higher currents, the filler metal is melted from the wire tip and transferred across the arc as a spray of molten droplets, *spray transfer*. This condition gives far lower spatter levels and deeper penetration into the parent metal than dip transfer.

When MIG welding aluminium, the low melting point of the aluminum results in spray transfer down to relatively low welding currents gives a spatter-free joint. Table 2-4 lists the likely and/or commonest methods of metal transfer with respect to wire diameter.

Table 2-4 Metal transfer modes and wire diameter [24]

Metal transfer mode	Wire diameter
Dip	0.8mm
Pulsed	1.2 and 1.6mm
Conventional spray	1.2 and 1.6mm
High-current spray	1.6mm
High-current mixed spray/globular	2.4mm

2.4.3 Shielding Gases Selection

The shielding gases, similar to TIG welding, are the inert gases argon and helium or combinations of these two. Other active gases such as oxygen or nitrogen even in small amounts could cause porosity and smutting problems. The most commonly used gas is argon which is used for both manual and some automatic welding. It is substantially cheaper than helium and

produces smooth, quiet and stable arc, giving a wide, smooth weld bead with a finger-like penetration to give a mushroom-shaped weld cross-section. Argon, however, gives the lowest heat input and the slowest welding speeds. There is a risk of lack of fusion defects and porosity on thick sections. Argon may also give a black sooty deposit on the surface of the weld. This can be easily removed by wire brushing. Sections of 3 mm thick butt welds using conventional and pulsed current are illustrated in Figure 2-6. Thicker section butt and fillet welds are illustrated in Figure 2-7. In these thicker section welds, the characteristic finger penetration of an argon gas shield can be seen [26].

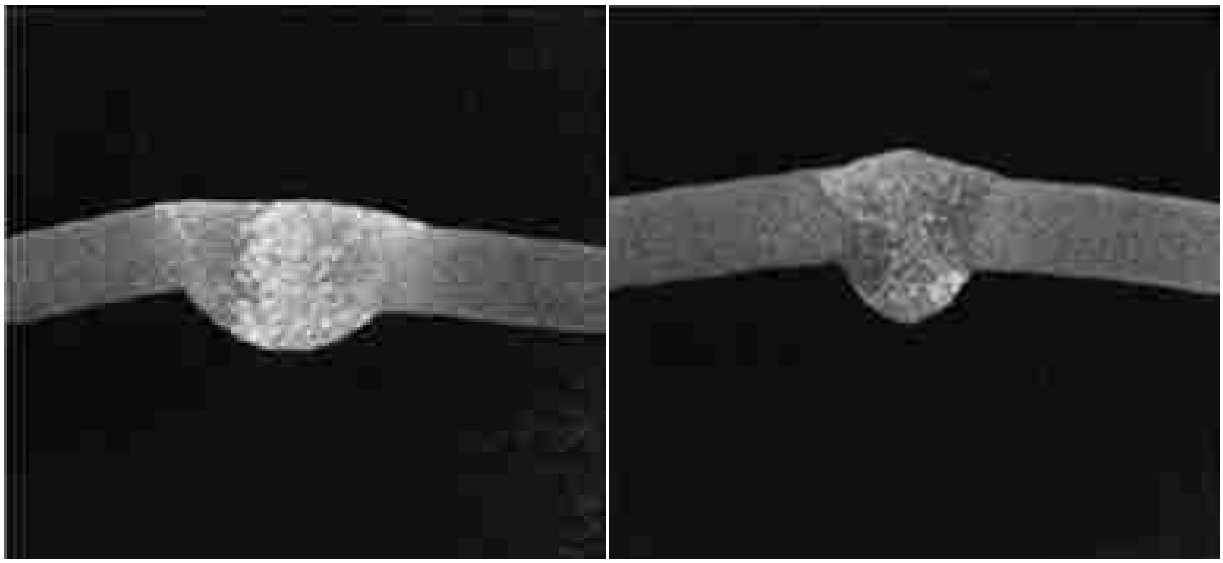

(a) (b)

Figure 2-6 (a) MIG, argon shielded 0.8mm wire, 3mm thick unbacked plate butt, and

(b) Pulsed MIG, argon shielded, 0.8 mm diameter wire, 3mm thick unbacked plate butt, flat position [23].

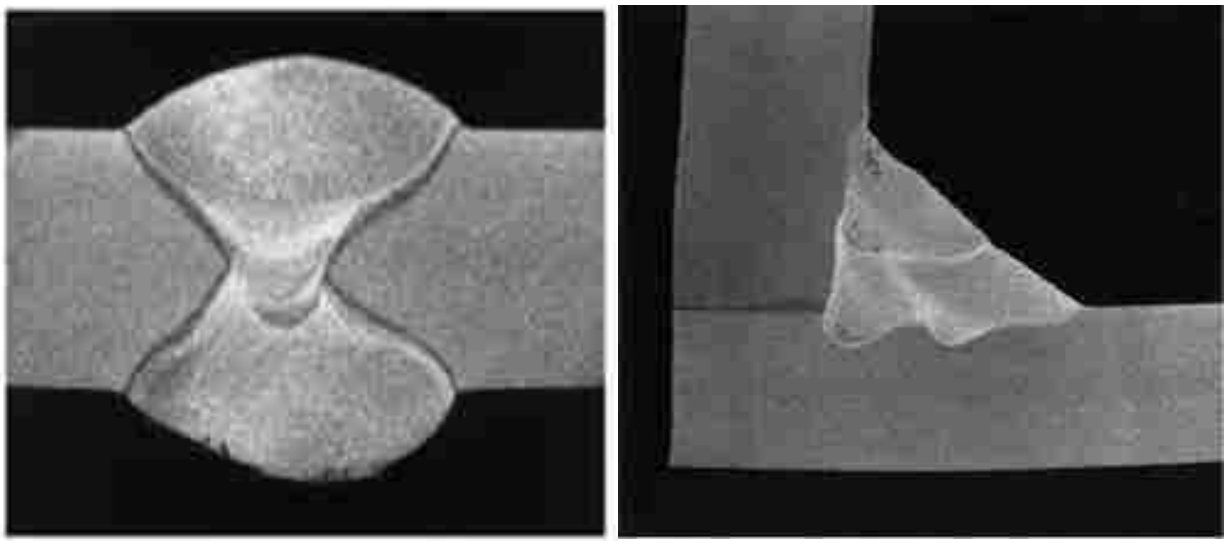

(a) (b)

Figure 2-7 (a) MIG, argon shielded, two pass, double sided, 12mm thick, and
(b) MIG, argon shielded, 15mm leg length fillet, 12mm thick plate, horizontal-vertical [23].

Helium increases the arc voltage by as much as 20% compared with argon [27], resulting in a far hotter arc, increased penetration and wider weld bead. The wider bead requires less critical positioning of the arc and avoiding missed edge and lack of penetration-type defects. The hotter, slower cooling weld pool also allows hydrogen to diffuse from the molten weld metal, making a method that may be used to reduce the amount of porosity. The increased heat also enables faster welding speeds to be achieved, as much as three times that of a similar joint made using argon as a shielding gas.

Helium, however, is expensive and gives a less stable arc than argon. Pure helium therefore finds its greatest use in mechanized or automatic welding applications. Helium shielded manual welds are illustrated in Figure 2-8.

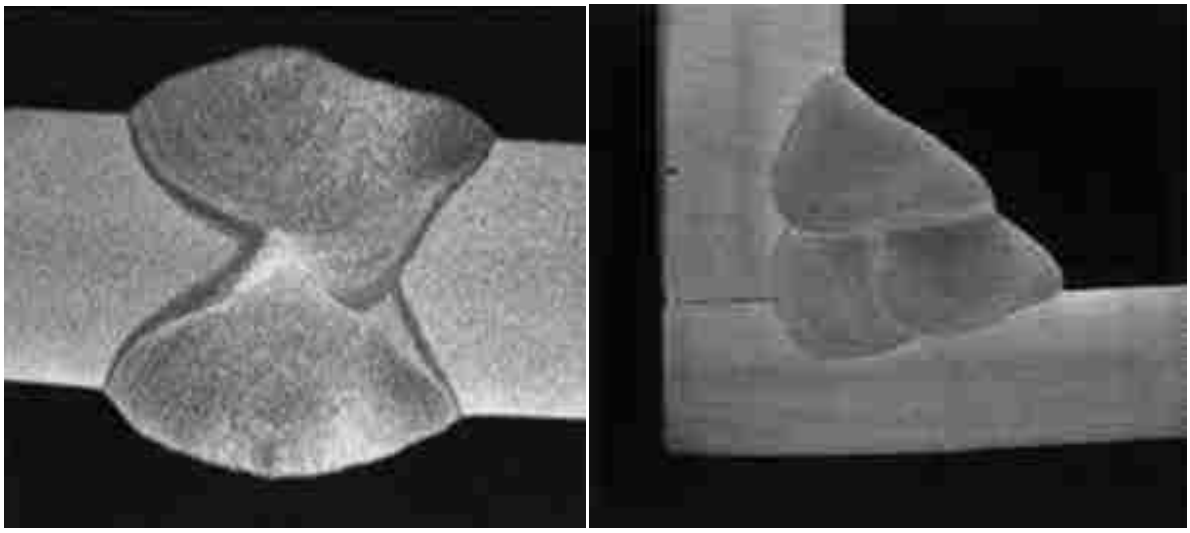

(a) (b)

Figure 2-8 (a) MIG, helium shielded, two pass, double sided, 12mm thick, and
(b) MIG, helium shielded, 15mm leg length fillet, 12mm thick plate [23].

For manual welding, mixtures of argon and helium give good results with characteristics intermediate between the two gases. These mixtures are useful on thicker materials because they increase the heat input and provide a wider tolerance box of acceptable welding parameters than pure argon. They also improve productivity by enabling faster travel speeds to be used. The most popular combinations are 50% and 75% of helium in argon. Typical welds using the 50% helium and the 50% argon are illustrated in the Figure 2-9 [28].

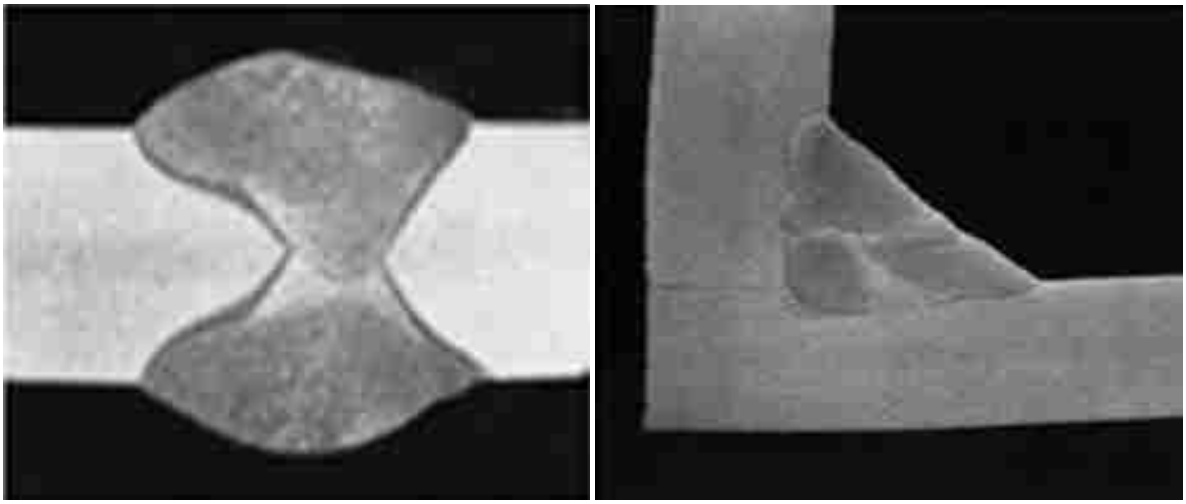

(a) (b)

Figure 2- 9 (a) MIG, helium–argon shielded, two pass, double sided, 12mm plate, and

(b) MIG, helium–argon shielded, 15mm leg length fillet, 12mm thick plate horizontal–vertical [23].

2.5 MIG and TIG Comparison

2.5.1 Process Difference

Either MIG or TIG welding is a process involving the fusing together of metals by melting the metal where they meet and come joined. In many cases, pressure and / or filler material is used to aid in the fusion process.

Both MIG and TIG welds are types of arc welding, which utilizes the concentrated heat of an electric arc to join together metals by fusion of the parent metal by a consumable electrode. Depending on the material to be welded and the electrode used, the process utilizes either direct or alternating current for the welding arc.

The MIG weld process, or Metal Inert Gas weld, fuses the metal by heating with an arc. With this type of weld, the arc is placed between the filler metal electrode and the work piece. Shielding gas is provided by outwardly supplied gas or gas mixtures.

A TIG weld or Tungsten Inert Gas, on the other hand, functions by joining metals through the process of heating with tungsten electrodes that do not become part of the completed weld. The process utilizes argon or other inert gas mixtures as shielding and filler metals are rarely used.

2.5.2 Advantages and Disadvantages

Some of the basic differences between the two types of welds are that MIG welding is faster than using TIG welding, as utilizing TIG welding requires more skill that MIG welding. A solid wire is used in the MIG Flux Cored Arc Welding-Gas Shield (FCAW-G) while TIG uses a flux cored electrode.

Another obvious difference is that TIG uses Tungsten to carry the arc, and a user of a TIG welder needs to have sufficient experience in the craft of welding. A MIG weld user, meanwhile, can carry on working despite being a novice welder.

Overall, while both MIG and TIG are gas shielded arc welding processes, the primary difference lies in the way the filler metal is added to produce the weld.

With the TIG process, the arc is created between a tungsten electrode mounted in a hand-held torch and the work piece to be welded. The welder initiates the arc by means of a switch. The filler metal, in the form of a hand held rod, is then added to the weld puddle by the welder as the torch is manipulated along the joint which is to be welded.

The MIG process uses a filler metal which is the electrode and the arc is created when the filler metal comes into contact with the work surface [29].

2.6 Other Welding Processes

2.6.1 Introduction

While MIG and TIG welding may be regarded as the most frequently used processes for joining aluminium and its alloys, there are a large number of other processes that are equally useful and are regularly employed although perhaps in rather more specialised applications than the conventional fusion welding processes. Some of these processes are discussed here.

2.6.2 Plasma-Arc Welding

A modification to the TIG welding torch enables a strong plasma jet to be produced that has some very desirable features for both welding and cutting. Despite these advantages, the process finds little application for the welding of aluminium when DC electrode negative or electrode positive is used because of extensive lack of fusion defects. Alternating current give no better results as high currents are required, resulting in rapid electrode deterioration. The pulsing of the current also causes weld pool instability, poor bead shape and lack of fusion defects. These limitations are overcome with the development of square wave power sources, since time plasma-TIG has become accepted as a viable production process [30].

2.6.3 Laser Welding

Laser welding is being used increasingly in both the automotive and aerospace industries for the welding of a range of materials. The laser welding of aluminium and its alloys has, however,

presented problems to the welding engineer [31]. Poor coupling of the beam with the parent metal, high thermal conductivity, high reflectivity and low boiling point alloying elements, prevents the achievement of consistent weld quality.

Defects in laser welded joints are similar to those encountered in welds made by other fusion welding processes. Porosity is caused by hydrogen from the environment, dissolved in the parent metal, contained in the oxide film or from an unstable keyhole condition. The solution to this problem is careful surface preparation including pickling and scraping, gas shielding and the use of adequate power to ensure the creation of a stable keyhole. Most of the non-heat-treatable alloys are capable of being welded successfully, hot cracking may be encountered, particularly in those alloys that are sensitive. This can be reduced or eliminated by the addition of a suitable filler wire. The last difficulty is caused by the low viscosity of the molten weld metal. This causes the problem of 'drop-through', where the weld metal falls out of the joint when welds are made in the flat position. This problem can be overcome by welding in the horizontal–vertical (PC) position [31].

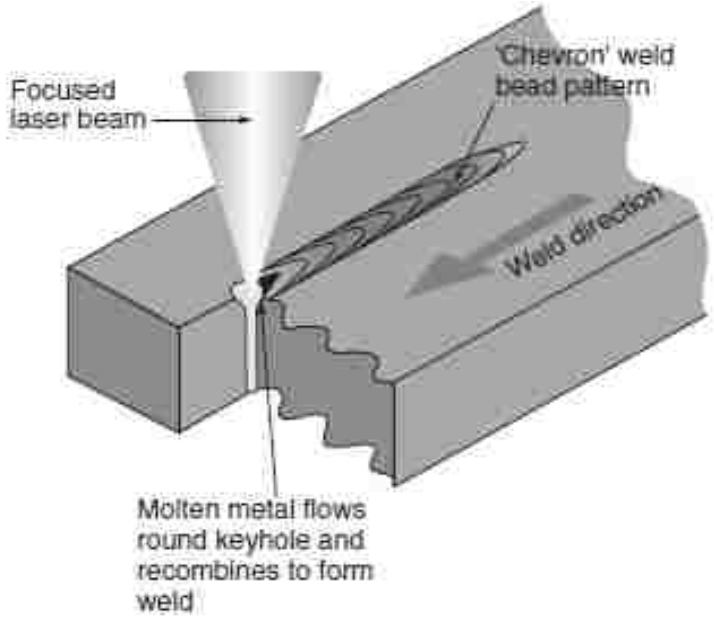

Figure 2-10.Principle of laser welding [31].

2.6.4 Electron Beam Welding

Electron beam welding is, like laser welding, a power beam process ideally suited to the welding of close square joints in a single pass. Unlike the laser beam, however, the electron beam process utilises a vacuum chamber in which is generated a high-energy density beam of electrons of the order of 0.25–2.5 mm diameter [32].

The beam is generated by heating a tungsten filament to a high temperature, causing a stream of electrons that are accelerated and focused magnetically to give a beam that gives up its energy when it impacts the target– the weld line. This enables very deep penetration to be achieved with a keyhole penetration mode at fast travel speeds, providing low overall heat input.

The process may be used for the welding of material as thin as foil and up to 400 mm thick in a single pass [32]. The keyhole penetration mode gives almost uniform shrinkage about the neutral axis of the component, leading to low levels of distortion. This enables finish machined components to be welded and maintained within tolerance. The transverse shrinkage also results in the solidifying weld metal being extruded from the joint to give some excess metal outside the joint.

2.7. Filler Metal (Alloy) Selection Cateria

2.7.1 Introduction

When choosing the optimum filler alloy, the application of the welded part and its desired performance must be prime considerations. Many alloys and alloy combinations can be joined

using any one of several filler alloys, but only one filler may be optimal for a specific application.

Both aluminium and magnesium react with the atmosphere to produce tightly adherent refractory oxides that melt at high temperatures (>2000^{o}C) and protect the underlying metal against corrosion. The oxides do not melt during welding and have to be dispersed or removed from the weld area to ensure full fusion. This is usually accomplished by the use of alternating current with the GTAW process and electrode positive polarity in the GMAW process [31].

2.7.2 Primary Factors

The primary factors commonly considered when selecting a welding filler alloy are: Ease of welding; Tensile or shear strength of the weld ; Weld ductility; Service temperature; Corrosion resistance; Color match between the weld and the base alloy after anodizing and Sensitivity to Weld Cracking.

Ease of welding is the first consideration for most welding applications. In general, the non-heat-treatable aluminum alloys can be welded with a filler alloy of the same basic composition as the base alloy.

2.7.3 Types for Filler Metals

The heat-treatable aluminum alloys are somewhat more metallurgically complex and more sensitive to "hot short" cracking, which results from heat - affected zone (HAZ) liquidation during the welding operation. Generally, a dissimilar alloy filler having higher levels of solute (for example, copper or silicon) is used in this case.

The high-purity 1xxx series alloys and 3003 are easy to weld with a base alloy filler, 1100 alloy, or an aluminum - silicon alloy filler, such as 4043; Alloy 2219 exhibits the best weldability of the 2xxx series base alloys and is easily welded with 2319, 4043 and 4145 fillers.

Aluminum-silicon-copper filler alloy 4145 provides the least susceptibility to weld cracking with 2xxx series wrought copper bearing alloys, as well as aluminum-copper and aluminum-silicon-copper aluminum alloy castings; The cracking of aluminum-magnesium alloy welds decreases as the magnesium content of the weld increases above 2%. The 6xxx series base alloys are most easily welded with the aluminum-silicon type filler alloys, such as 4043 and 4047. However, the aluminum-magnesium type filler alloys can also be employed satisfactorily with the low-copper bearing 6xxx alloys when higher shear strength and weld metal ductility are required [33]. The 7xxx series (aluminum-zinc-magnesium) alloys have a narrow melting range and can be readily joined with the high magnesium filler alloys 5356, 5183 and 5556. The 7xxx series alloys that possess a substantial amount of copper, such as 7975 and 7178, have a very wide melting range with a low solidus temperature and are extremely sensitive to weld cracking when are welded [33].

2.8. Defect Prevention

The specific properties that affect welding are its oxide characteristics, its thermal, electrical, and non-magnetic characteristics, lack of color change when heated, and wide range of mechanical properties and melting temperature that result from alloying with other metals.

2.8.1 Oxide

Aluminum oxide melts at about 2050 ^{o}C which is much higher than the melting point of the base alloy [34]. If the oxide is not removed or displaced, the result is incomplete fusion. In some joining processes, chlorides and fluorides are used in order to remove the oxide contain. Chlorides and fluorides must be removed after the joining operation to avoid a possible corrosion problem in service.

2.8.2 Hydrogen Solubility

Hydrogen dissolves very rapidly in molten aluminum. However, hydrogen has almost no solubility in solid aluminum and it has been determined to be the primary cause of porosity in aluminum welds. High temperatures of the weld pool allow a large amount of hydrogen to be absorbed, and as the pool solidifies, the solubility of hydrogen is greatly reduced [34]. Hydrogen that exceeds the effective solubility limit forms gas porosity, if it does not escape from the solidifying weld.

2.8.3 Electrical Conductivity

For arc welding, it is important that aluminum alloys possess high electrical conductivity -- pure aluminum has 62% that of pure copper. High electrical conductivity permits the use of long contact tubes guns, because resistance heating of the electrode does not occur, as is experienced with ferrous electrodes [35].

2.8.4 Thermal Characteristics

The thermal conductivity of aluminum is about 6 times that of steel [35]. Although the melting temperature of aluminum alloys is substantially below that of ferrous alloys, higher heat inputs

are required to weld aluminum because of its high specific heat. High thermal conductivity makes aluminum very sensitive to fluctuations in heat input by the welding process.

2.8.5 Forms of Aluminum

Most forms of aluminum can be welded. All the wrought forms (sheet, plate, extrusions, forgings, rod, bar and impact extrusions), as well as sand and permanent mold castings, can be welded. Welding on conventional die-castings produces excessive porosity in both the weld and the base metal adjacent to the weld because of internal gas. Vacuum die-castings, however, have been welded with excellent results. Powder metallurgy (P/M) parts also may suffer from porosity during welding because of internal gas [35].

The alloy composition is a much more significant factor than the form in determining the weldability of an aluminum alloy.

2.9 Solution Treatment Work on 3xx Serial Alloys

2.9.1. Morphology of Silicon Phase during Solution Treatment

Apelian et al.[36] have analyzed the extensive information available on the heat treatment of commercial Al-Si-Mg alloys (ASTM B108 A356.2). According to them, the purpose of solution-heat treatment in cast Al-Si-Mg alloys is: 1) to obtain a maximum concentration of the age-hardening constituent (Mg_2Si) in solid solution, 2) to homogenize the casting, and 3) to change the structural characteristics of the eutectic Si particles. As the solution time increases at 540°C, Si particles undergo necking and are broken down into smaller fragments. The

fragmented particles are gradually spheroidized. Prolonged solution treatment leads to extensive coarsening of the particles.

Modification is a technique through adding electropositive elements like sodium, calcium or strontium into Al-Si alloy, to completely change the morphology of the eutectic silicon crystals from large flakes into a fibrous structure, thus improve the mechanical properties of alloys [37].

The rate of spheroidization is extremely rapid in modified alloys compared to unmodified samples. Due to large differences in particle size distribution, the driving force for coarsening is greater in unmodified alloys than in modified ones. Consequently, unmodified alloys exhibit a higher coarsening rate.

In modified castings, particle growth obeys equations developed for diffusion controlled growth and particle volume is proportional to $t^{1/3}$ (t is time here) [38]. This relationship is shown as Equation 2-1, known as LSW equation. In unmodified sand castings, the dependence of particle size on $t^{1/3}$ is observed only after large solution times (>200 min). In this case, the assumption of spherical morphology for Si particles is not valid at short solution times.

$$R_m^3 - R_o^3 = \frac{8}{9} \frac{D \sigma \Omega^2 c_\infty}{K_B T (c_\beta - c_\infty)} t = \frac{K t}{T} \qquad (2\text{-}1)$$

Where D is the diffusion coefficient of solute in the matrix, σ the interfacial tension, Ω the atomic volume, and c_∞ and c_β the equilibrium concentrations of solute in the matrix and the particle at a planar interface, respectively.

Shivkumar et al [36] studied the changes of silicon particle parameters with solution time in Figure 2-11. The average diameter initially registers a decrease because off fragmentation of the

particle. Subsequently, particle coarsening leads to a significant increase in the average diameter. Because of the higher cooling rate, the average diameter is much smaller in permanent mold than in sand cast specimens.

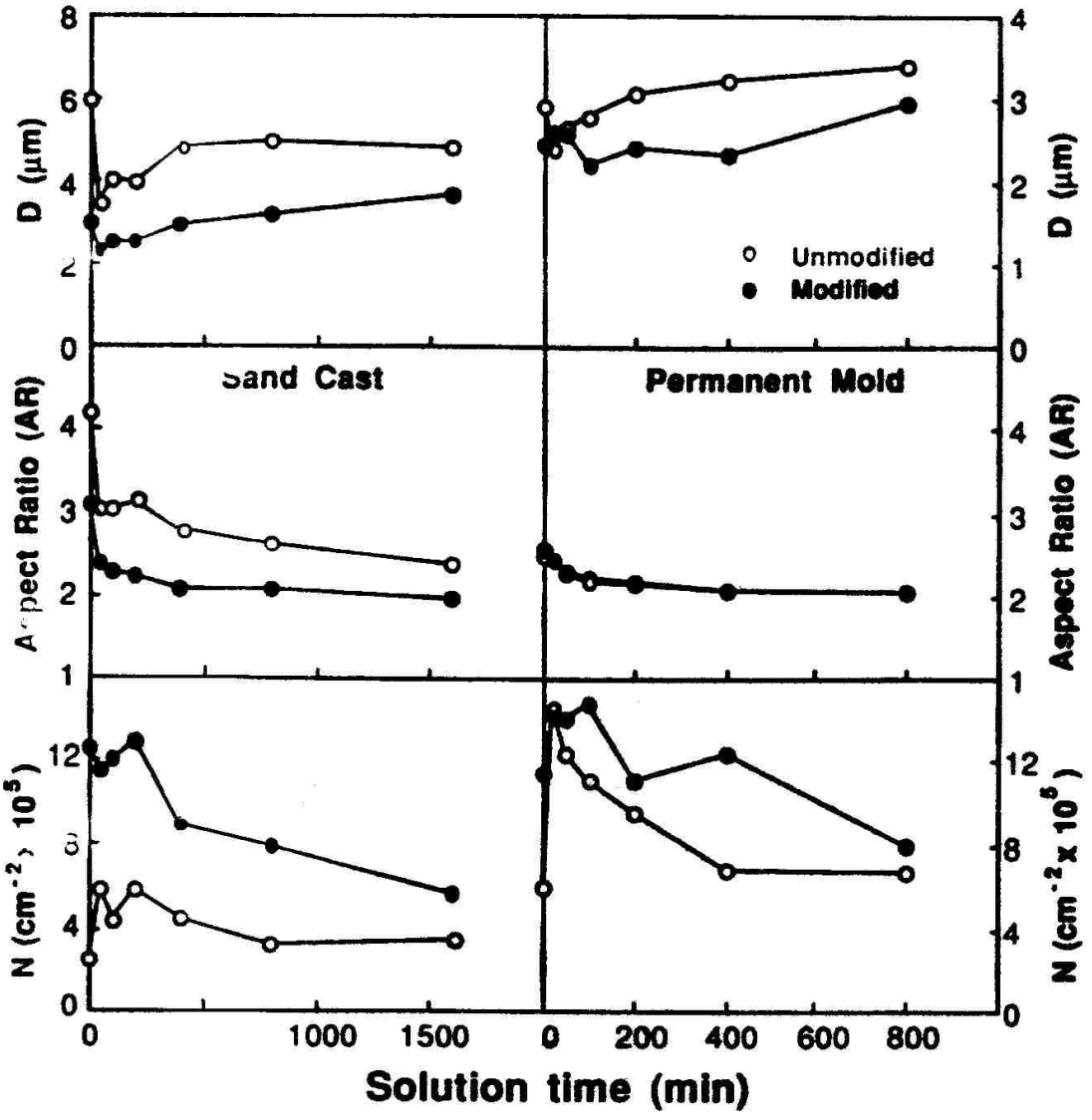

Figure 2-11 Variation of silicon particle average diameter (D), aspect ratio, and number of silicon particles (N) with solution time (solution temperature = 540°C) [36].

Meyers [39] has conducted a detailed study of the silicon particle coarsening process in unmodified A357 samples, and has shown that the silicon particle volume increase is directly proportional to time. Under the assumption that growth is not diffusion controlled, the growth of silicon particles is independent of alloy composition, that is, independent of the particle spacing. The number of particles varies inversely with the particle diameter since the total volume of silicon remains constant. The aspect ratio of silicon particles decreased rapidly up to 100 minutes of solution treatment. Subsequently, the reduction tendency of their aspect ratio slows down. Figure 2-12 shows their result of mean particle volume as a function of time duration.

The result of Shivkumar et al. [40] on the A356 alloy castings (Si 7.3%, Fe 0.09%, Cu 0.002%, Mn 0.009%, Mg 0.36%, Ni 0.001%, Zn 0.02%, 0.06%) indicates that the solution temperature has a strong effect on the Si morphology. Higher temperatures result in coarser particles. Increasing the solution temperature from 540 to 550ºC may benefit strength properties.

According to the study of M. Tsukuda and S. Koike [41], the distribution and morphologies of eutectic Si have a greater influence on mechanical properties than dendrite arm spacing (DAS). The effect of solution temperature and time on mechanical properties are shown in Figure2-13 for a permanent mold cast Al-6.85%Si-0.3%Mg-0.2%Fe-0.12%Ti-0.006%Na alloy in T4 condition. At 520°C or 530°C, UTS (Ultimate Tensile Strength), elongation and impact strength increase with solution time. The yield strength decreases marginally with solution time. At 540°C, UTS and elongation attain a peak value in a very short time and then show a slight decrease.

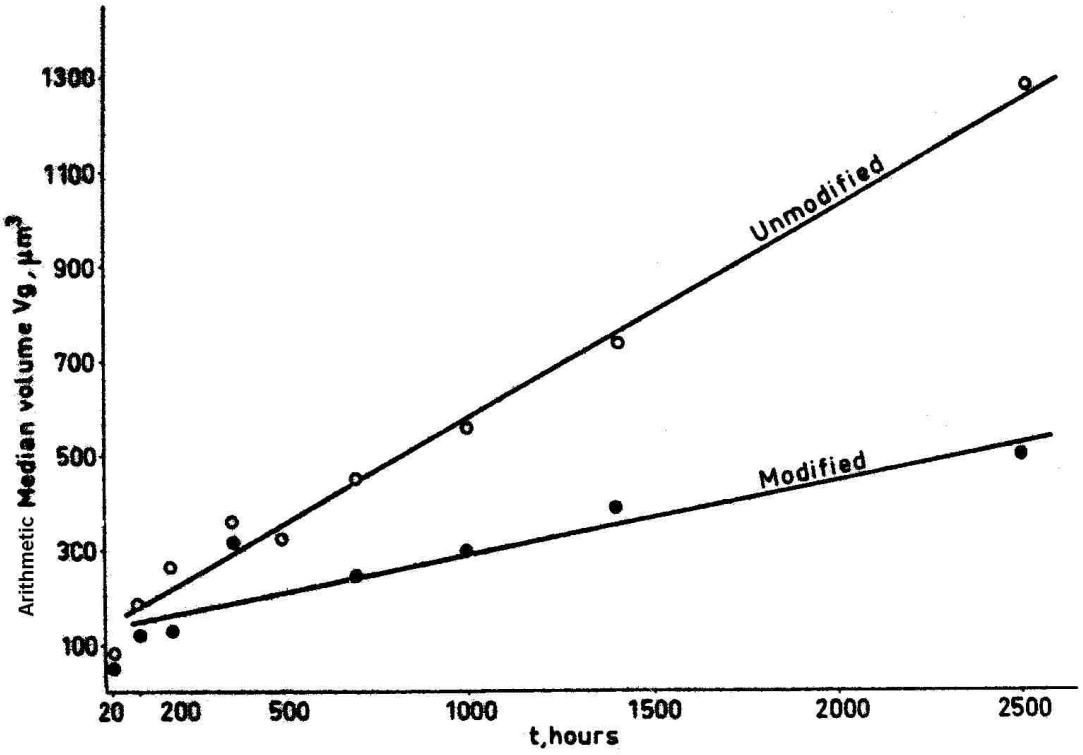

Figure 2-12 Arithmetic mean particle volume (V_v/N_v) vs. time at 540°C for modified alloys, lower plot; unmodified alloys, upper plot [39].

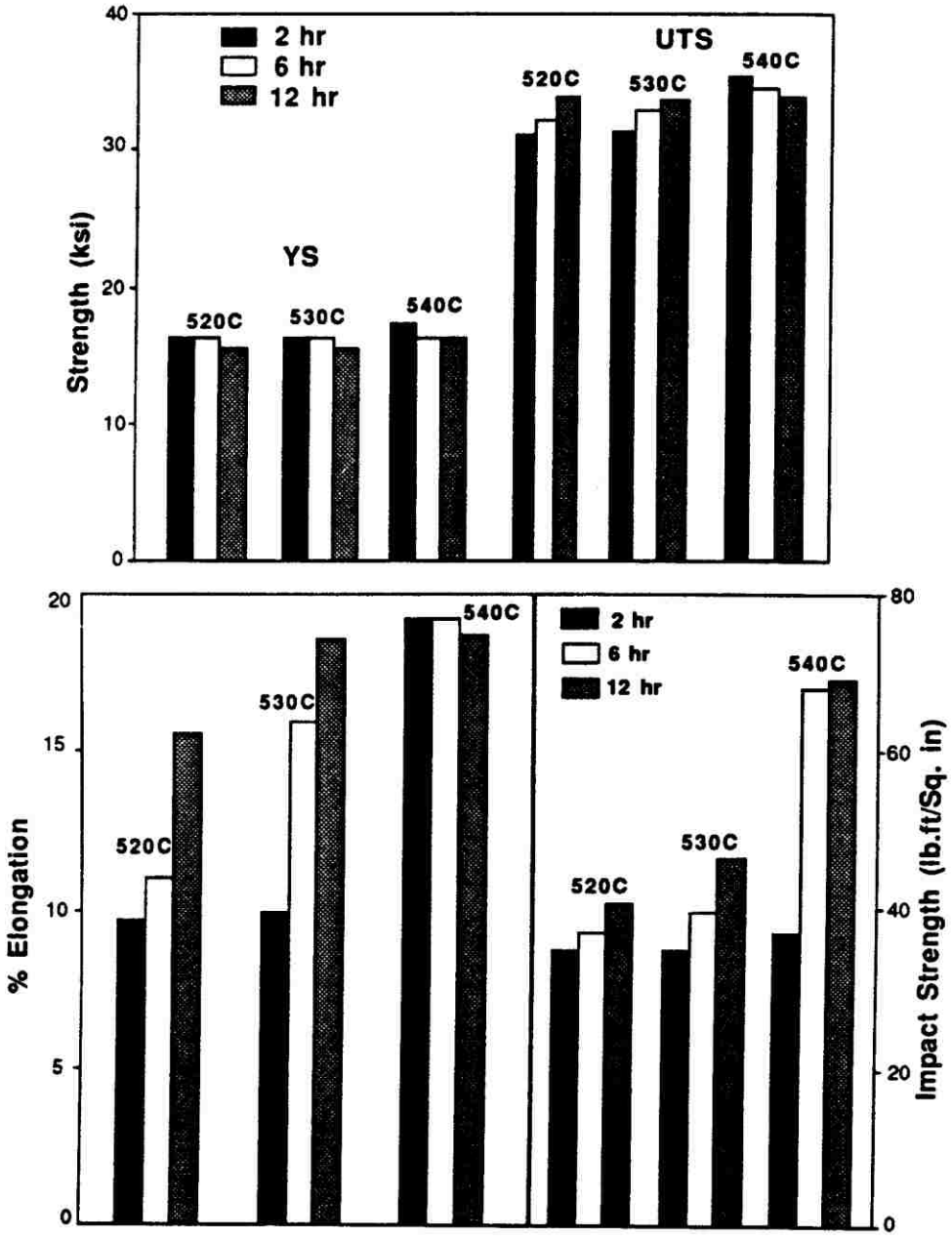

Figure 2-13 Effect of solution heat treatment temperature and time on mechanical properties of A356 alloy in the T4 condition [41].

Gauthie et al [42,43] have studied solution-heat-treated behavior of 319.2 alloys (Si 6.23%, Cu 3.77%, Fe 0.46%, Mn 0.14%, Mg 0.06%, Zn 0.08%), which differ from A380 in silicon content. Figure 2-14 shows their results on silicon particle growth through different solution temperatures and times. In the temperature range 480-525°C, the Si particles initially undergo a decrease in area, indicating fragmentation of the particles into smaller segment. This period (2-4hrs) is followed by a steady coarsening of the particles. A solution treatment of 2hr at 540°C leads to instant particle coarsening, indicating that fragmentation at this temperature may take place much earlier.

According to their research, solutionizing 319.2 alloy for 8hr at 515ºC improves the alloy ductility through partial spheroidization of the Si particles. A high solution temperature enhances partial melting of Al_2Cu, resulting in porosity formation and the structure less form of the phase upon quenching, which leads to deterioration of the mechanical properties [44].

Also they used a two-step procedure that yields better results compared to other treatments. Increasing the solution time to 12hr at 515°C prior to heating at 540°C for another 12hr, followed by cooling to 515°C and then quenching in water at 60°C resulted in superior tensile properties, as shown in Figure 2-15.

Schneider and Feikus [45] have discovered that for $AlSi_9Cu_3$ alloy (Si 8.65%, Cu 2.65%, Fe 0.69%, Mn 0.24%, Mg 0.33%, Cr 0.047%, Zn 0.81%, Ti 0.053%, produced by a 3.2MN vacuum die casting machine), the maximum tensile strength and hardness were attained after solution treatment 60 minutes at 480ºC, and maximum elongation value after 15 minutes. This observation indicates that a solution treatment time of 15 minutes is fully sufficient to dissolve the precipitation hardening phases (Figure 2-16).

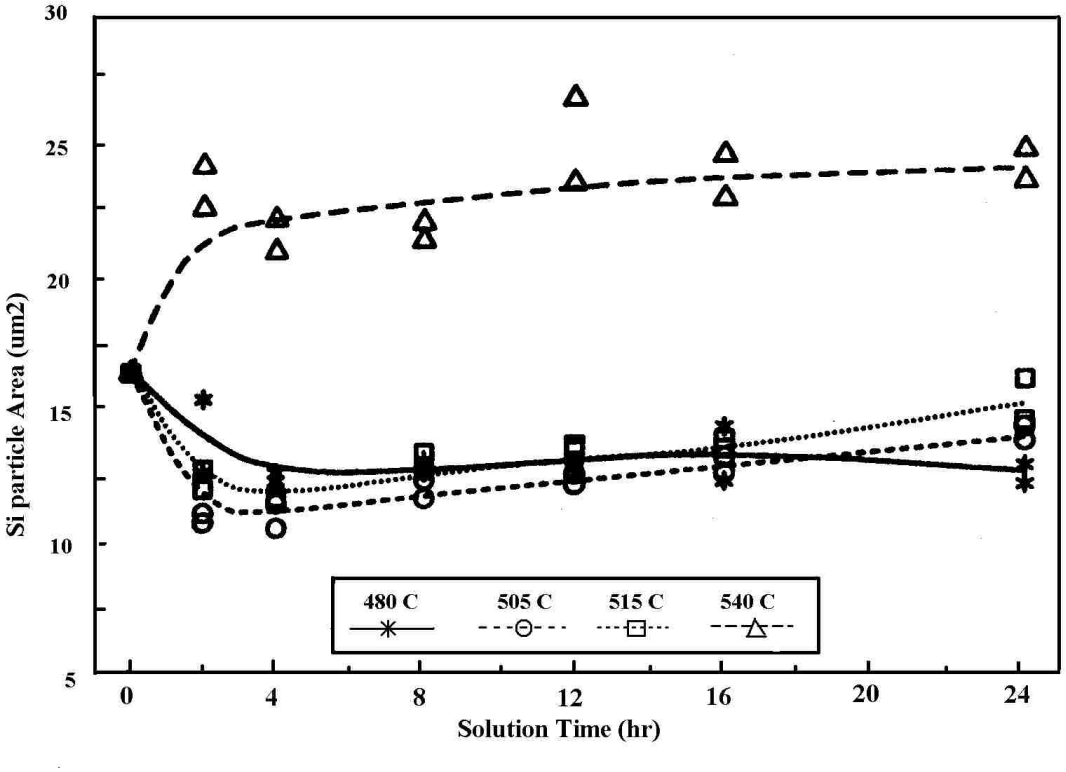

Figure 2-14 Variation in eutectic silicon particle area as a function of solution time in the range 480ºC to 540ºC [44].

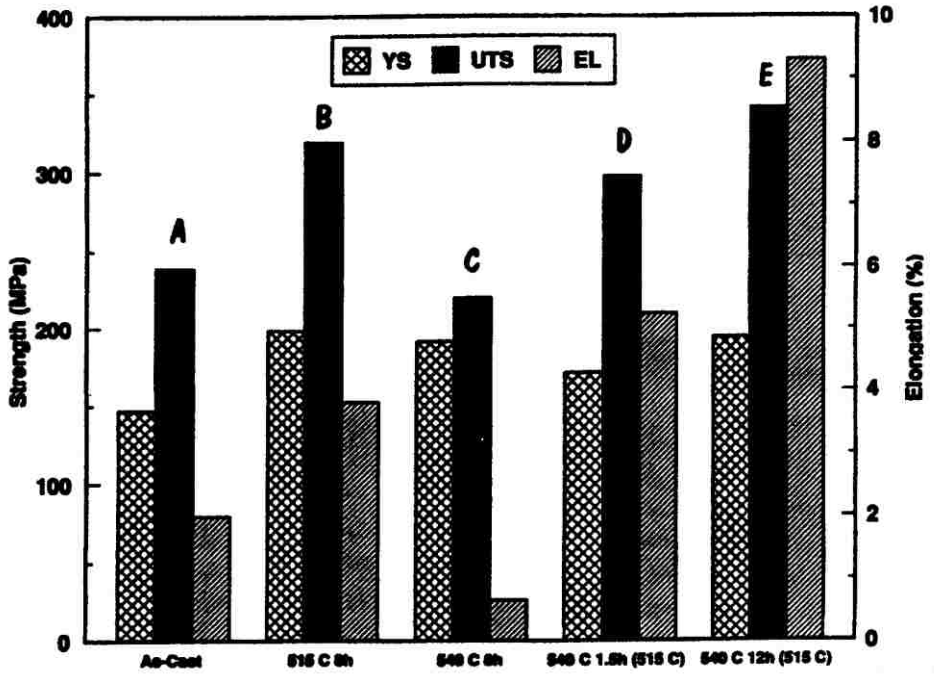

Figure 2-15 Comparison of the tensile properties of test bars. Solution treated according to the following treatments:

A: as cast;

B: 8hr/515C/water quench;

C: 8hr/540C/water quench;

D: 1.5hr/540C→cooling to 515C/1hr/515C/water quench;

E: 12hr/515C→heating to 540C/12hr/540C/water quench [44]

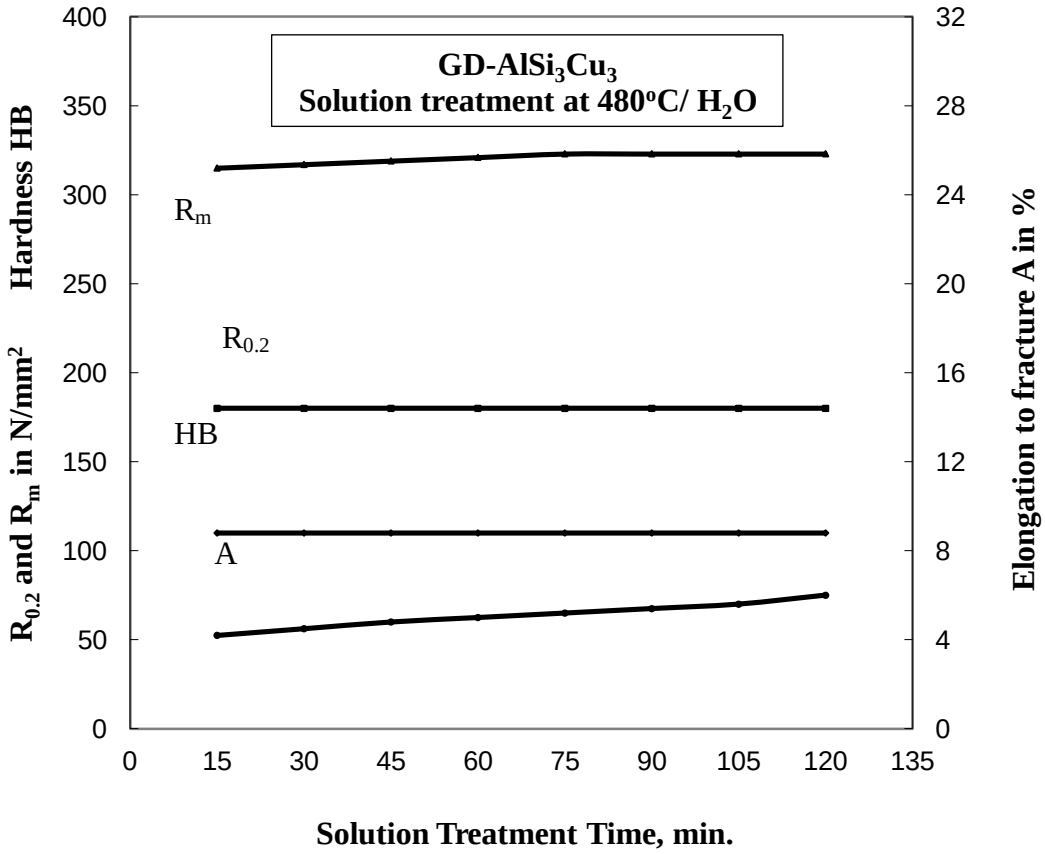

Figure 2-16 Effect of solution treatment time on the mechanical properties of solution treated $AlSi_9Cu_3$ [45]

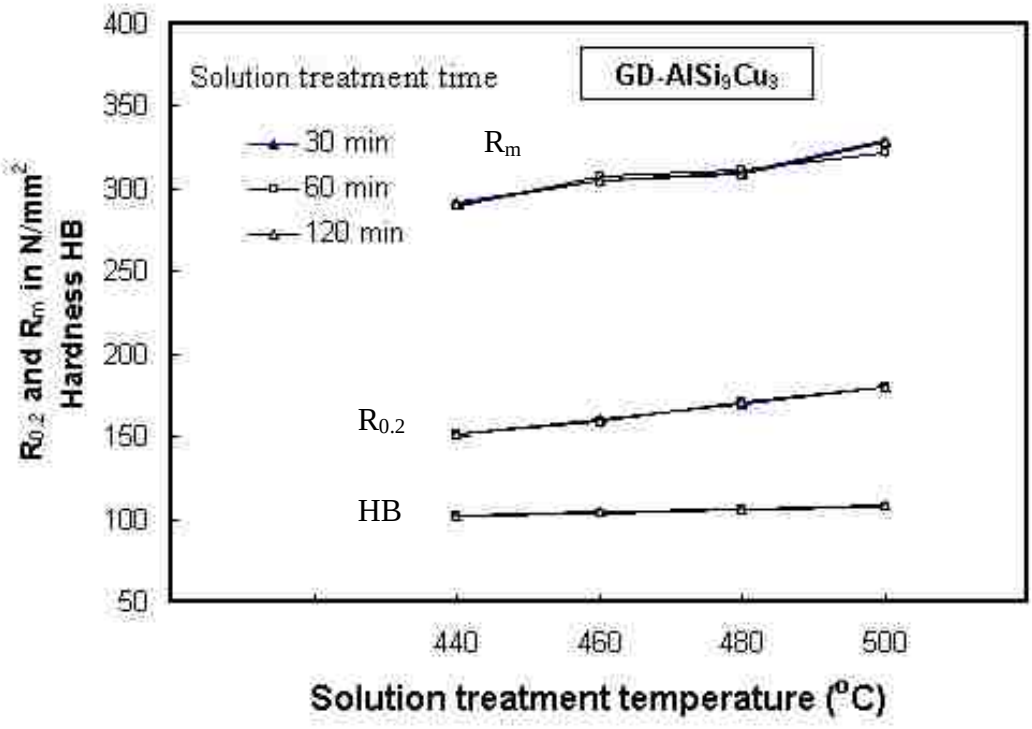

Figure 2-17 Effect of solution treatment temperature on the mechanical properties of solution treated $AlSi_9Cu_3$ [45]

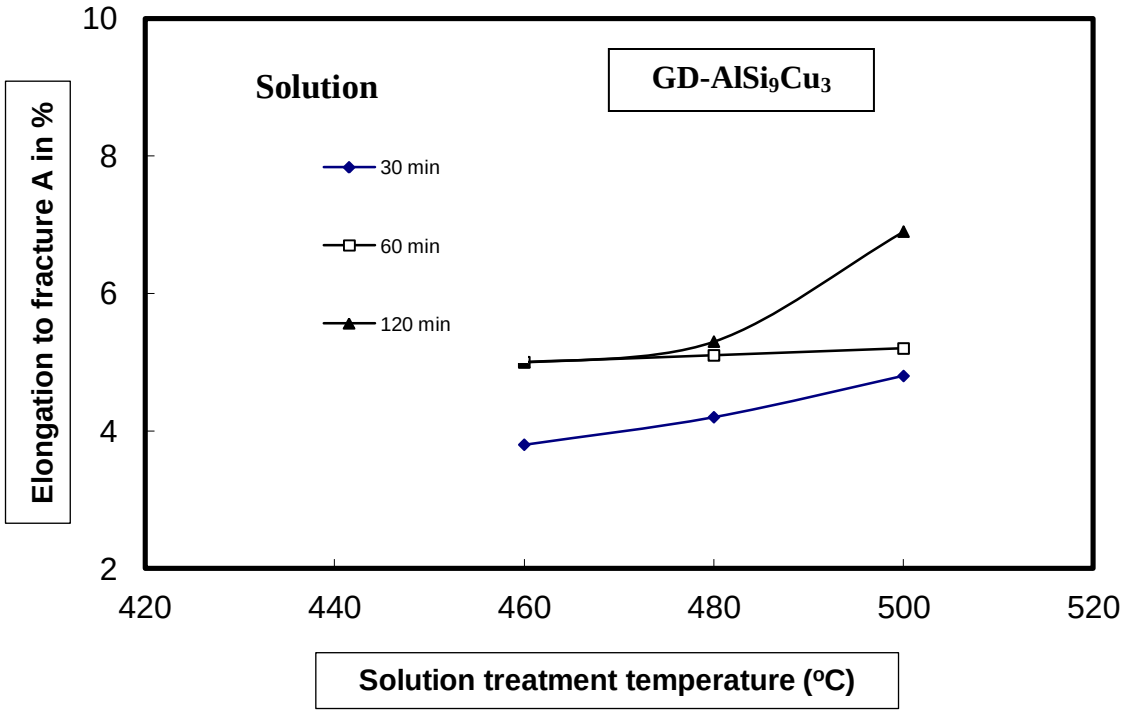

Figure 2-18 Effect of solution treatment temperature on the elongation of$AlSi_9Cu_3$ test bars in the solution treated condition [45]

They pointed out that the morphology of the silicon eutectic has a decisive effect on elongation, and solution treatment can be used to produce uniform silicon particles. It was also observed that as the solution treatment time extended, the silicon particles became coarse without affecting the elongation or the sphericity of particles. Attributed to an increased strengthening of the solid solution due to increasing solubility of the alloying elements in the solid solution, the yield strength, tensile strength and hardness increased with the temperature. Figure 2-17 and 2-18 show the influence of solution temperatures on mechanical properties of the alloy.

2.9.2 Effect of Porosity Influence on Mechanical Properties

Porosity is another important phenomena that can affect mechanical properties of aluminum alloys. Porosity in aluminum die casting is attributed to three main sources: solidification shrinkage, gas entrapment, and the rejection of gas from the liquid metal during solidification [46].

The formation of porosity is also controlled by other factors such as grain refinement and inclusion content. When grain refiner like $TiAl_3$ particles acts as nucleation sites for the formation of primary α-aluminum dendrites and promotes a uniform, equaxied grain structure, it leads to fine dispersion of, and in some cases, a reduction in the amount of porosity [47].

Modification of Al-Si alloy melts through the addition of Sr or Na to the melt changes the shape of the eutectic Si from acicular to fibrous, which enhances the mechanical properties[48]. However, the modification process tends to increase the amount of porosity**.**

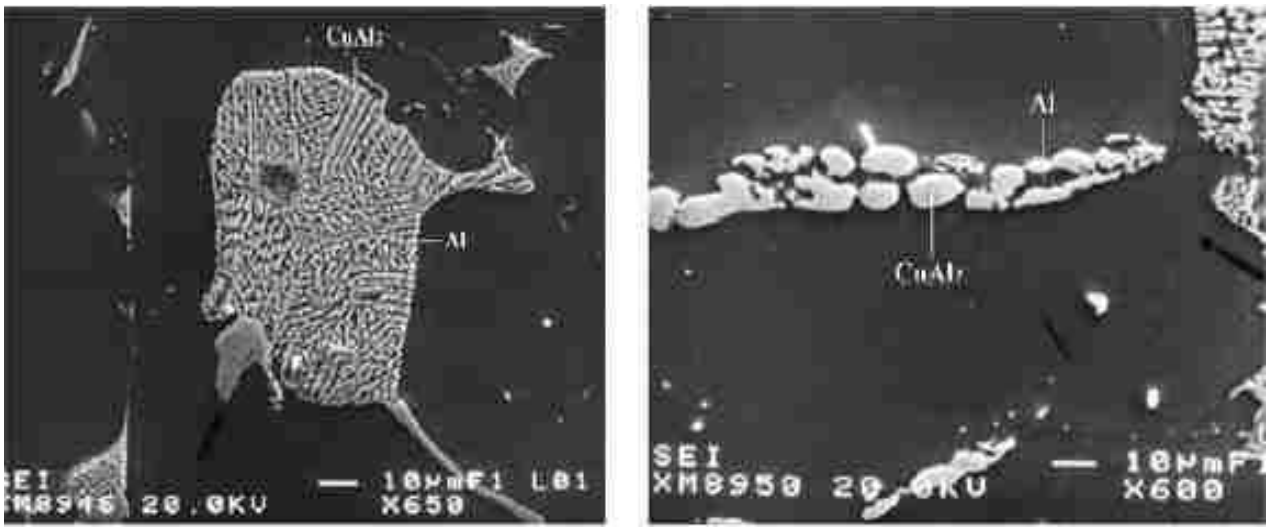

(a) (b)

Figure 2-19 Back scattered images of: (a) eutectic Al-Al_2Cu, (b) blocky Al_2Cu [43]

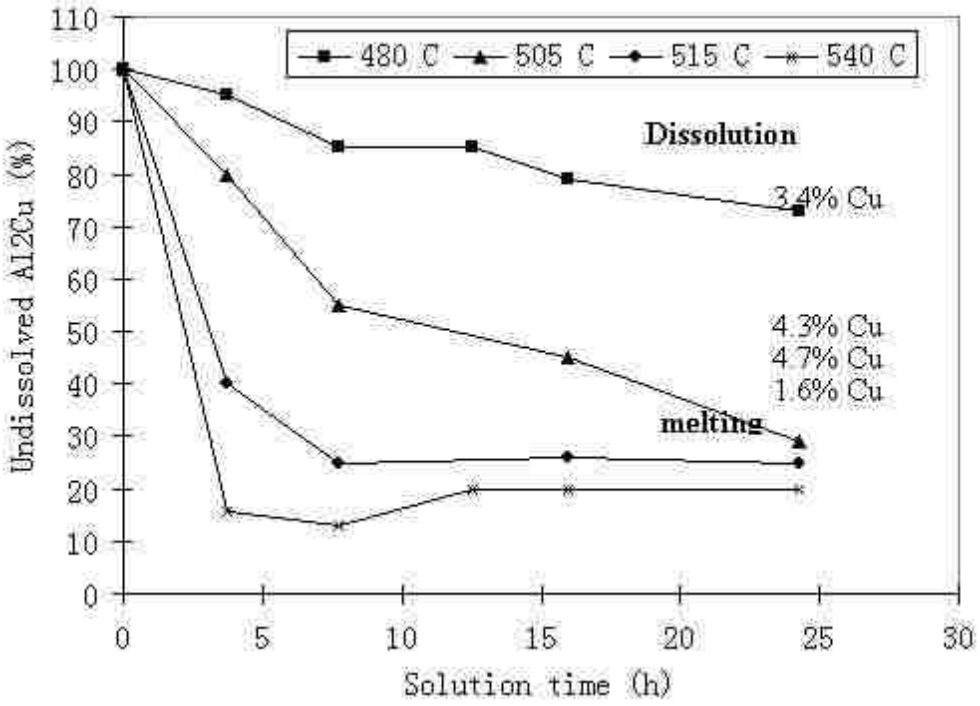

Figure 2-20 Variation in the percentage of undissolved Al_2Cu as a function of solution time in the temperature range 480ºC to 540ºC[43]

The effect of porosity is not always detrimental to the tensile properties of casting, but instead depends upon the base properties of the alloy, in particular, the inherent ductility of the matrix material [38]. Porosity levels of 2% or 3% would often not be significant within the normal variations observed in the tensile properties of a casting. It was also observed that large changes in pore size had a small effect on the tensile properties [49].

2.10 Summary

Currently, there are very few publications in the open literature which discussed the welding of high pressure die cast aluminum and its alloys by using either MIG or TIG methods. This survey reviewed recent progresses on fusion welding of cast aluminum alloys. The compilation of the primitive results could be used to assist in establishing baseline parameters for the use of aluminum as well as magnesium alloys in welding applications. Furthermore, a detailed overview of the welding process was provided, which is meant to serve as a guide for future research in the field. According to the tables and data that has been presented throughout this review, the following general statements regarding the welding process with respect to aluminum alloys have been concluded,

- Both MIG and TIG are gas shielded arc welding processes, the primary difference lies in the way the filler metal is added to produce the weld.
- Thermal treatments should be applied as a post-welding process to improve dimensional stability and relieve residual stress.
- The distribution and morphologies of eutectic Si have a greater influence on mechanical properties than DAS.
- Because of the higher cooling rate, the average diameter is much smaller in permanent mold than in sand cast specimens.
- Porosity levels of 2% or 3% would often not be significant within the normal variations observed in the tensile properties of a casting.
- Large changes in pore size had a small effect on the tensile properties

CHAPTER 3.

EXPERIMENTAL PROCEDURES

3.1 Materials

Two types of aluminum alloys, casting alloy A356 and wrought alloy 6061 were used in this study. The basic chemical compositions of alloys A356 and 6061 are shown in Tables 3-1 and 3-2. A356 alloy was high pressure die cast in a plate shape with the dimensions of 300 mm long, 100 mm wide and 4 mm thick provided by Ryobi Die Casting (USA), Inc. To facilitate the welding of the cast plate and the selected wrought alloy, commercially-available 4-mm thick 6061 was sectioned into rectangular plates with the same dimensions as the cast ones. It should be pointed out that the cast plates were also subjected to thermal treatments, i.e. Solution Treatment (T4: 2 hr at 470^{o}C), Aging (Stress-Relief) (T5: 2 hr at 200^{o}C), and Solution Treatment +Aging (T6).

Table 3-1 Chemical Composition of Cast alloy A356

Cast Alloy A356	**Chemical Composition (mass %)**
Copper	0.20 max
Magnesium	0.25 – 0.45
Manganese	0.10 max
Silicon	6.50-7.50
Iron	0.20 max
Zinc	0.10 max
Titanium	0.20 max

Table 3-2 Chemical Composition of Wrought alloy 6061

Wrought Alloy 6061	**Chemical Composition (mass %)**
Aluminum	Balance
Chromium	0.04 - 0.35
Copper	0.15 - 0.4
Iron	0 - 0.7
Magnesium	0.8 - 1.2
Manganese	0.15 max
Other	0.15 max
Remainder Each	0.05 max
Silicon	0.4 - 0.8
Titanium	0.15 max
Zinc	0.25 max

3.2 Gas Metal Arc Welding (GMAW)

A GMAW machine (Lincoln electric power wave 300 welder, Cleveland, Ohio, USA) with semi-automatic wire feeding system was employed for welding operation in Agreatsun Welding LTD. The applied filler metal was ER4303, of which chemical composition was given in Table 3-3. The shielding gas of Argon was applied during welding with a gas flow rate of 25 L/Min. The welding speed was set at 8.6 mm/s. The detailed process parameters of GMAW for welding the A356 and 6061 alloys are presented in Table 3-4. Before GMAW, the surfaces of the specimens were necessarily cleaned by brushing to remove surface oxide.

For the purpose of comparison, one representative combinations of the selected plates were welded, which were as-cast A356/ 6061, T4 A356/ 6061, T5A356/ 6061, T6 A356/ 6061 shown in Figure 3-1.

Table 3-3 Chemical Composition of Filler metal ER4043

Fillers	**Si**	**Fe**	**Cu**	**Mn**	**Mg**	**Zn**	**Cr**	**Ti**	**Al**
ER4043 (wt %)	5.0	0.8	0.3	0.05	0.05	0.1	-	0.2	Balance

Table 3-4 Process Parameters of GMAW

Welding Process	**Gas Metal Arc Welding (GMAW)**
Welding current	115-130A
Welding voltage	17.4-19V
Welding Speed	8.6mm/s
Shielding gas	Ar
Gas flow rate	20-25 L/Min
Filler metal	ER4043
Wire Diameter	1.2mm
Wire feed method	Semi-automatic
Wire feed rate	5.2 M/Min
Tip angle	80°

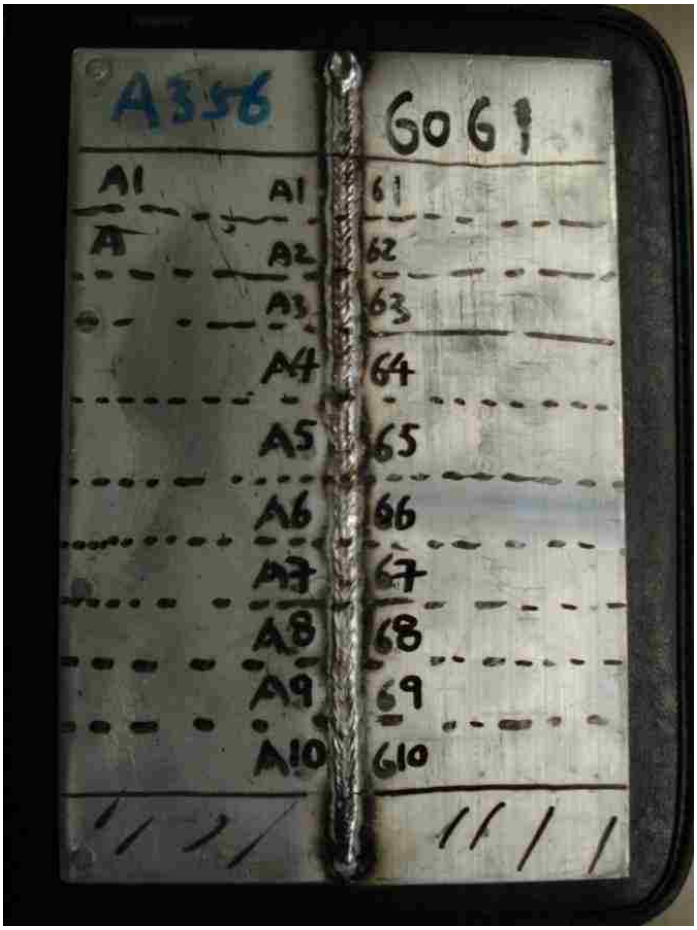

Figure 3-1 Representative welded pair of two plates of as-cast alloy A356 and Wrought Alloy 6061.

3.3 Tensile Testing

3.3.1 Specimens Preparation

The welded plates were marked perpendicularly along the welding bead. The marked plates as shown in Figure 3-2a, were sectioned to prepare specimens for testing and analyses. Ten specimens were cut from each pair of the welded plates. Five specimens were used for tensile testing while the other five specimens were kept for microstructural analysis (Figure 3-2 b).

In addition, specimens cut from unwelded part of the plate away from the welding bead were also tensile tested and analyzed for establishment of a property baseline. Figure 3-3 schematically shows the geometry and dimensions of the tensile specimen used in this study.

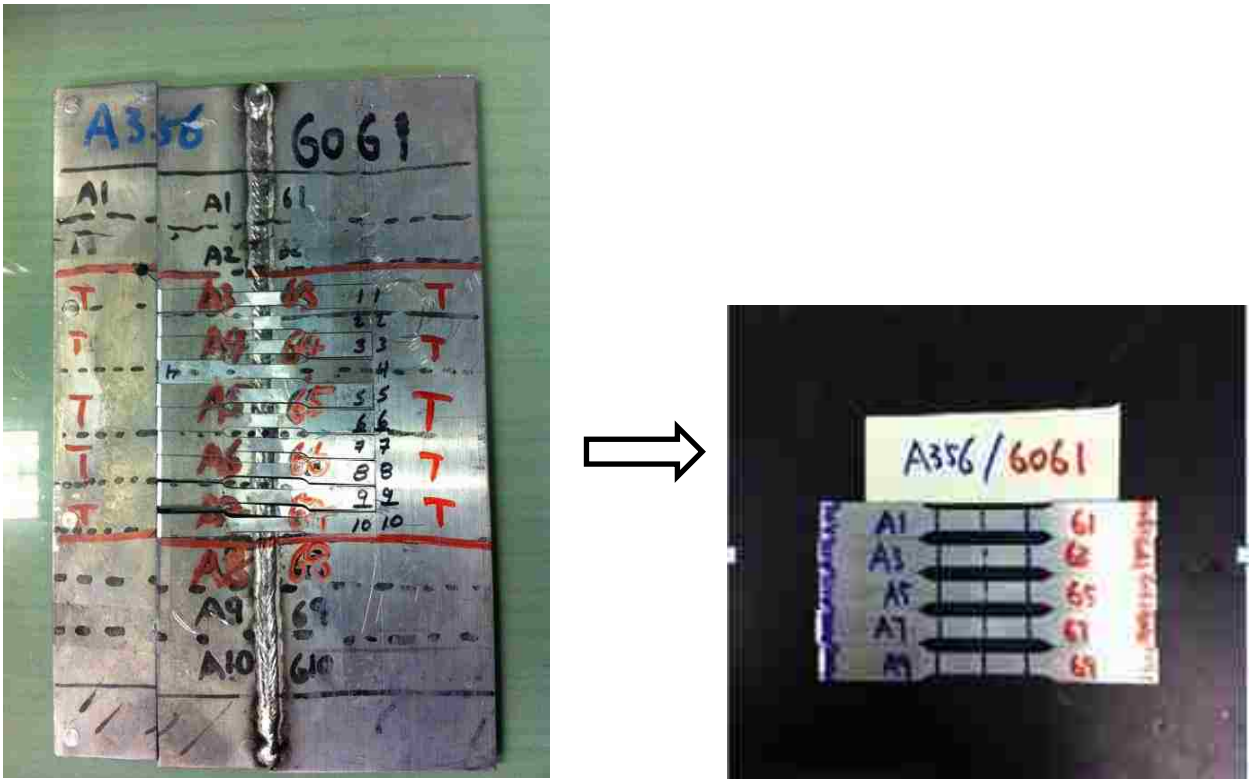

(a) (b)

Figure 3-2. (a) Representative welded plates and (b) cutted specimens which joined cast alloy A356 to wrought alloy 6061.

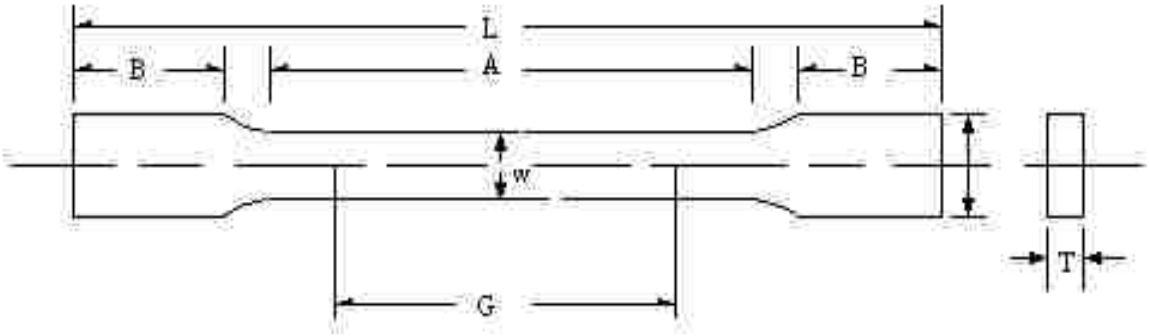

Figure 3-3 Schematic illustration of Tensile Test Specimen

G – Gage length: 25.0 ± 0.1 mm W – Width: 6 ± 0.1 mm

T – Thickness: 3 ± 0.1mm R – Radius of fillet, min: 6 mm

L – Overall length, min: 100mm A – Length of reduced section: 32 mm

B – Length of grip section, min: 30 mm C – Width of grip section: 10 mm

3.3.2 Tensile Testing

According to the ASTM standard B557M, subsize tensile specimens were prepared. The samples were tested at room temperature on an Instron 30KN Materials Test System equipped with a data acquisition system (Figure 3-4). The load cell and test speed were set up at 10KN and 2 mm/min. The output data, including the displacement measured by extensometer, and tensile load, were analyzed. The ultimate tensile strength (UTS), 2% offset yield strength (YS) and elongation (Ef%) were determined for tested welded samples. The machined specimens were tensile tested to fracture at room temperature.

Figure 3-4 Instron Tensile Test Machine (Model 8562).

3.4 Microstructural Analysis

3.4.1 Specimen Preparation

Samples for metallographic observation were prepared following the conventional preparation procedure. Following steps were carried out for sample preparation for microstructural analysis:

1. Samples were cut into rectangular shape;
2. Mounted with DIALLYL PHTHALATE (Mounting powder);
3. Polished with emery paper (to 600 grades);
4. Fine polishes using 1 µm gamma alumina powder; and
5. Etched with 0.5% HF acid solution. Performed by submerging the sample into the etchant for 20/25 seconds for optical microscope and about 40 seconds for SEM, rinsing with water and finally cleaned with ethanol specimen surface with running water and ethanol.

3.4.2 Metallographic Analysis

Microstructural characteristics of prepared specimens were examined using an optical microscope with a Buehler optical image analyzer (model 2002) and a SEM (JEOL Model JSM – 5800 LV) shown in Figures 3-5 and 3-6 respectively.

Figure 3-5 BUEHLER Optical Image Analyzer Model 2002.

The microstructure of prepared welded and unwelded specimens was analyzed by an optical and image analysis technique to assess the significant microstructural changes that occurred during welding. The Buehler optical image analyzer 2002 system (Figure 3-5) was used to determine structural characteristics of silicon particles as well as to observe the porosity severity in the associated samples. The observation fields were selected randomly. At least 10 fields were analyzed from a single specimen in each location. The dendrite arm spacing, porosity size, silicon morphology as well as its distribution was observed. Grain size and porosity size were measured by using IMAGE TOOL for Windows software (Version 3.00).

A JSM-5800 scanning electron microscope (SEM) was employed (Figure 3-6) with a maximum resolution of 200nm in a backscattered mode / 2µm in X-Ray diffraction mapping mode for

elemental analysis in a particular phase. Both higher and lower magnification was used to analyze different phases as well as to characterize the microstructure of specimens. Eutectic particles were also analyzed by using higher magnification to observe their morphology at different heat treating condition.

Fracture surface of tensile specimens were also analysed by the SEM to ascertain the fracture surface, different significant scenario (gas porosity when they exist, shape of eutectic silicon and primary dendrites) as well as to observe the nature of fracture mechanism.

Figure 3-6 Scanning Electron Microscope (JEOL Model JSM – 580).

CHAPTER4.

RESULTS AND DISCUSSION

4.1. Tensile Properties

4.1.1 Based Alloys and Filler Metal (ER 4043)

To compare the mechanical properties between the base metal and filler alloy, the ultimate tensile strength(UTS), 2% offset yield strength(YS) and elongation(E_f) of unwelded samples were determined first.

4.1.1.1 6061 Wrought Alloy

Based on the size of the aluminum plate, five base tensile test specimens were cut from 6061 samples. Figure 4-1 shows the representative engineering stress-strain curves of 6061 wrought alloy specimens with no heat treatment. Table 4-1 shows the corresponding strength and elongation of the specimens. It can be seen that the ultimate tensile strength (UTS), yield strength (YS) and elongation (E_f) are 217.5±6.8 MPa, 116.10±1.5 MPa and 16.18±1.3%.

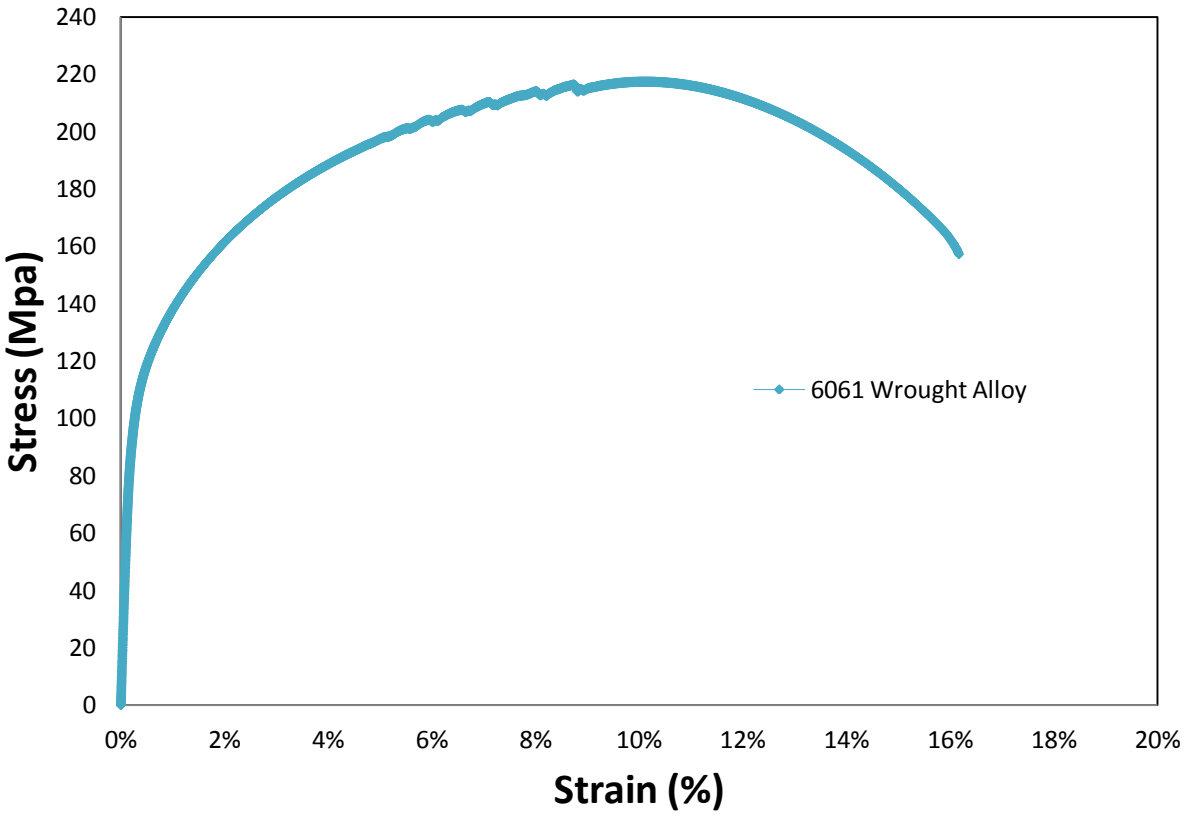

Figure 4-1 Representative engineering stress-strain curves for 6061 wrought alloy.

Table 4- 1 Tensile properties of 6061wrought alloy

Specimens ID	Ultimate Tensile Strength (MPa)	Yield Strength (Offset 0.2%) (MPa)	Elongation (%)
Wrought alloy 6061-1	213.9±3.2	118.6±4.1	14.50±1.2
Wrought alloy 6061-2	224.1±2.7	116.3±7.2	18.68±2.2
Wrought alloy 6061-3	208.6±5.9	113.5±4.3	16.43±1.3
Wrought alloy 6061-4	218.4±5.4	120.8±4.3	15.78±3.2
Wrought alloy 6061-5	217.5±6.8	116.1±1.5	16.18±1.3
Mean	**216.5±4.3**	**117.1±2.2**	**16.31±2.1**

4.1.1.2 As-cast Alloy A356

Figure 4-2 shows a typical engineering stress-strain curve of the as-cast alloy A356 without heat treatment. Table 4-2 shows the corresponding strength and elongation of the specimens. The average ultimate strength, yield strength and elongation of the as-cast alloy are 221.70±2.3 MPa, 137.10±4.2 MPa and 11.13±1.3 %.

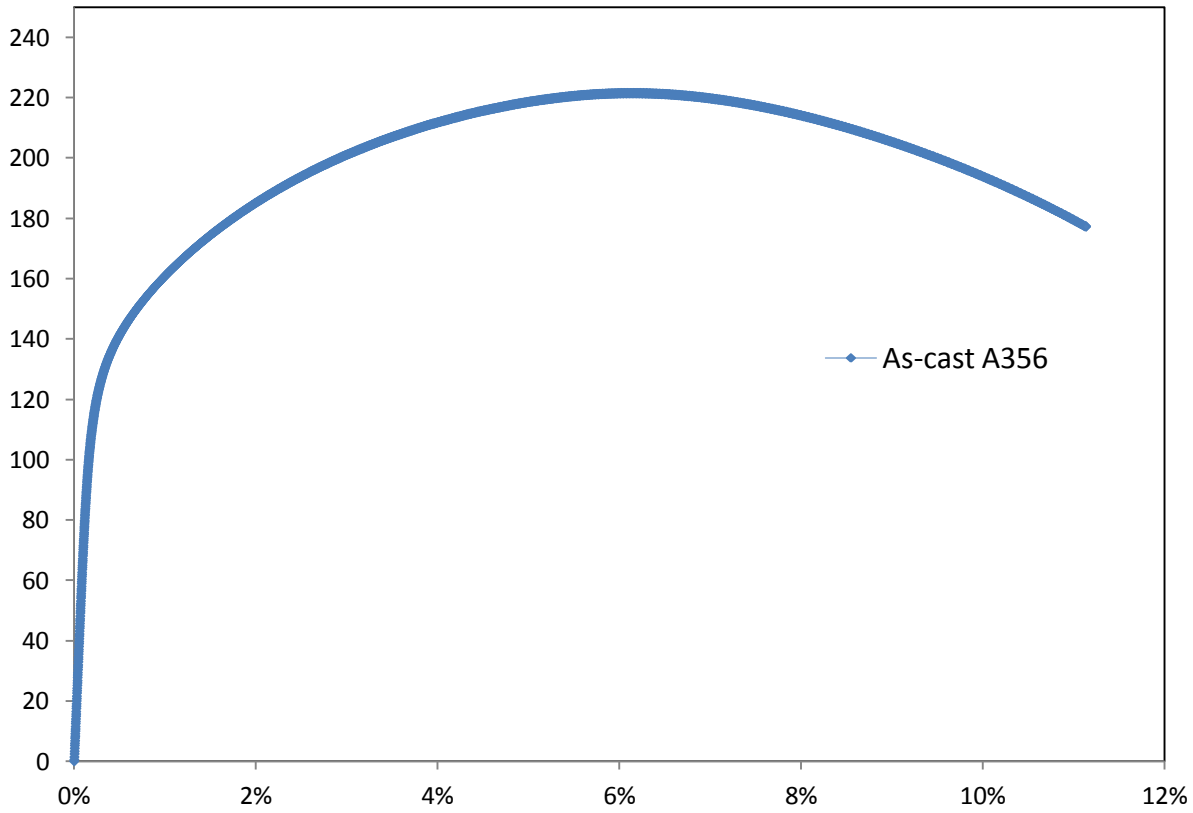

Figure 4-2 Representative engineering stress-strain curves for as-cast A356 alloy.

Table 4- 2 Tensile properties of as-cast A356 alloy

Specimen ID	Ultimate Tensile Strength (MPa)	Yield Strength (Offset 0.2%) (MPa)	Elongation (%)
As-cast A356-1	221.7±2.3	137.1±4.2	11.13±1.3
As-cast A356-1	224.3±3.4	133.0±3.2	6.15±2.6
As-cast A356-1	225.9±6.2	139.7±3.3	11.37±2.7
As-cast A356-1	211.1±5.2	140.1±6.1	10.39±2.2
As-cast A356-1	222.0±4.3	131.7±7.9	11.58±2.9
Mean	**221.0±3.6**	**136.3±7.2**	**10.12±3.3**

4.1.1.3 T4 Cast Alloy A356

The aluminum alloy A356 was treated under T4 heat treatment scheme. Figure 4-3 shows a representative engineering stress-strain curve of T4-A356 cast alloy. Table 4-3 shows the corresponding strength and elongation of the five tested specimens, and their averages. The T4 A356 exhibits the average of UTS of 169.90±3.3 MPa, YS of 104.90±3.1 MPa and E_f of 9.48±2.2 %.

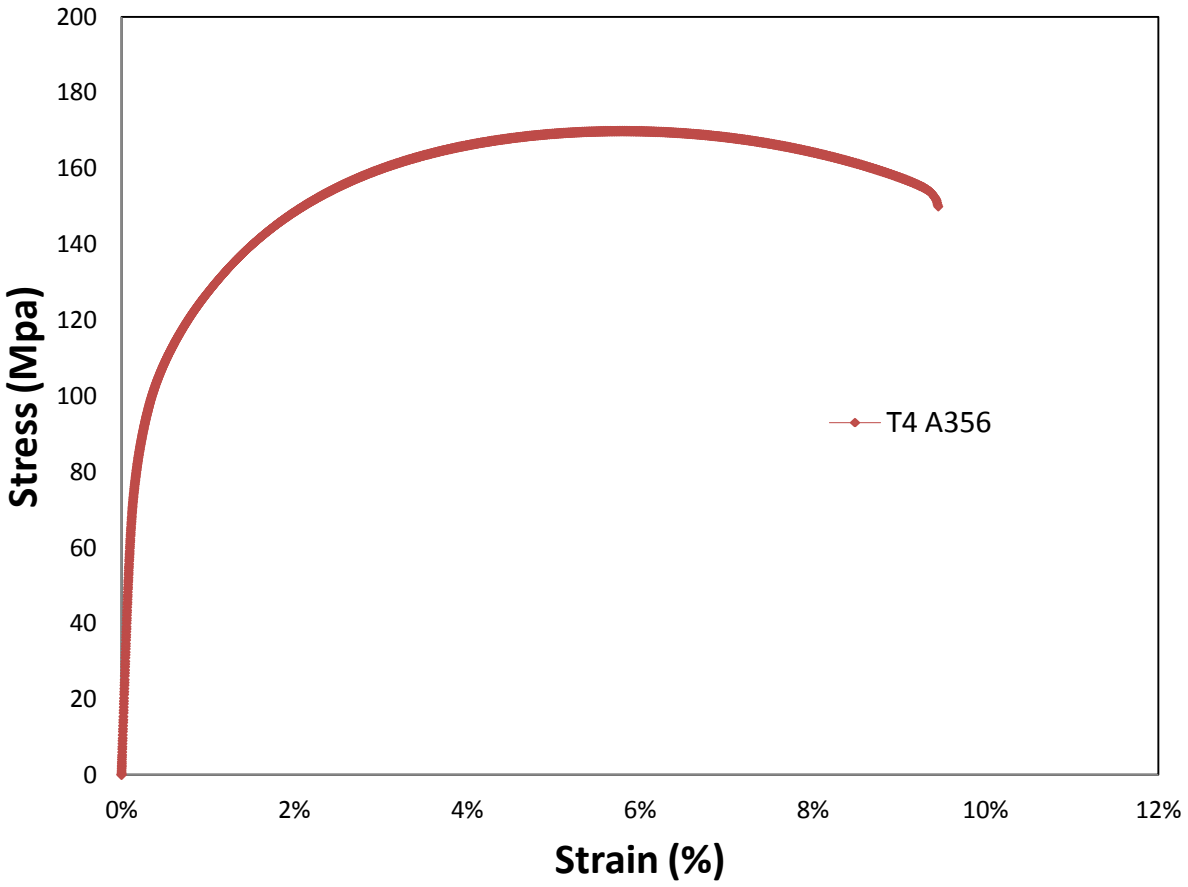

Figure 4-3 Representative engineering stress-strain curves for T4 A356 cast alloy.

Table 4- 3 Tensile properties of T4 A356 cast alloy

Specimens ID	Ultimate Tensile Strength (MPa)	Yield Strength (Offset 0.2%) (MPa)	Elongation (%)
T4 A356-1	169.1±3.1	107.8±2.2	10.29±1.3
T4 A356-2	169.9±3.3	104.9±3.1	9.48±2.2
T4 A356-3	171.4±3.9	105.9±3.2	10.85±2.6
T4 A356-4	169.4±4.2	105.7±4.2	8.11±1.8
T4 A356-5	167.8±6.2	106.5±5.3	7.77±1.8
Mean	**169.5±2.1**	**106.2±4.0**	**9.30±2.1**

4.1.1.4 T5 Cast Alloy A356

The cast aluminum alloy A356 was also treated in T5 stress-relief treatment. Figure 4-4 shows the representative engineering stress-strain curves of T5 A356 cast alloy specimens. Table 4-4 shows the corresponding strength and elongation of the specimens. The UTS, YS and Ef for T5 A356 are 286.6±2.3 MPa, 140.1±2.3 MPa and 11.21±2.0%, respectively.

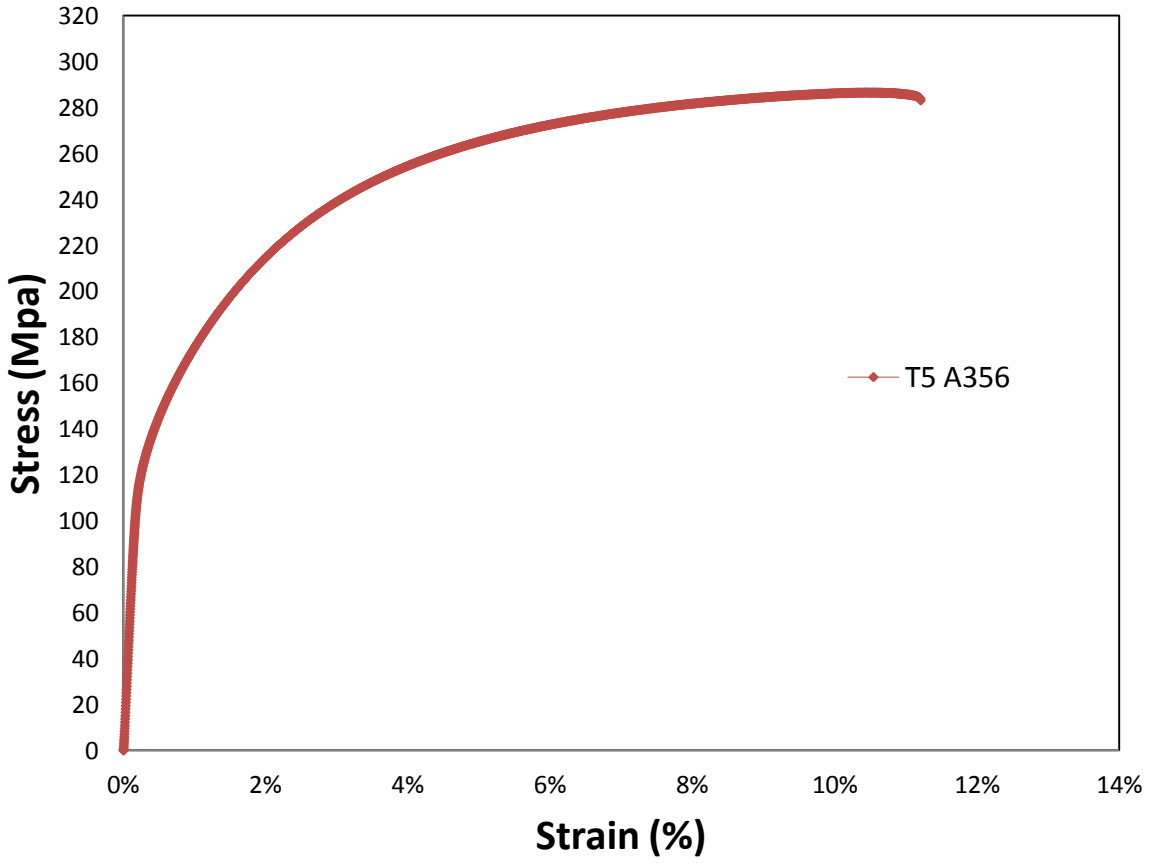

Figure 4-4 Representative engineering stress-strain curves for T5 A356 cast alloy.

Table 4- 4 Tensile properties of T5 A356 cast alloy

Specimens ID	Ultimate Tensile Strength (MPa)	Yield Strength (Offset 0.2%) (MPa)	Elongation (%)
T5 A356-1	302.4±3.2	143.3±1.3	15.49±1.3
T5 A356-2	286.6±2.3	140.1±2.3	11.21±2.0
T5 A356-3	279.7±3.9	130.7±3.3	9.53±3.4
T5 A356-4	278.3±4.8	136.2±4.2	11.05±2.3
T5 A356-5	269.9±6.4	132.8±6.1	9.64±2.4
Mean	**283.4±2.4**	**136.6±6.2**	**11.38±2.0**

4.1.1.5 T6 Cast Alloy A356

The cast aluminum alloy A356 was also treated in T6 heat treatment. Figure 4-5 shows the representative engineering stress-strain curve of T6 A356 cast alloy specimens. Table 4-5 shows the corresponding strength and elongation of the specimens. The tested results show that the UTS, YS and E_f are 191.20±1.9 MPa, 107.40±5.3 MPa and 9.82±2.3 %.

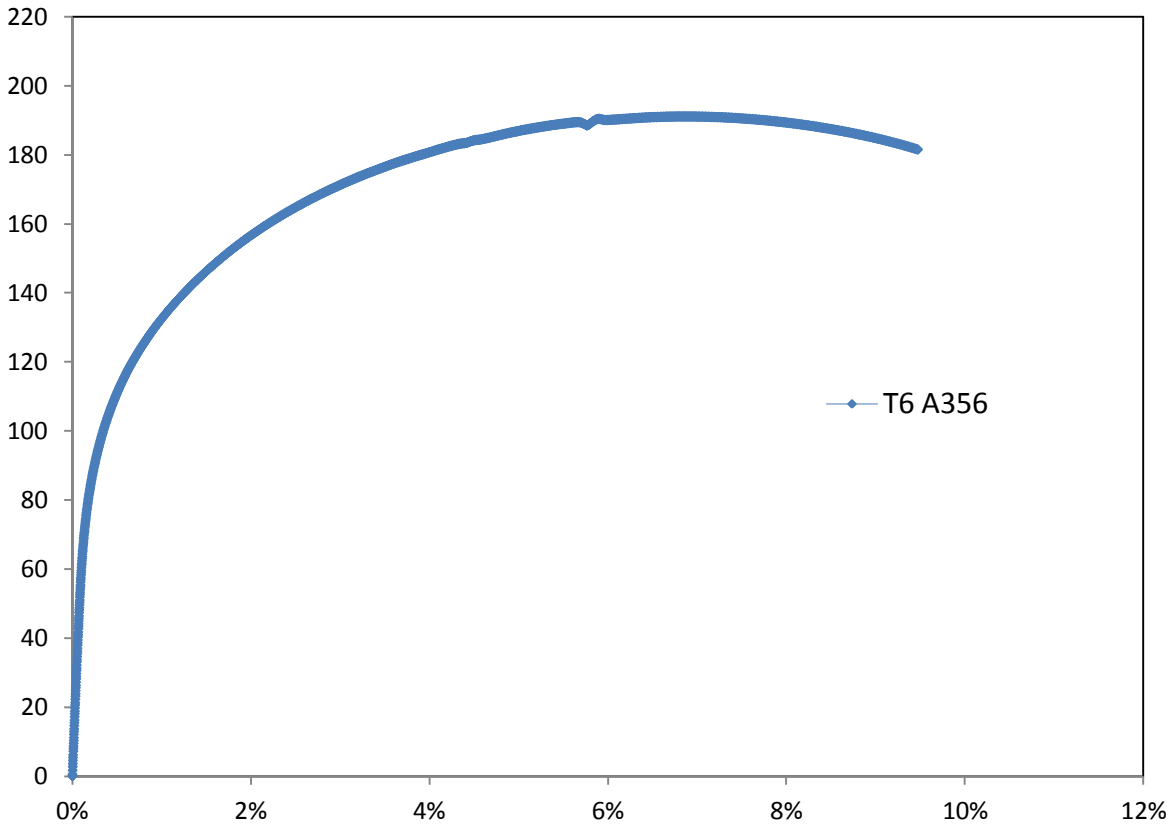

Figure 4-5 Representative engineering stress-strain curves for T6 A356 cast alloy.

Table 4- 5 Tensile properties of T6 A356 cast alloy

Specimens ID	Ultimate Tensile Strength (MPa)	Yield Strength (Offset 0.2%) (MPa)	Elongation (%)
T6 A356-1	129.8±3.2	109.4±6.3	1.28±1.2
T6 A356-2	191.2±1.9	107.4±5.3	9.82±2.3
T6 A356-3	189.1±1.6	111.0±6.1	10.08±2.0
T6 A356-4	188.1±2.3	106.3±2.9	9.93±1.5
T6 A356-5	193.0±2.6	110.4±4.8	10.38±3.1
Mean	**191.7±2.7**	**108.9±3.9**	**9.30±2.1**

4.1.1.6 Filler Alloy (ER 4043)

The tensile property of filler alloy 4043 was obtained in the following table. Table 4-4 shows the corresponding strength and elongation of the filler alloy.

Table 4- 6 Mechanical property of Filler alloy 4043[20]

Types of Filler Alloy	Tensile strength (MPa)	Yield strength (0.2% offset)	Elongation, %
ER 4043	285±3.5	270±2.3	22±1.6

Based on the tested mechanical properties of 6061 wrought, as-cast, T4 A356, T5 A356, T6 A356 cast alloy and filler alloy 4043, the best mechanical properties was obtain from both Filler Metal ER4043 and T5 A356 cast alloy, which the highest Ultimate Tensile Strength (UTS) and 0.2% Yield Strength (YS) were around 285 MPa, and 170 MPa for the filler alloy and 137 MPa for T5 A356; and the highest elongation value was 22% from the filler metal ER4043.

4.1.2 Joined Cast alloy A356 with Wrought alloy 6061

Joining cast A356 aluminum alloys with a wrought aluminum alloy 6061 was divided into 3 experiments. Different types of heat treatments (T4, T5 and T6) were applied to A356 casting alloy to show their effect on mechanical properties and weldability, comparing to the 6061 wrought alloy and filler metal (ER4043). Table 4.7 summarize the results of fracture location for joined A356/6061.

Table 4- 7 Fracture location of joined A356/6061

Joined Part (A356/6061)	Fracture Location
As-cast A356/ 6061	6061
T4-A356/6061	T4-A356
T5-A356/6061	6061
T6-A356/6061	T6-A356

4.1.2.1 As-cast A356& 6061 Wrought Alloy

For joining the A356 and 6061, the first trial for the casting process and heat treatment was focused on the as-cast A356/6061 system. A typical engineering stress-strain comparison curve of welded as-cast A356/6061 is graphically depicted in Figure 4-6. Tensile properties and fracture location of A356 alloy with no heat treatment and wrought alloy 6061 are summarized in Tables 4-2, 4-2 and 4-7, respectively.

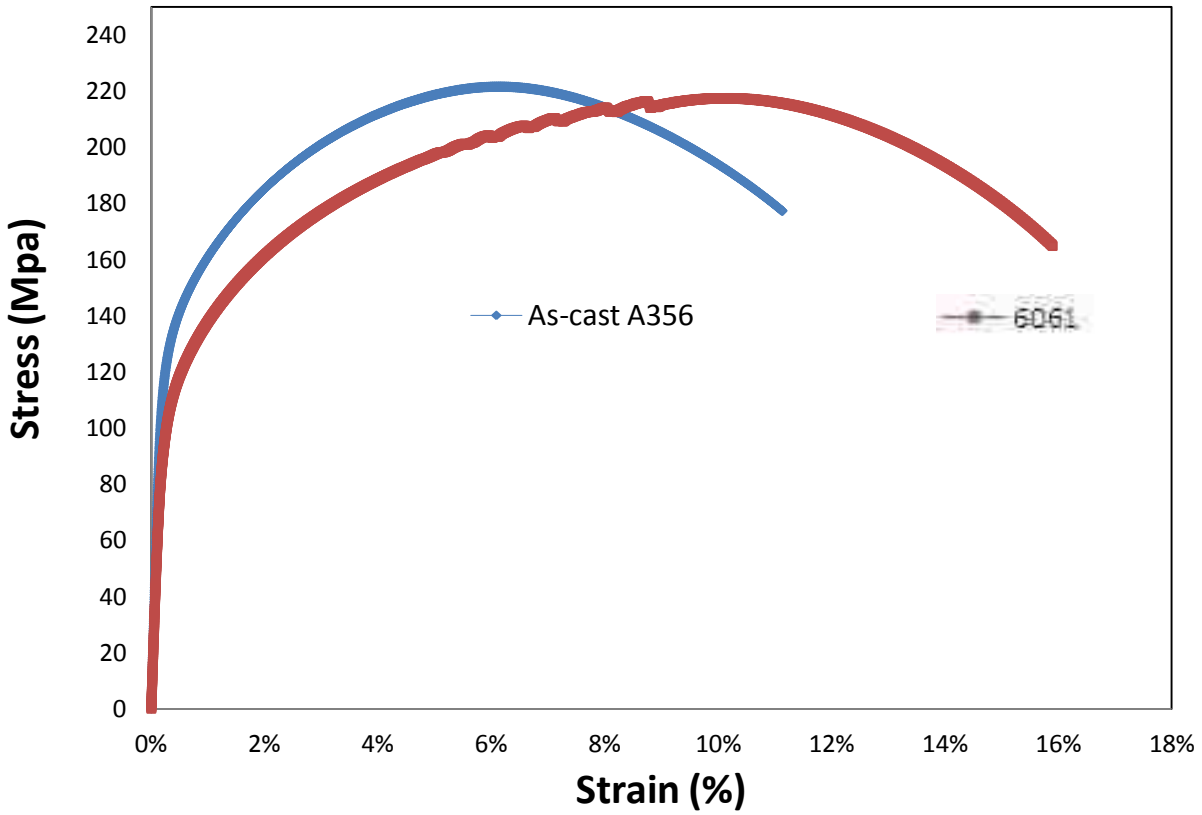

Figure 4-6 Typical Engineering stress-strain curve for welded as-cast A356/6061 alloys.

As listed in Table 4-2, as-cast A356 had the UTS, YS and elongation of 221.70 MPa, 137.1 MPa and 11.13%, respectively. They were higher than the 6061, of which the UTS, YS and elongation were 217.50 MPa, 116.1 MPa and 16.18% respectively (Table 4-1). As such, the fracture of the joined as castA356/6061 took place in 6061since the tensile properties of the 6061 were lower than both the as cast A356 and filler alloy (ER 4043).

4.1.2.2 T4 A356& 6061 Wrought Alloy

The second trial for the casting process and heat treatment was focused on the T4 A356/6061 system. The representative engineering stress-strain curve of the joined T4-A356 and 6061 is showed in Figure 4-7.

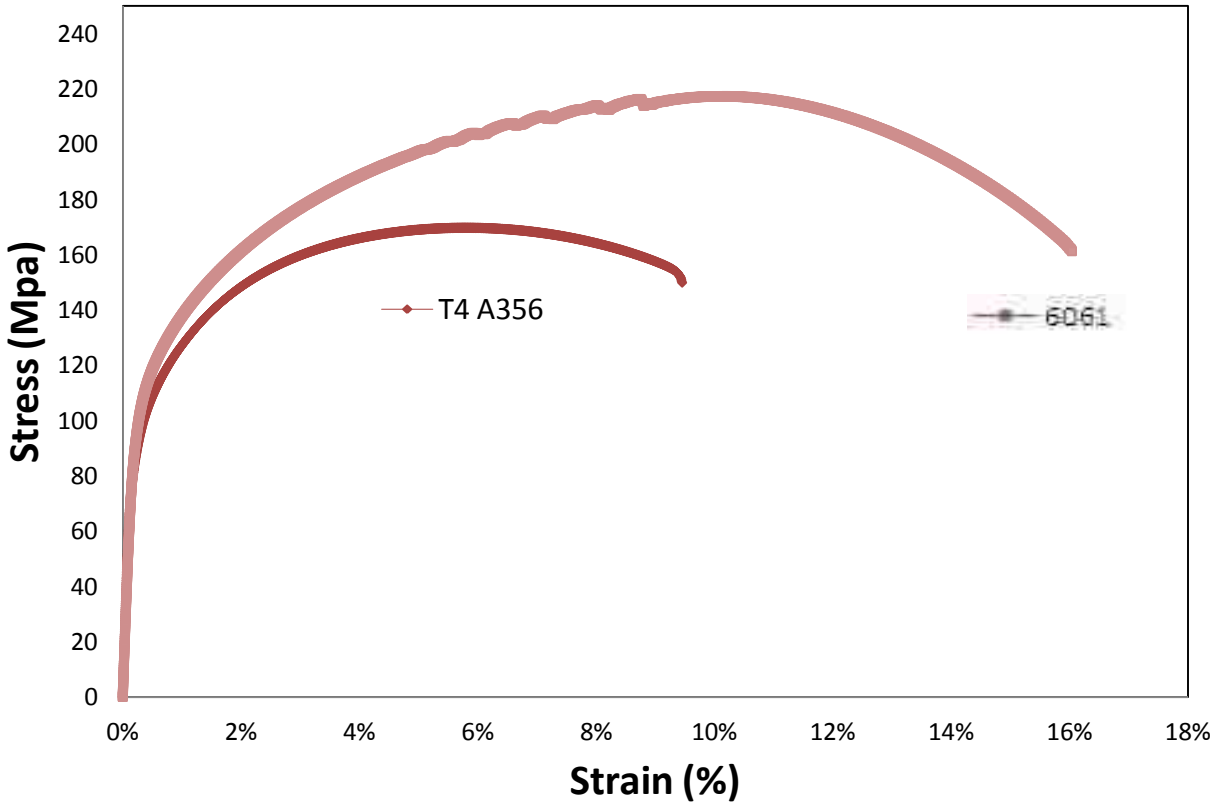

Figure 4-7 Typical engineering stress-strain curve for welded T4 A356/6061 alloys.

After the T4 heat treatment, both the ultimate tensile strength (UTS) and yield strength (YS) of A356 decreased and became lower than those of 6061 wrought alloy. From the table 4-3 and 4-1, average UTS and YS of T4 A356 were only maintained at 169.90 MPa and 104.90 MPa; and the elongation just changed to 9.48%, which was lower than those of the wrought alloy 6061 (UTS: 217.50 MPa, YS: 116.10 MPa and 16.18%).

4.1.2.3. T5 A356& 6061 Wrought Alloy

To understand the effect of T5 stress relief treatment on tensile properties of joined part, T5 A356 and 6061 were weld together. The representative engineering stress-strain curve of the welded T6 A356 and 6061 is shown in Figure 4-8.

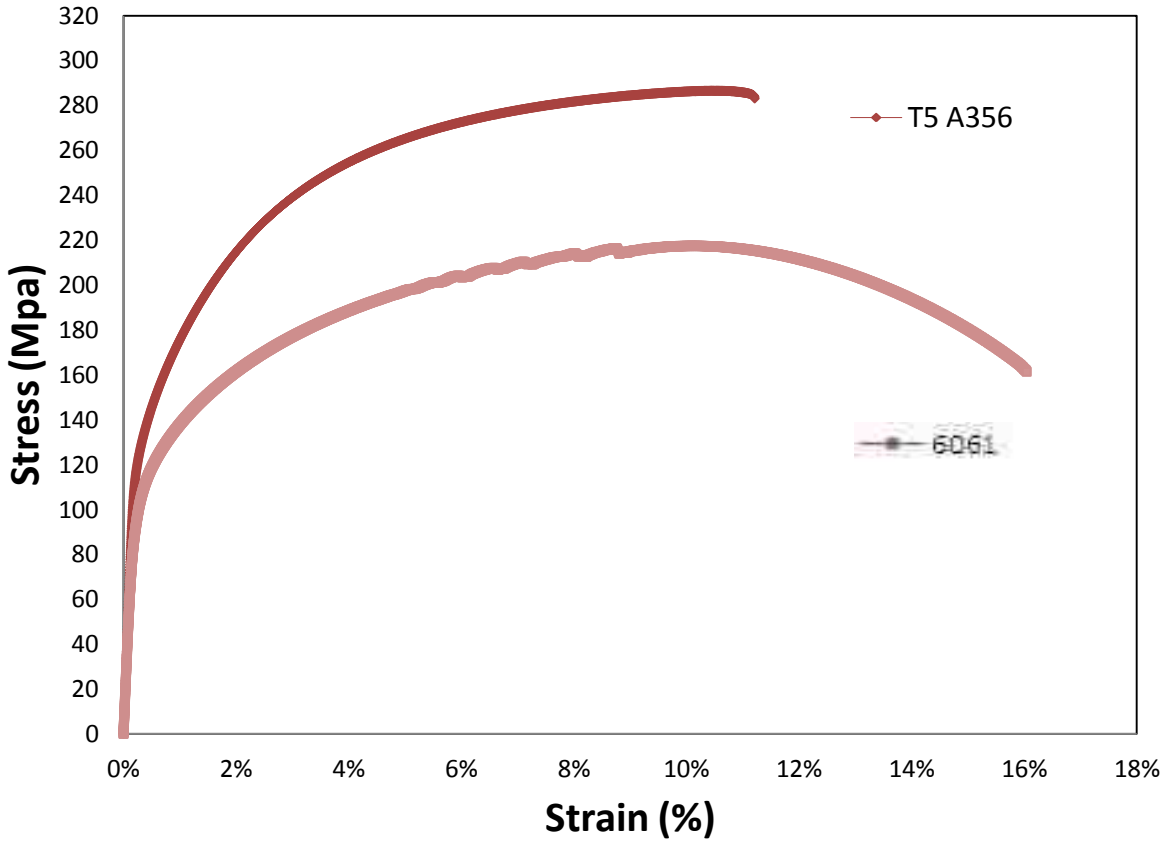

Figure 4-8 Typical engineering stress-strain curve for welded T5 A356/6061 alloys.

After joining T5 A356 cast alloy with 6061 wrought alloy, the ultimate tensile strength (UTS) and yield strength (YS) of T5 A356 were being improved as 286.60 MPa and 140.10 MPa (Table 4-4), and become higher than the wrought alloy 6061, which was the fracture location of welding samples. This is because the T5 A356 has stronger mechanical properties than both filler metal and 6061 wrought alloy.

4.1.2.4. T6 A356& 6061 Wrought Alloy

For the condition of T6 heat treatment on tensile properties of joined part, T6 A356 and 6061 were weld together. The representative engineering stress-strain curve of the welded T6 A356

and 6061 was shown in Figure 4-10. Tensile properties of the specimens are summarized in Table 4-5.

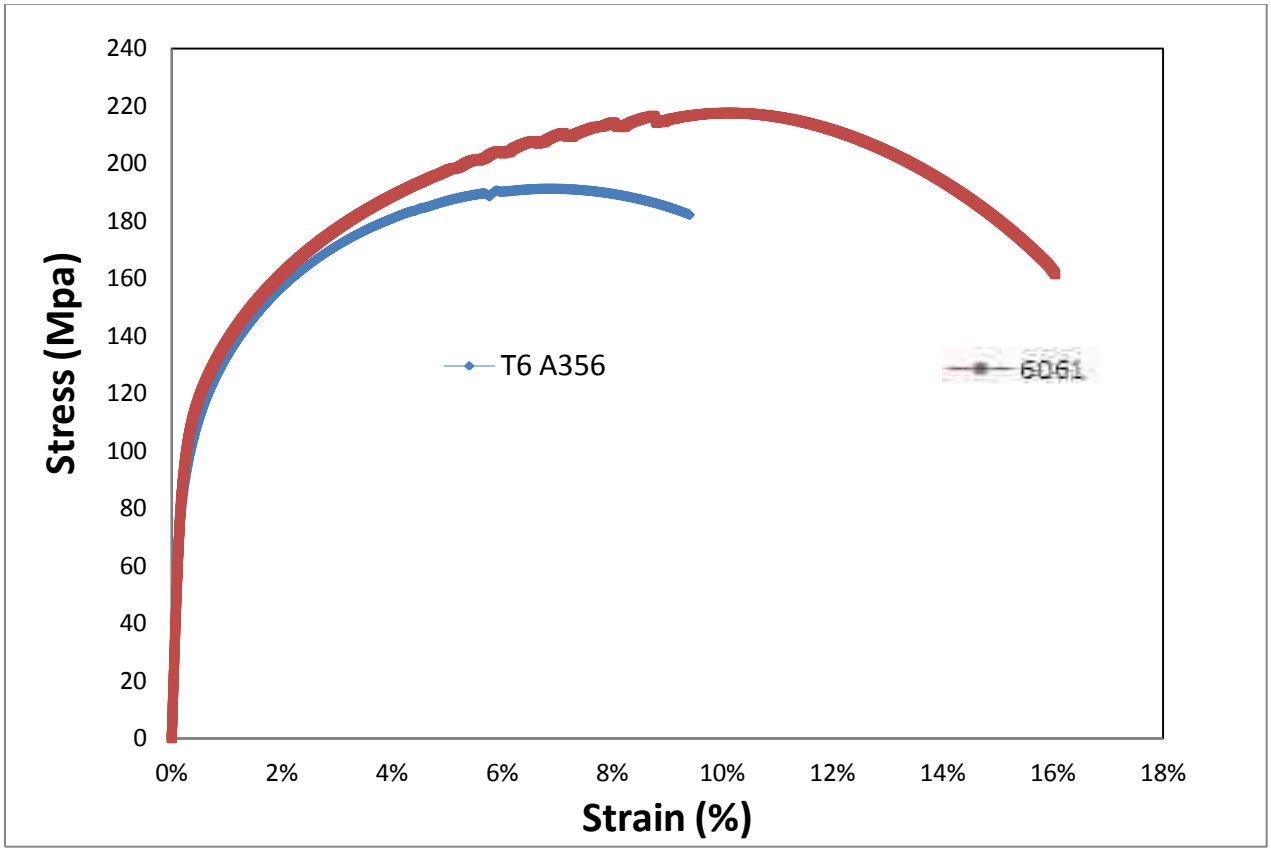

Figure 4-9 Typical engineering stress-strain curve for welding T6 A356/6061 alloys.

After joining T6 A356 cast alloy with 6061 wrought alloy, the ultimate tensile strength (UTS) and yield strength (YS) of T6 A356 were identified as 191.20 MPa and 107.40 MPa (Table 4-5), and became lower than the wrought alloy 6061. The fracture position was located on T6 A356. This is due to the fact that the T6 A356 cast alloy has the mechanical properties weaker than both filler metal ER4043 and wrought alloy 6061.

4.2. Microstructure

4.2.1. T4 A356 Alloy /Wrought Alloy 6061

For the T4 heat treatment system, the samples of T4 A356 cast alloy had the primary Al and the eutectic phase at the boundary of the primary Al dendrites. Figure 4-10 shows the microstructures of the joined T4 heat treatment A356 cast alloy revealing from the Base Metal, Heat Affected Zone (HAZ) to Fusion Zone, respectively. It has been reported that fine eutectic silicon along with fine primary aluminum grains improved mechanical properties [38].

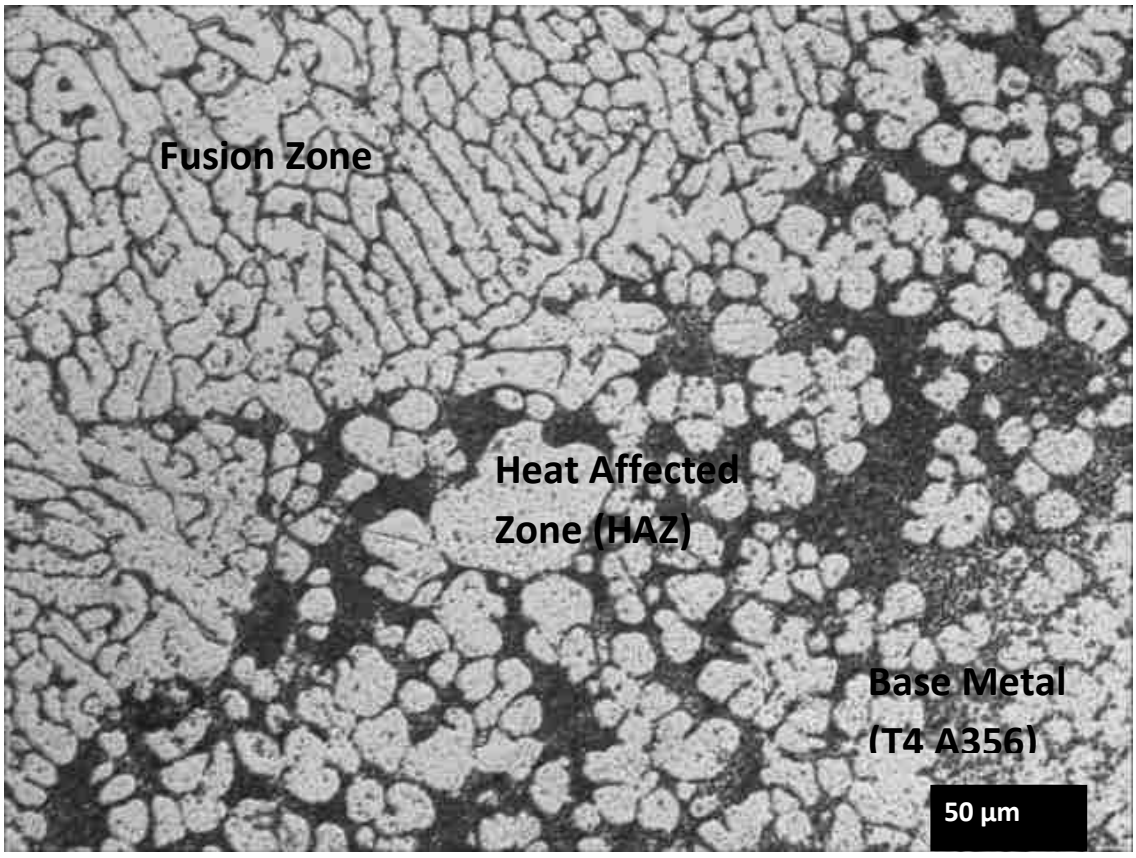

Figure 4-10 Optical Micrograph showing the Grain Structure of the Welded T4 A356 cast alloy with Filler Metal ER 4043.

Comparing the dendrite arm spacing (DAS) and silicon particles from three effected zones (Figure 4-11), there is an increasing trend in DAS from Fusion Zone, Heat Affected Zone (HAZ) to Base Metal. Accordingly, there were 74.98% and 157.02% increments from 10.87 microns to 19.02 and 27.17 microns. The improvement in the tensile properties should be attributed to the fine grain structure of thin specimen.

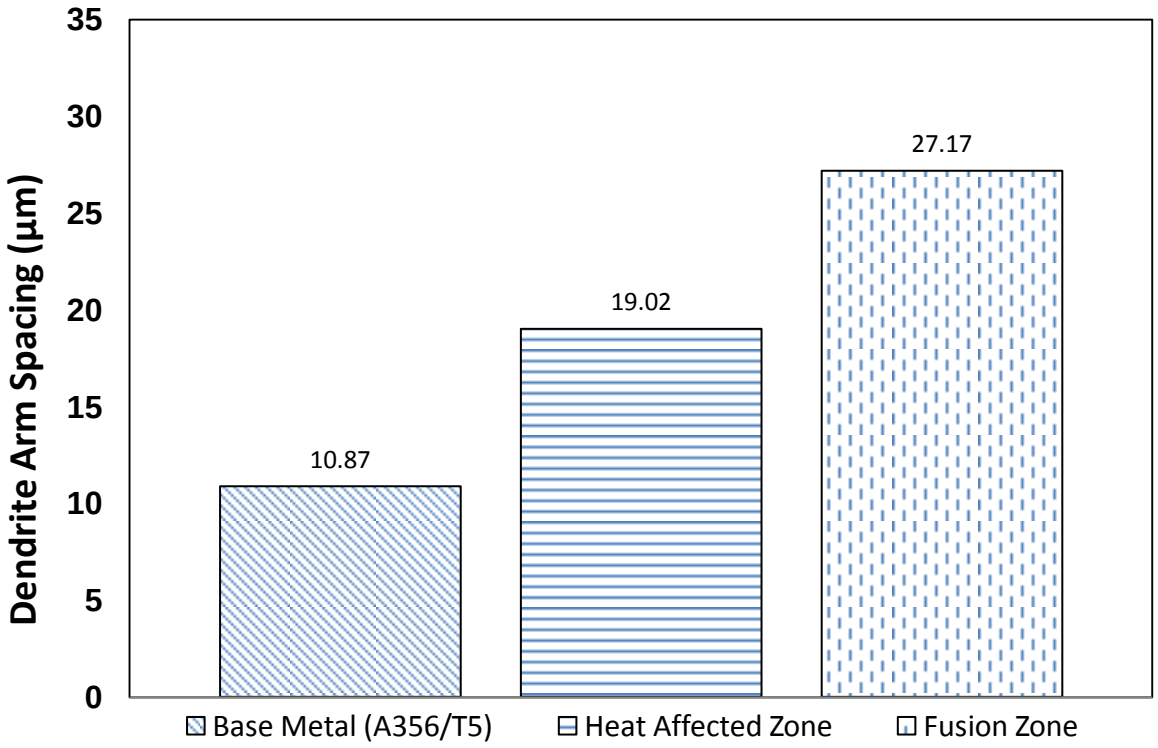

Figure 4-11 Dendrite arm spacing in Fusion Zone, Heat Affected Zone and Base Alloy (A356).

Figures 4-12 and 4-13 show the presence of phases in the A356 alloy after T4 heat treatment. SEM and EDS analyses on the specimens treated at T4 thermal treatment schemes indicated that, no Mg_2Si, a strengthening intermetallic phase, was detected, despite that it was found in the as-cast A356 in the previous study [36]. The microstructure observation suggested that the dissolution of the Mg_2Si might take place during the solution treatment. As a result, the strengths of the T4 A356 alloy were reduced.

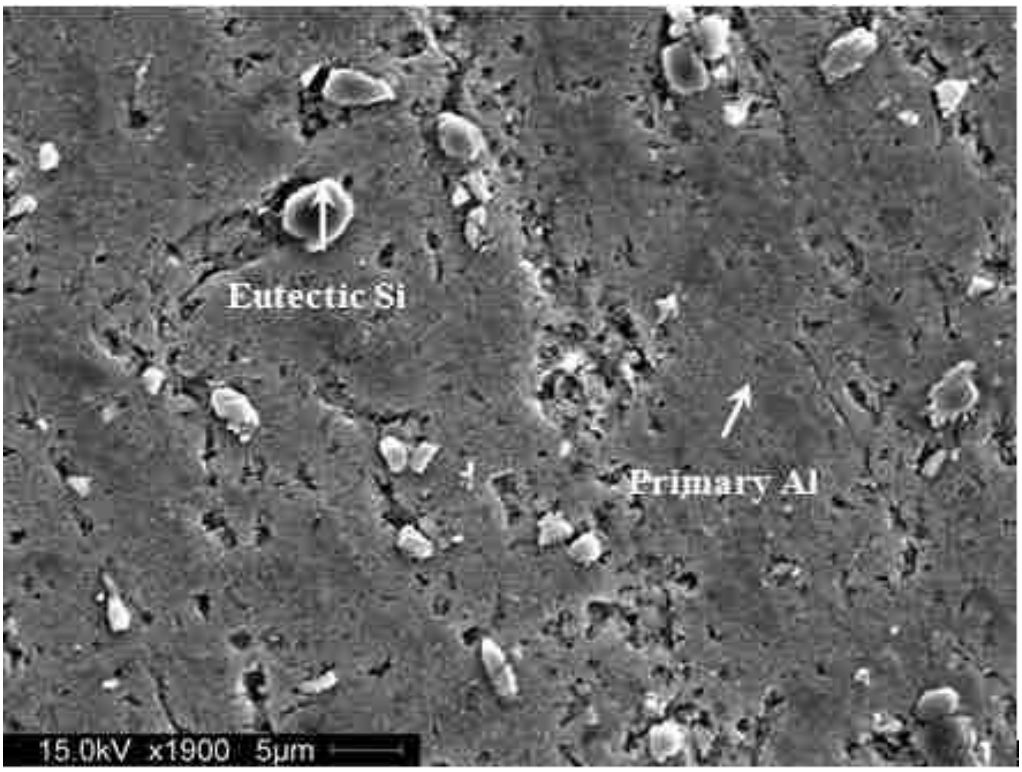

Figure 4-12 SEM Micrograph showing phases present in the T4 Cast Alloy in the joined part.

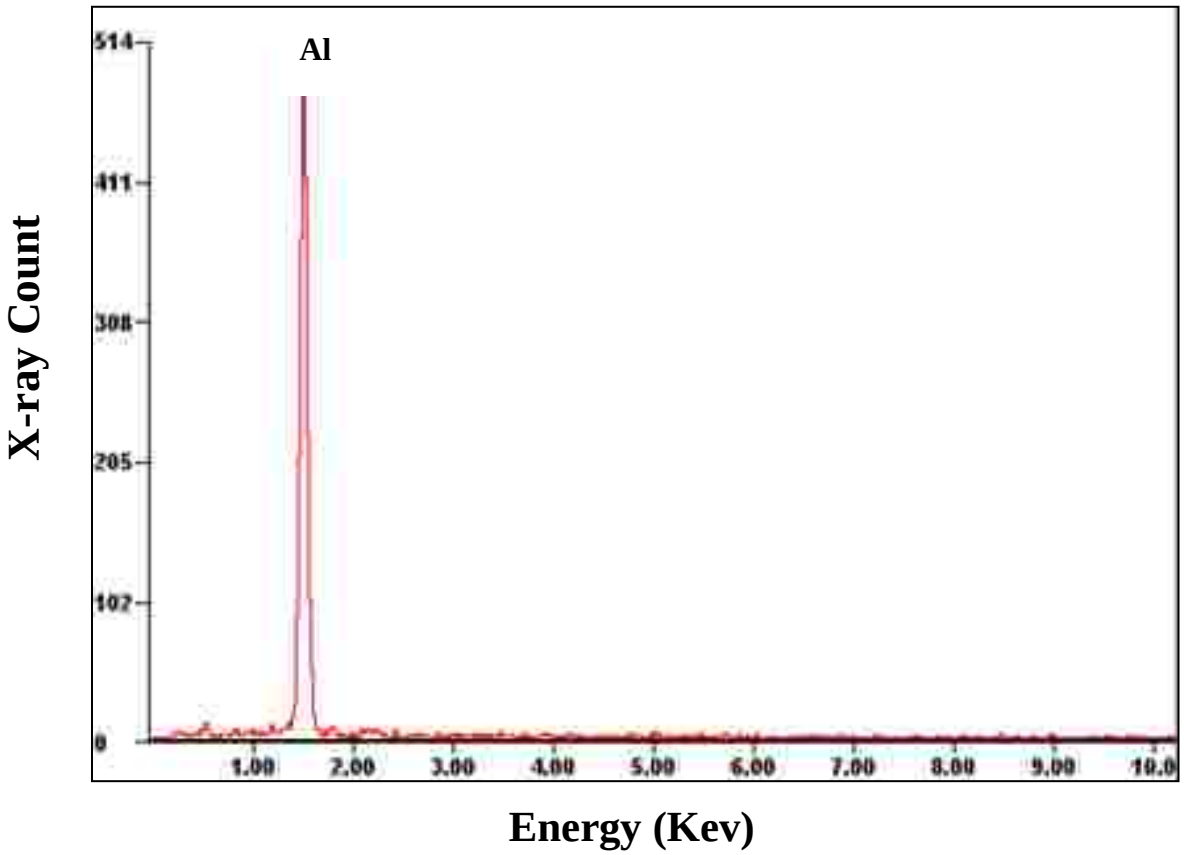

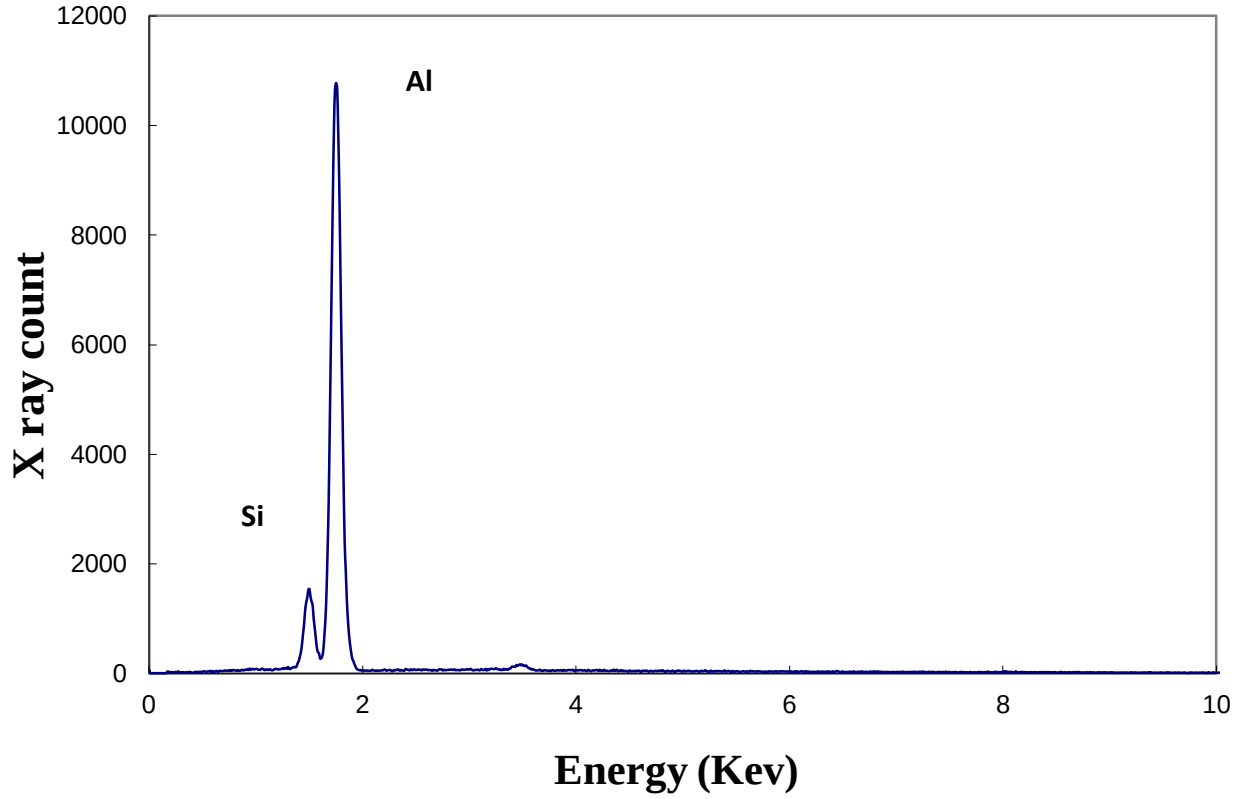

(b)

Figure 4-13 EDS spectra for identified phases, (a) primary Al and (b) eutectic Si.

For joined T4 A356 cast alloy system with wrought alloy 6061 by using the filler metal (ER 4043), the microstructural comparison among Base metal, HAZ and fusion zone was attempted. It has been reported [37] that the magnesium containing intermetallic significantly influenced the mechanical properties of the alloy. Since Mg could form intermetallic phases with Si, Mg-phases in A356 would precipitate in forms of Mg_2Si. But under T4 heat treatment condition, the Mg_2Si was dissolved, which would cause the strength reduction in A356 cast alloy. In addition, the DAS and silicon particle in the fusion zone (ER4043) were finer than those base metal, which resulted in an increase in strengths of the fusion zone of the filler alloy (4043). As a result, the fracture occurred in the T4 A356, which had lower strengths.

4.2.2. T5 A356 Alloy/Wrought Alloy 6061

After the T5 heat treatment, the samples of T5 A356 cast alloy had not only the primary Al and the eutectic phase at the boundary of the primary Al dendrites, but a Mg-containing intermetallics, Mg_2Si, precipitated in the matrix of cast A356 alloy. Figure 4-14 show the microstructures of the joined T5 heat treatment A356 cast alloy revealing from the Base Metal, Heat Affected Zone (HAZ) to Fusion Zone, respectively. As mentioned in the review, a fine eutectic silicon along with fine primary aluminum dendrites improved mechanical properties of aluminum alloys.

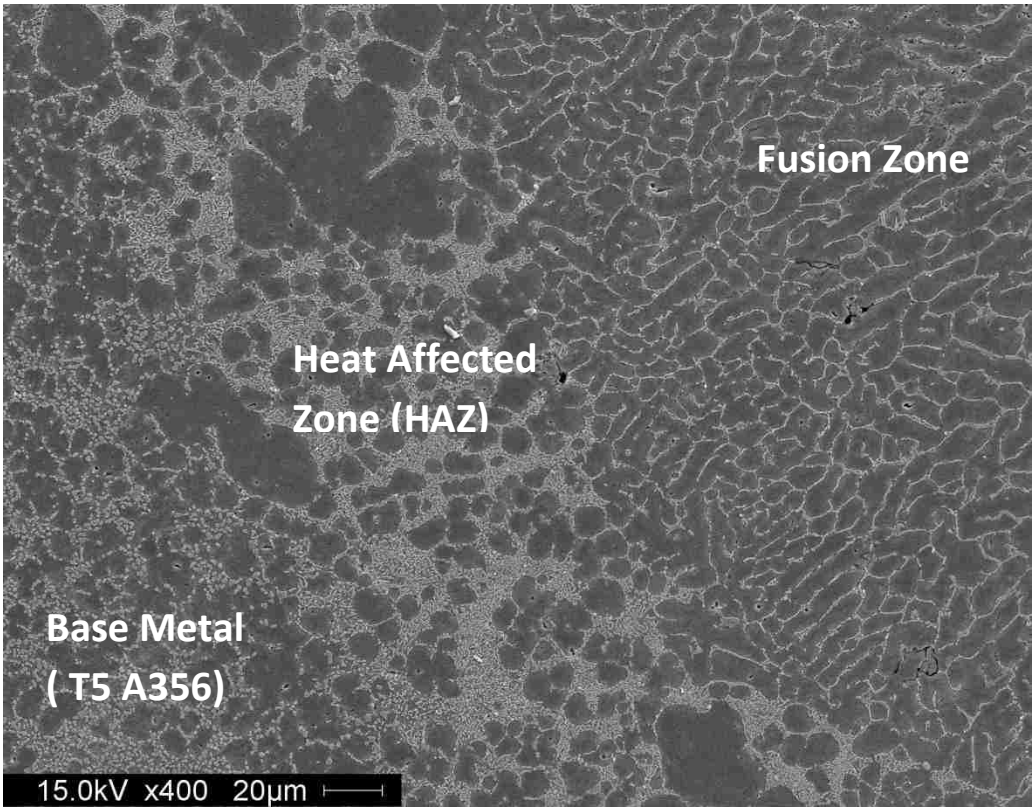

Figure 4-14 SEM micrograph showing the dendritic structure of the welded T5 A356 Cast alloy with Filler Metal ER 4043.

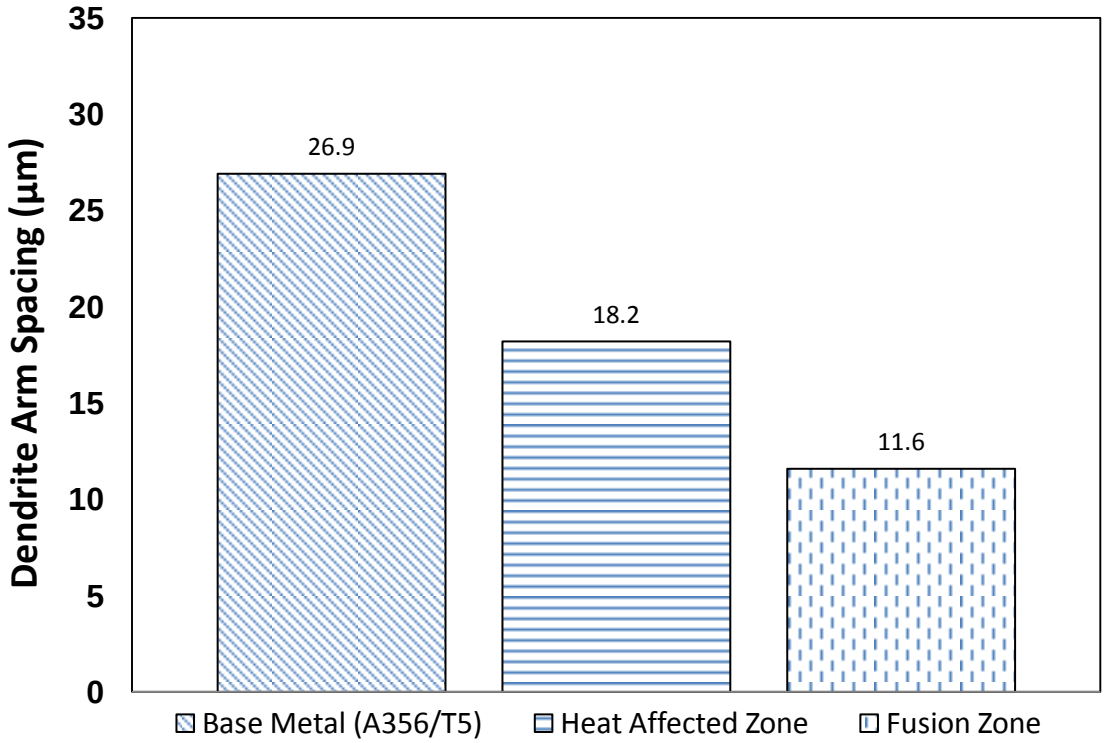

Figure 4-15 Dendrite arm spacing in Fusion Zone, Heat Affected Zone and Base alloy (A356) of welded T5 A356/6061.

Examination of the dendrite arm spacing in three zones revealed a decreasing trend of their sizes from Base Metal (A356), Heat Affected Zone (HAZ) to Fusion Zone as shown in Figure 4-15. Accordingly, there were 74.98% and 153.07% decrements from 26.9 microns to 18.2 and 11.6 microns. The improvement in the tensile properties should be attributed to the fine grain structure resulting from the rapid cooling during fusion welding.

Based on the SEM analyses, the DAS and silicon particle in the base metal (A356) and fusion zone were finer than those in 6061, which resulted in an increase in strengths of the fusion zone and base metal of the T5 cast alloy A356, compare to wrought alloy 6061. As a result, the fracture occurred in the 6061, which had lower strengths.

Figures 4-16 and 4-17 show the presence of phases in the A356 alloy after T5 heat treatment. SEM and EDS analyses on the specimens treated at T5 stress relief treatment schemes indicated that, a strengthening intermetallic phase, Mg_2Si, was observed for a successful stress relief treatment (T5). The study of Koch et al [36] on Silafont-36 alloy, also found that the magnesium content influenced the mechanical properties and aging behavior of the alloy. It is always necessary to have a strong bond among particles to matrix to contribute strengths in alloys by particles or intermetallic phases. Moreover, the shape, size and distribution of the intermetallic phases also have significant influence on the matrix in terms of strengths of the alloy. As a result, the strength improvement of the T5 A356 alloy should be attributed to the presence of the strengthening intermetallic phases.

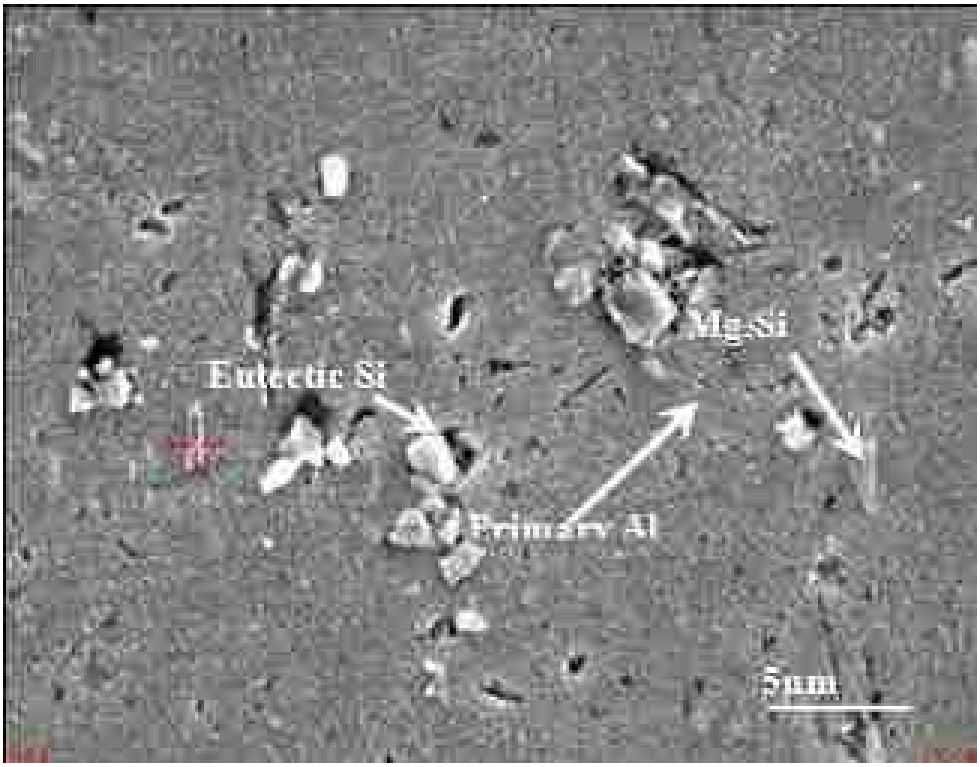

Figure 4-16 SEM Micrograph showing phases present in the T5 Cast alloy in joining part.

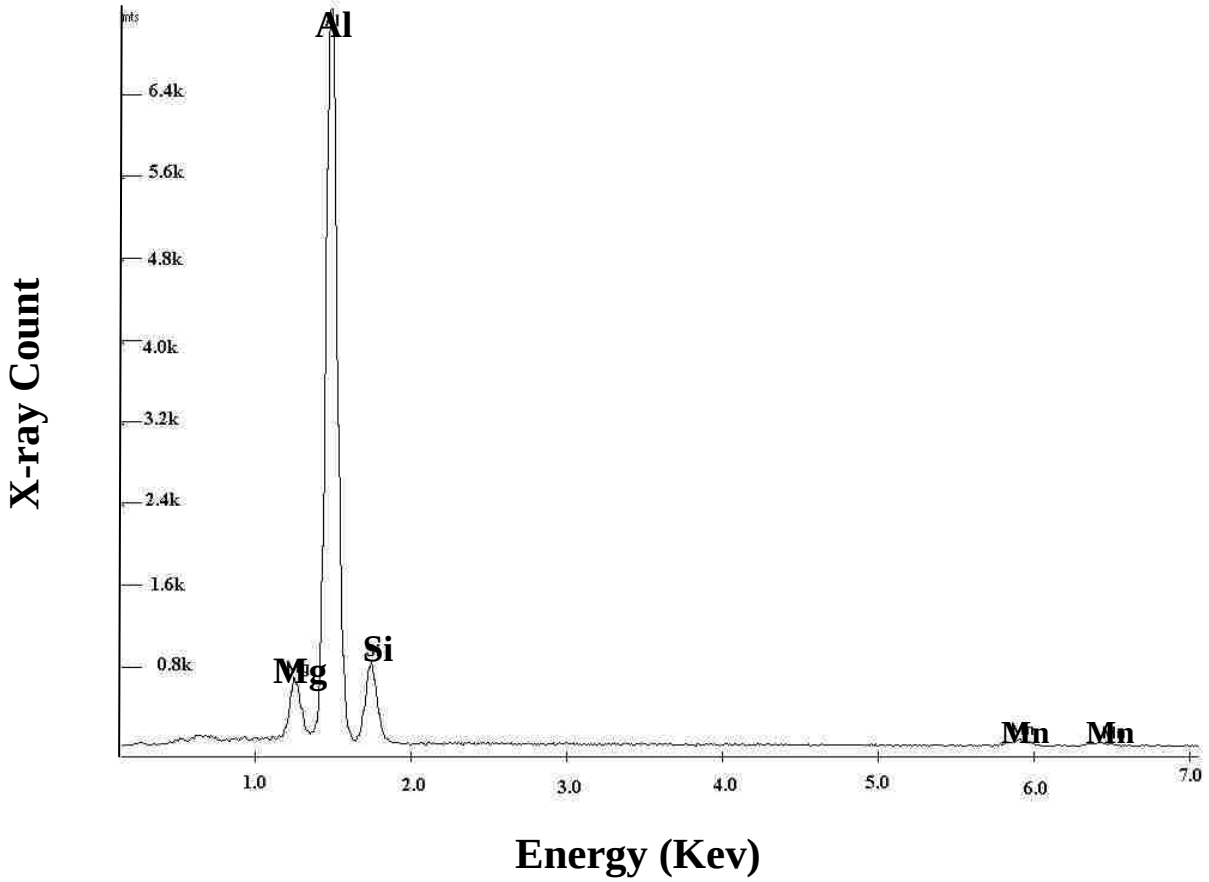

Figure 4-17 EDS analysis showing the elements contains in corresponding Mg-based phase

4.2.3. T6 A356 Alloy/Wrought Alloy 6061

After the T5 heat treatment, the A356 cast alloys under T6 heat treatment were joined together by using same Filler Metal (ER4043). Figure 4-18 shows the optical microstructures of the Base Metal, Heat Affected Zone (HAZ) to Fusion Zone for the joined T6 heat treatment A356 cast alloy with wrought alloy 6061.

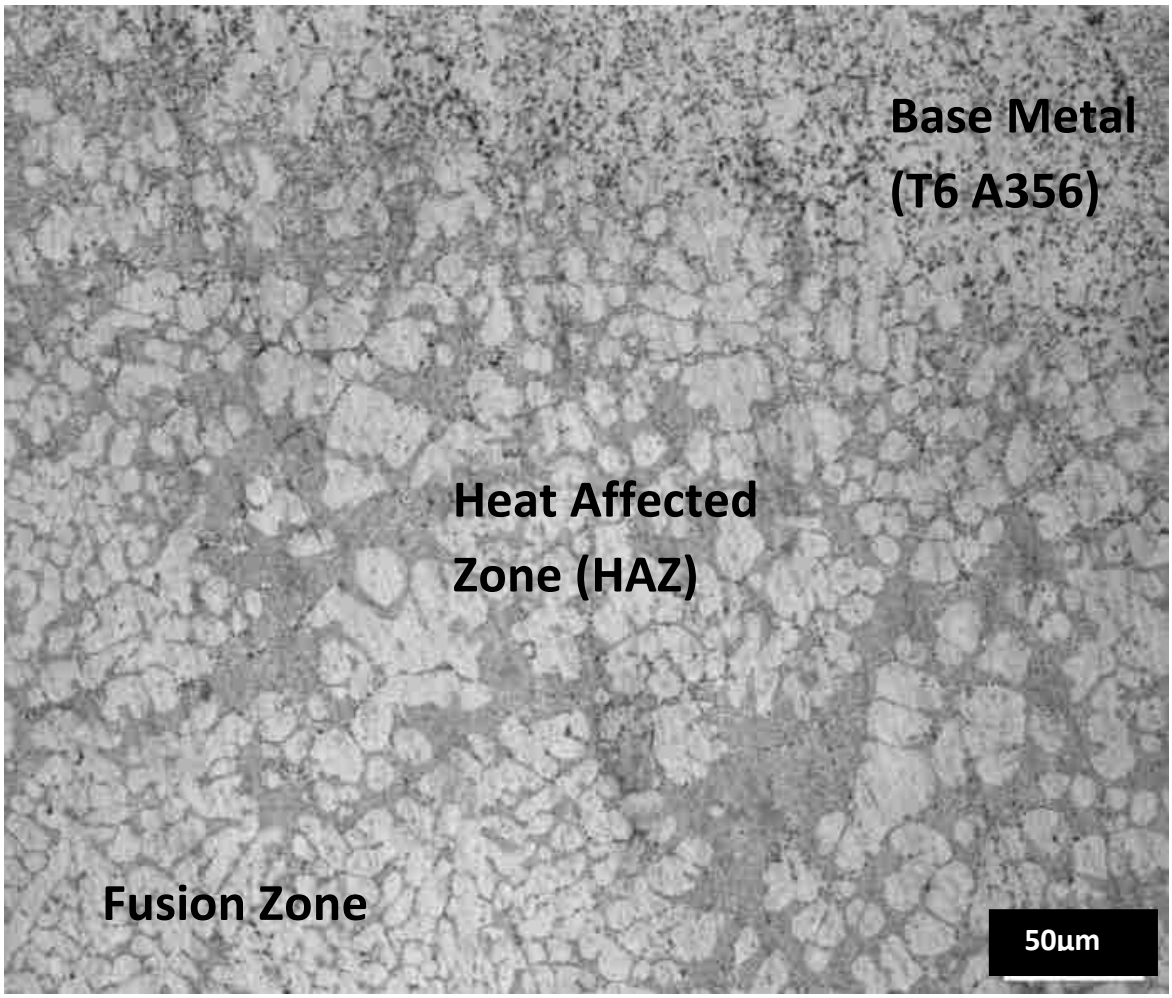

Figure 4-18 Optical micrographs showing the dendritic structure of welded T6 A356 cast alloy with filler metal ER 4043.

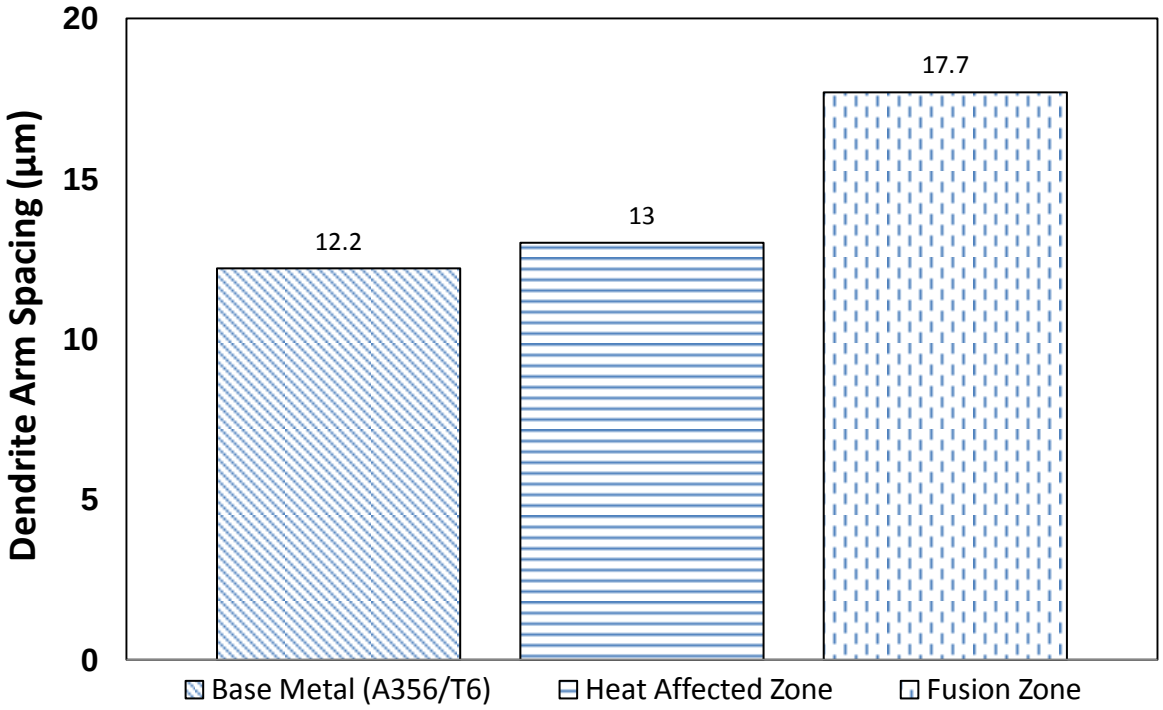

Figure 4-19 Dendrite arm spacing in Fusion zone, Heat affected zone and Base alloy (A356) of welded T6 A356/6061 alloys.

Examination of dendrites from three affected zones in Figure 4-19, revealed an increasing trend of dendrite size from Fusion Zone (12.2µm), Heat Affected Zone (13.0µm) to Base Metal (17.7µm). The improvement in the tensile properties should be attributed to the fine dendrite arm spacing structure of the HAZ and fusion zones. Also, based on the optical microstructural analyses, the dendrites and silicon particles in the fusion zone (ER4043) were finer than those base metal, which resulted in an increase in strengths of the fusion zone of the filler alloy ER 4043. As a result, the fracture occurred in the T6 A356, which had lower strengths.

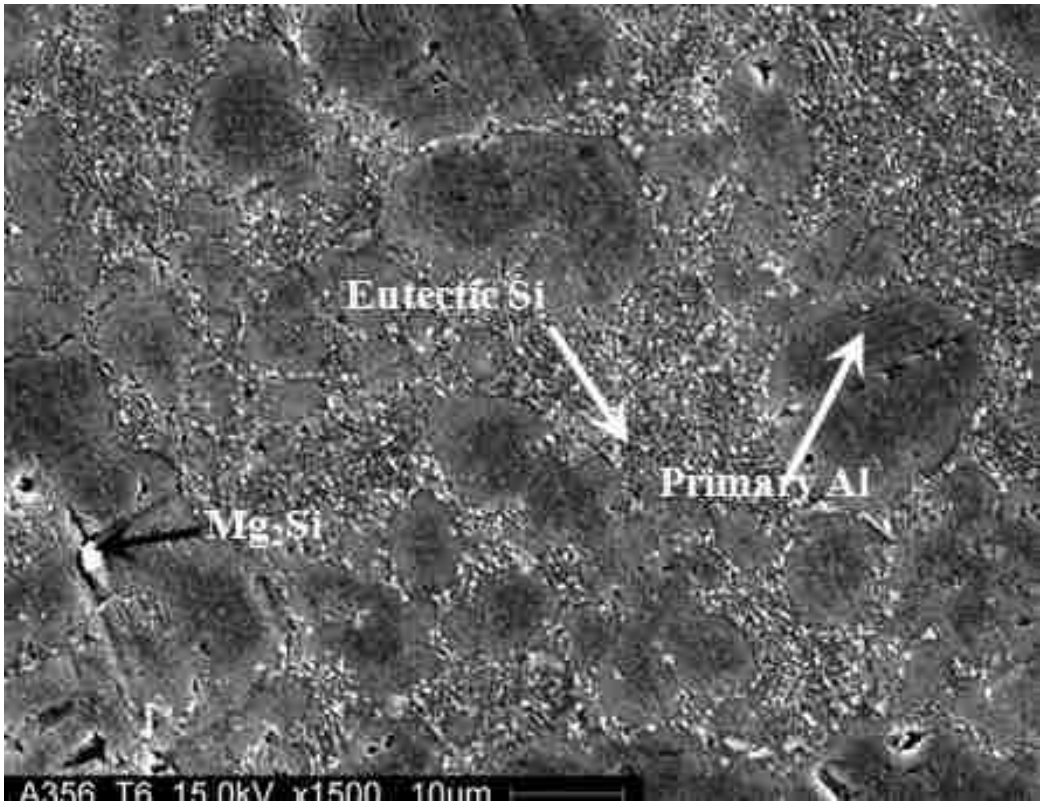

Figure 4-20 Micrograph showing phases present in the T6 A356

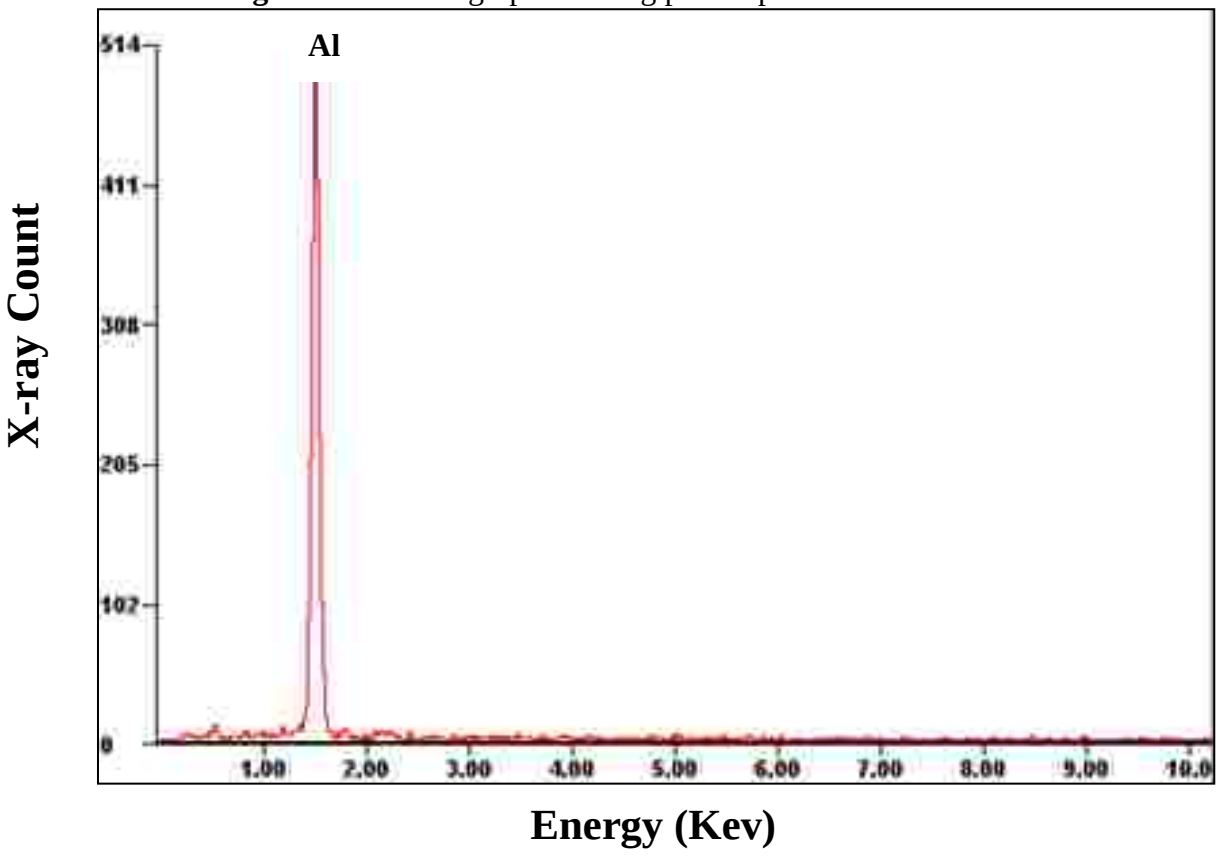

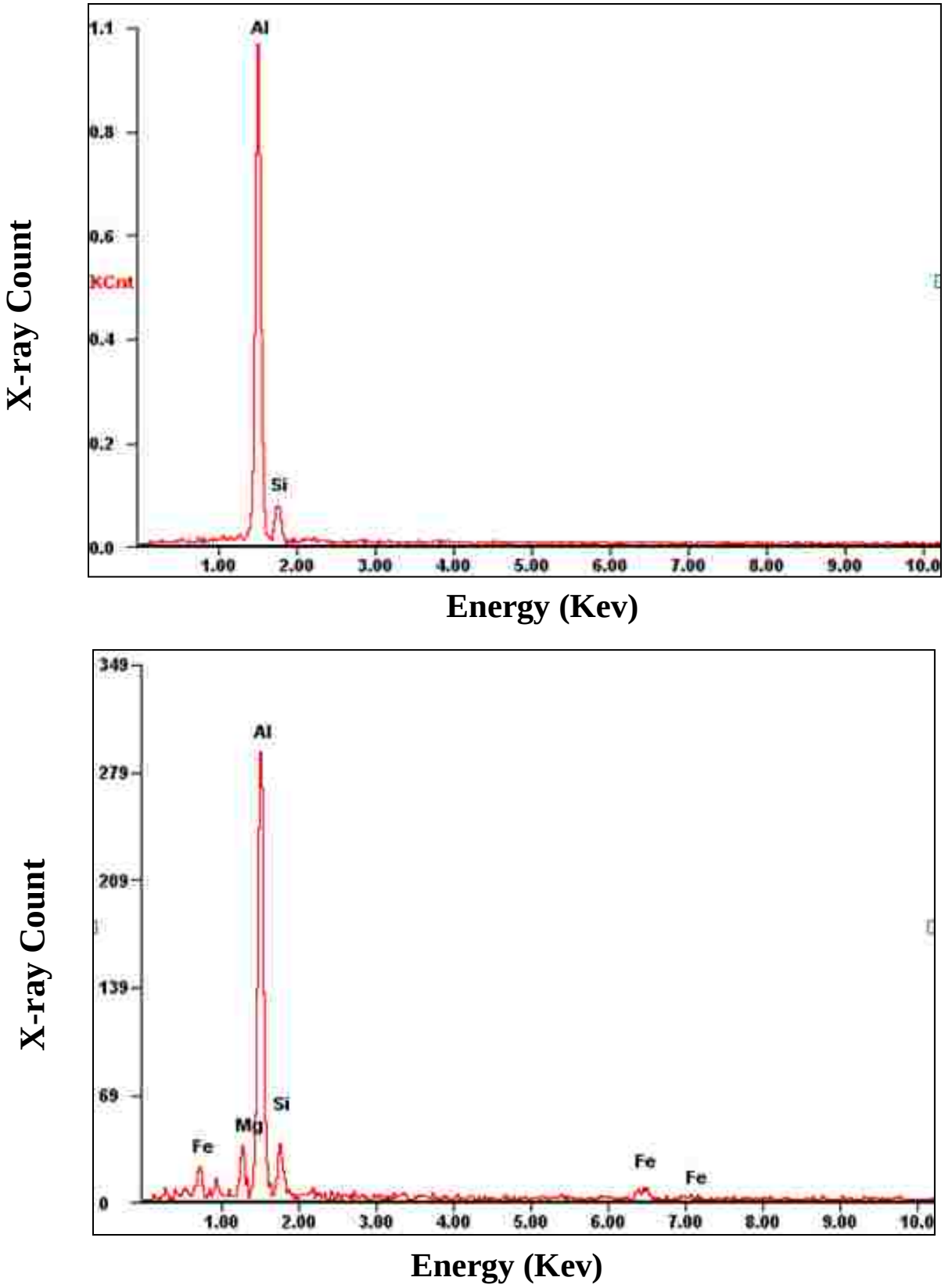

Figure 4-21 EDS analysis the presence of a) Primary Al, b) Eutetic Si and c) Mg- based phases.

Figures 4-20 and 4-21 show the presence of phases in the A356 alloy after T6 heat treatment. SEM analyses on the specimens treated at T6 thermal treatment scheme indicated that, although Mg_2Si, a strengthening intermetallic phase was detected, it was very hard to find them due to their scarce presence in the T6 treated A356 compared to the as-cast and T5 A356. The limited presence of the Mg_2Si phase in the T6 A356 alloy suggested that the dissolution of the Mg_2Si took place during the solution treatment. As a result, the strengths of the T6 A356 alloy were reduced.

4.3. Porosity

The porosity levels at different thermal treatment conditions were summarized in Figure 4-23. Due to vacuum assistance during the high pressure die casting process, the porosity level of the as-cast A356 alloy was the lowest in the cast components. Comparing the as-cast and T5 (220 ^{o}C) treatment conditions, it indicates that the T6 and T4 treated specimens had the relatively high amount of porosity, which resulted in high temperature treatment. The presence of gas porosity in castings is harmful to the mechanical properties of aluminum die castings. The relatively high porosity level in T4 and T6 specimens should be responsible for the poor mechanical properties, compared to both filler metal (ER 4043) and wrought alloy 6061.

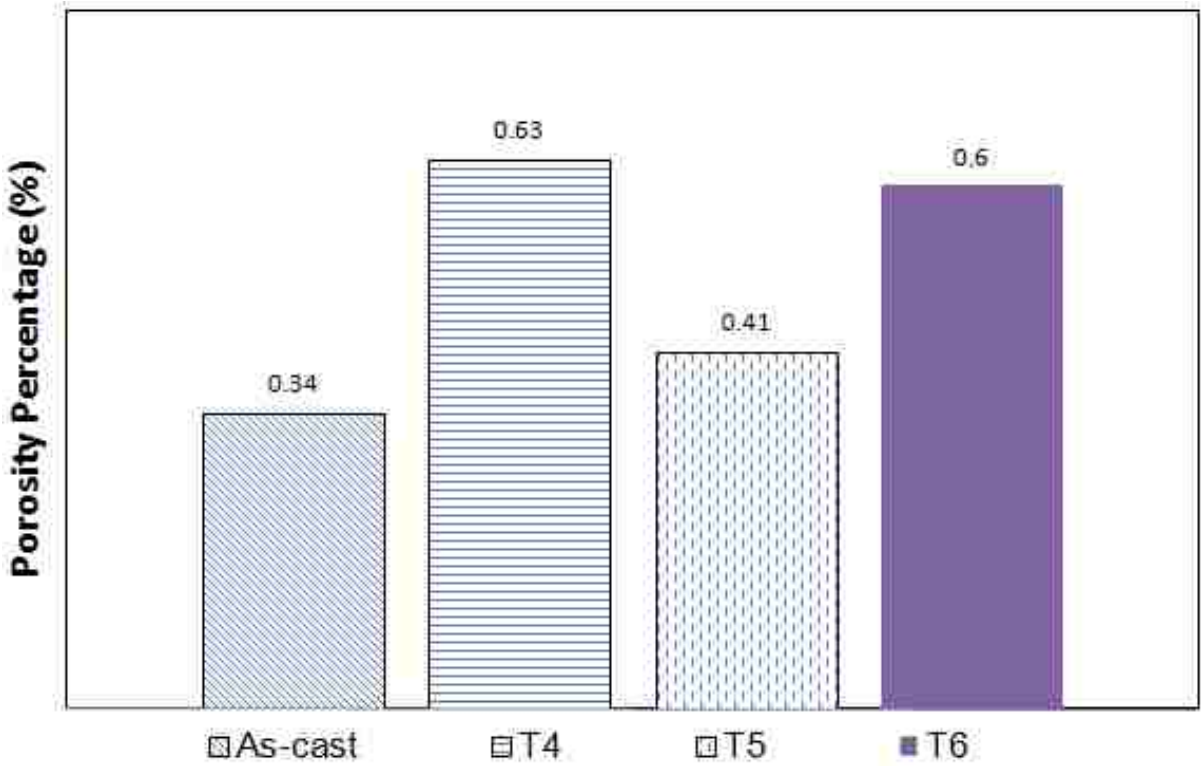

Figure 4-22 Porosity variation of aluminum alloy A356 at different thermal treatment conditions (As-cast, T4, T5 & T6).

4.4. Fracture Behaviors

To evaluate the fracture behaviour, fractured samples after tensile testing for different combination of alloys (A356-6061) were analyzed by a scanning electron microscope(SEM). Fracture surfaces of each samples were observed under two different magnifications, 500x and 1000x, which identify evident characteristics for making technical comparisons.

4.4.1 Fracture in T4 A356 part of T4 A356/6061 welding

Figure 4-23 shows the fractured tensile specimen of T4 A356/6061 under an optical microscope, in which fracture took place in the welded section of T4 A356.

Figure 4-23 Fractured tensile specimen of welded T4 A356/6061 alloys.

The longitudinal section of the fractured casting can be seen in Figure 4-24, which identified the DAS and silicon particles after applying tensile load. The fracture path was mainly along the boundary between the primary α-Al dendrites and the eutectic mixture which were clearly observed. The coarser dendrites in the fractured part resulted in relatively low tensile properties.

Fractographs in Figures 4-25 and 4-26 revealed the difference in the fracture behavior of T4 A356 cast alloy and 6061 wrought alloy. A ductile fracture surface containing deeper dimples with dramatic height variation resulted from the elongated fracture surface in 6061 wrought alloy than those in the fracture surface of T4 A356 cast alloy. This SEM observation indicated the T4 A356 cast alloy was less ductile than 6061 wrought alloy. This is in agreement with the results of tensile testing, which the fracture occurred in the T4 A356 cast alloy.

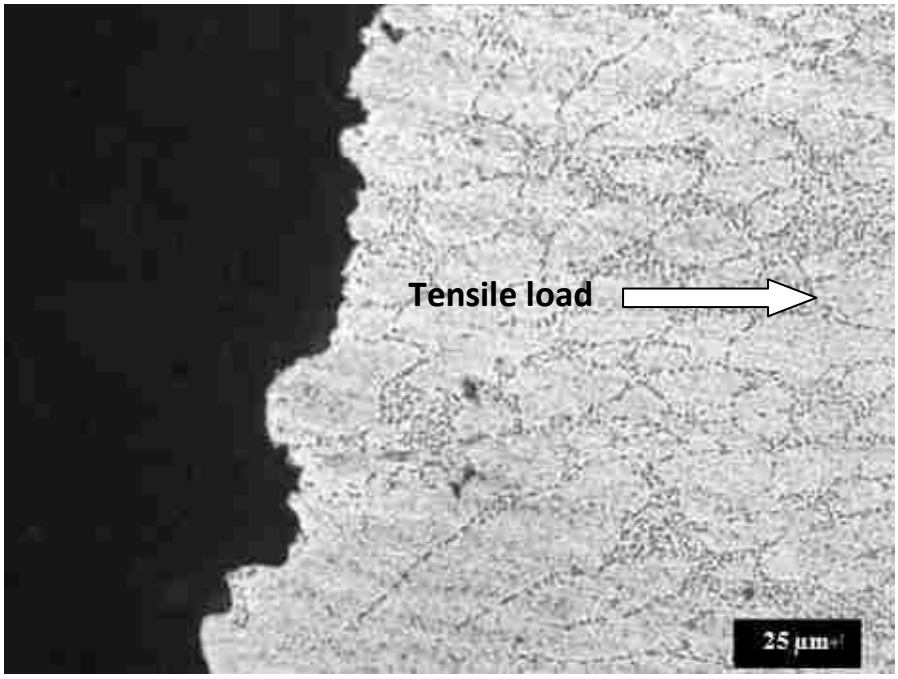

Figure 4-24 Optical micrograph showing the longitudinal section of a fractured casting (T4 A356).

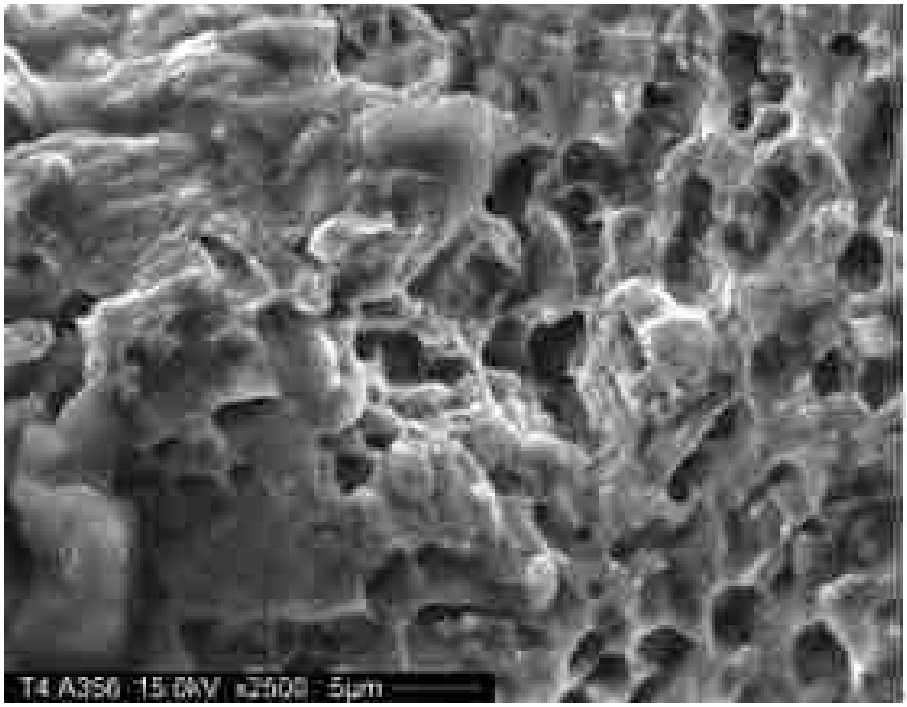

Figure 4-25 SEM fractograph showing the fracture surface of T4 cast alloy A356

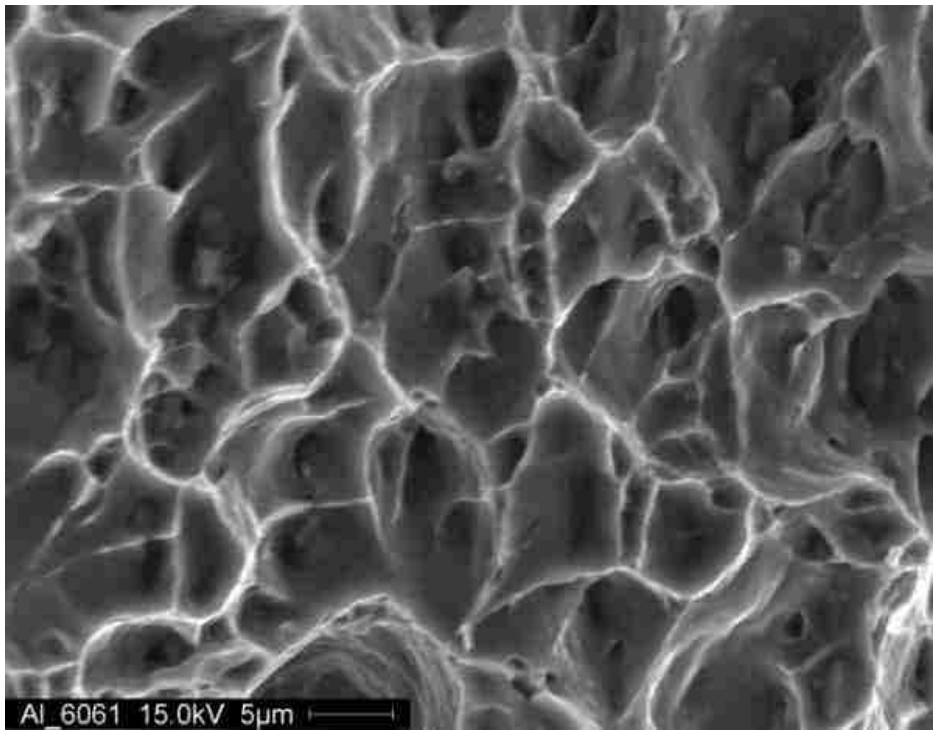

Figure 4-26 SEM fractograph showing the fracture surface of 6061 wrought alloy.

4.4.2 Fracture in 6061 part of T5 A356/6061 welding

Figure 4-27 depicts the fractured tensile specimen of T5 A356/6061, in which fracture occurred in 6061. Figures 4-28 and 4-29 illustrated the details of fractography of the welded T5 A356/6061.

Figure 4-27 Fractured tensile specimen of welded T5 A356/6061 alloys

Figure 4-28 shows the longitudinal section of the fractured casting, fracture path after tensile loading was applied. The fracture path was mainly along the boundary between the primary α-Al dendrites and the eutectic mixture which were clearly shown.

Fractograph in Figure 4-29 revealed the fracture behavior of T5 A356 cast alloy. Comparing to the fracture part in wrought alloy 6061 in Figure 4-26, the size of dimples became larger, which indicated the 6061wrought alloy was more ductile than T5 cast alloy. But the strength of 6061 was lower than A356 cast alloy as discussed early. This observation is in agreement with the result of tensile testing, which the fracture occurred in the 6061 wrought alloy.

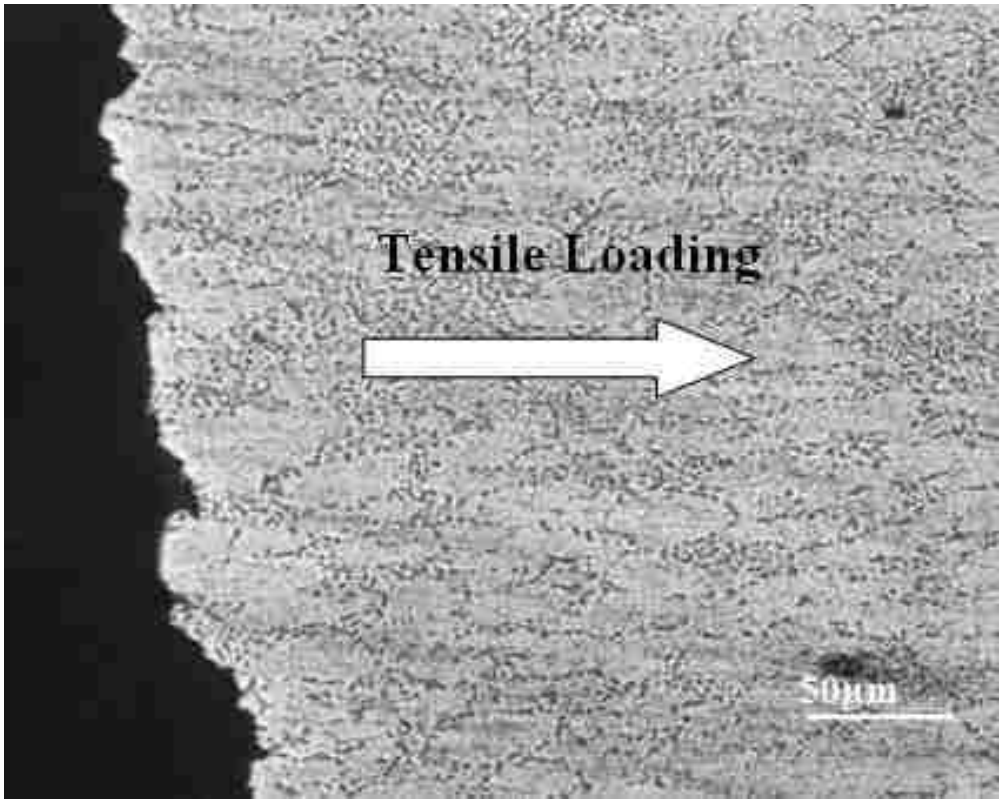

Figure 4-28 Optical micrograph showing the longitudinal section of a fractured tensile specimen of welded T5 A356/6061 alloys.

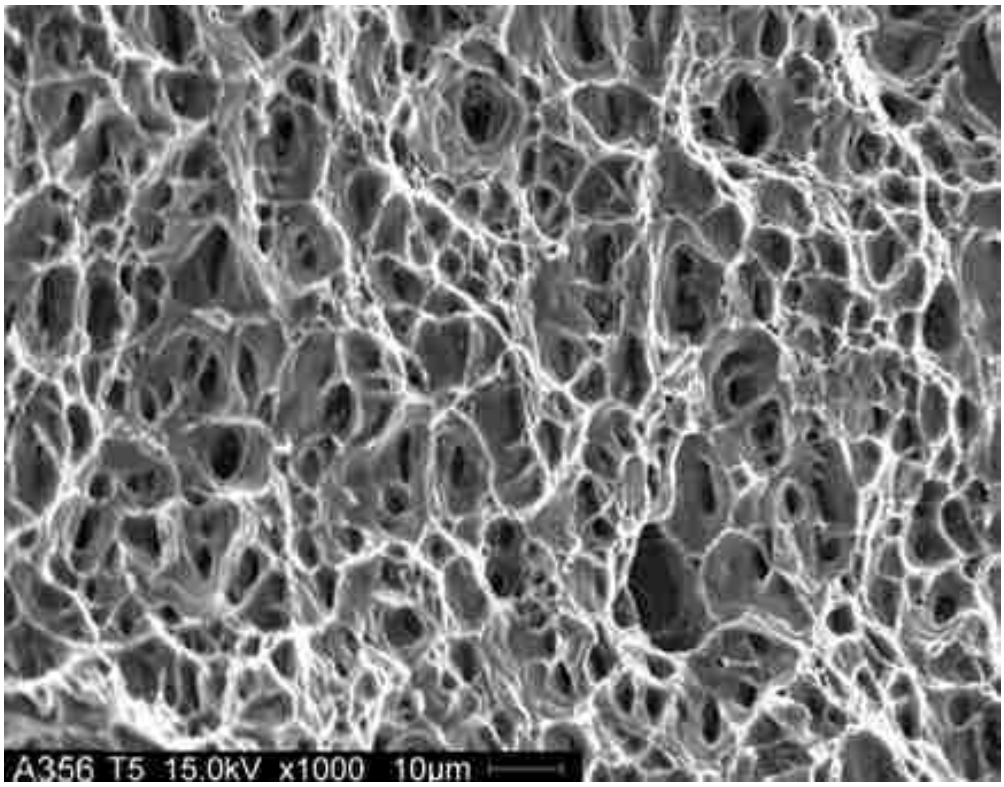

Figure 4-29 SEM fractograph showing the fracture surface of T5 cast alloy A356

4.4.3 Fracture in T6 A356 part of T6 A356/6061 welding

Figure 4-30 shows the fractured tensile specimen of T6 A356/6061, where fracture happened in T6 A356 part. Figures 4-31 and 4-32 illustrated the details of fractography of the welded T6 A356 and 6061.

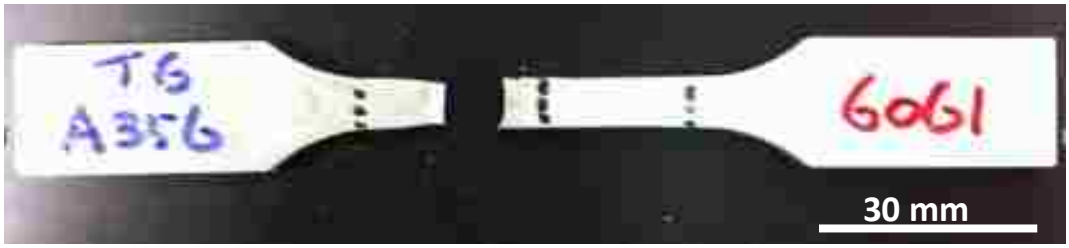

Figure 4-30 Fractured tensile specimen of welded T6 A356/6061alloys.

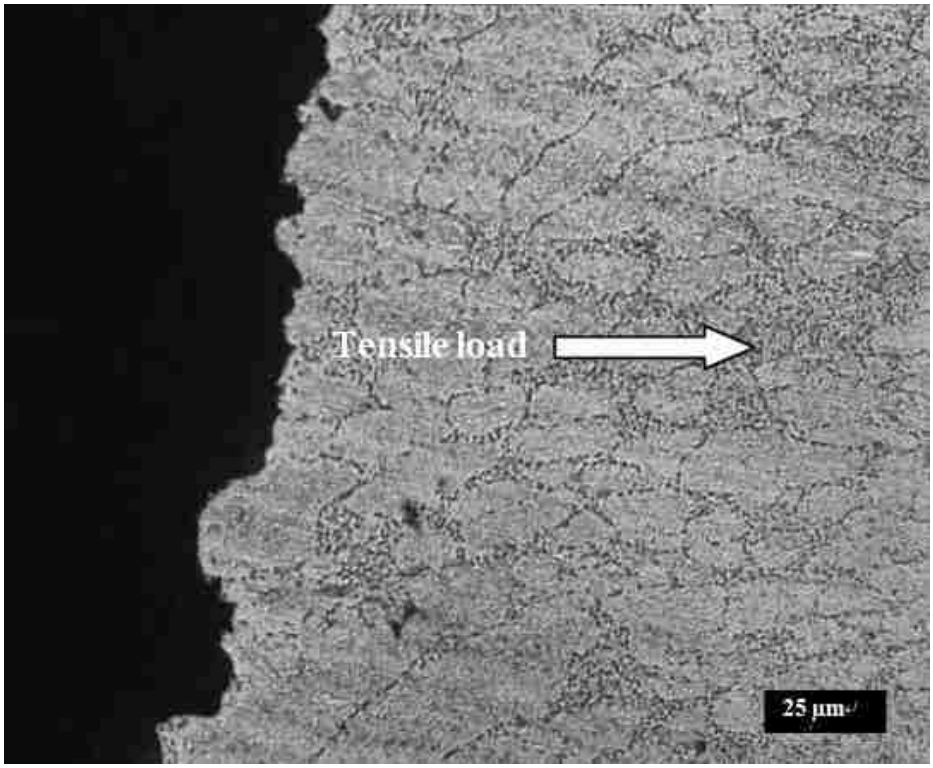

Figure 4-31 Optical micrograph showing the longitudinal section of a fractured tensile specimen of welded T6 A356/6061 alloys.

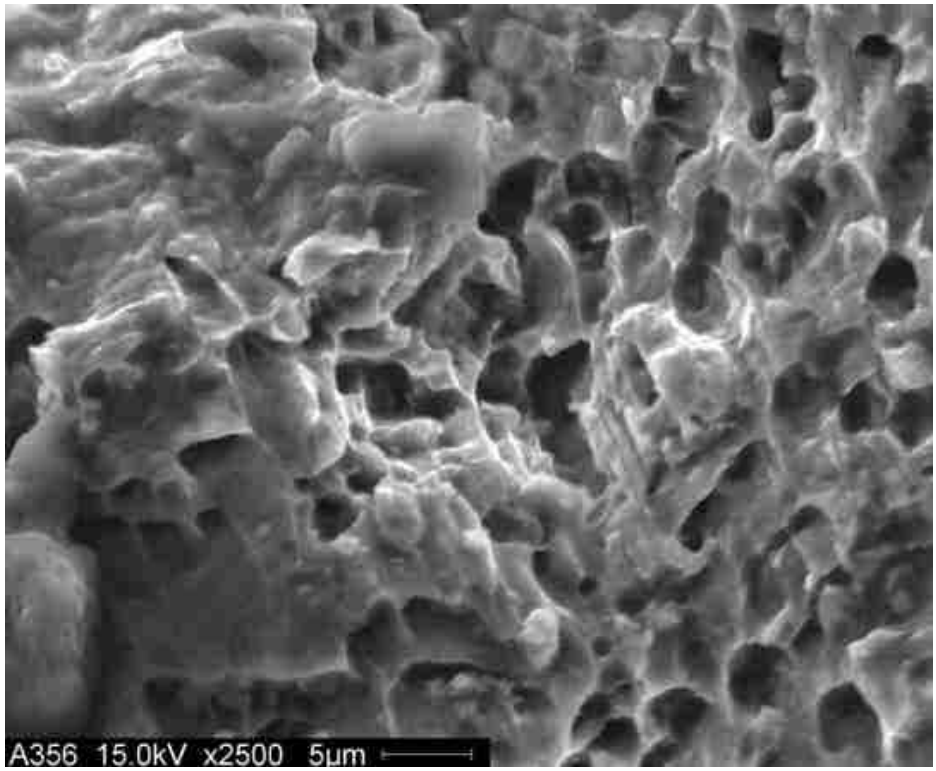

Figure 4-32 SEM fractograph showing the fracture surface of T6 cast alloy A356.

Fractograph in Figure 4-32 identified the fracture morphology of T6 A356 cast alloy. From the SEM observation, a ductile fracture surface containing deeper dimples with dramatic height variation resulted from the elongated fracture surface in the fracture surface of T6 A356 cast alloy. The SEM observation agrees to the results of tensile testing, in which the elongation of the T6 A356 cast alloy was somewhat high. But, the strengths of T6 A356 were lower than those of 6061 alloy, which caused the fracture of T6 A356 in the welded T6 A356/6061 alloys

CHAPTER 5.

CONCLUSIONS AND FUTURE WORK

5.1 Conclusions

1. Four pairs of A356 and wrought 6061 aluminum alloys for fusion welding were designed and experimented, which were T4 A356 cast alloy/6061 wrought alloy, T5 A356 cast alloy/6061 wrought alloy and T6 A356/ 6061wrought alloy by using the same filler metal (ER 4043). A356 alloy was cast by a vacuum high pressure die casting process (V-HPDC). The mechanical properties of the proposed alloys were evaluated by the tensile testing and their microstructures were characterized by scanning electronic microscopy (SEM).
2. The UTS, YS and E_f of as-cast, T4, T5,T6 and 6061 were 221.17±2.3 MPa, 137.1±4.2 MPa and 11.13±1.3%; 169.90±3.3 MPa, 104.90±3.1 MPa and 9.48±2.2%; 286.6±2.3 MPa, 140.1±2.3 MPa and 11.21±2.0%; 191.2±1.9 MPa, 107.4±5.3 MPa and 9.82±2.3%; and 217.5±6.8 MPa, 116.1±1.5 MPa and 16.18±1.3%.
3. Different fracture locations indicated the order of mechanical properties of materials.

- For the joined T4 A356 cast alloy/6061 wrought alloys, the results of tensile testing of welded samples showed the fracture of the joined T4-A356/6061 took place in T4-A356 due to its lower tensile properties than 6061 and the filler alloy (ER 4043).
- For the joined T5 A356/6061 wrought alloy samples, the results of tensile testing of the welded samples showed the fracture of the joined T5-A356/6061 occurred in 6061 due to its tensile properties lower than those of the V-HPDC A356 T5 alloy and the filler alloy (ER

4043).

- For the joined T6 A356/6061 wrought alloy samples, the results of tensile testing of the welded samples showed the fracture of the joined T6-A356/6061 happened in T6 A356 due to its tensile properties lower than wrought alloy 6061 and the filler alloy (ER 4043).

4. The content of magnesium based intermetallic phase, their morphology and distribution throughout the matrix affected the mechanical properties as well. The reduction in the strengths of the alloy treated at T4 condition should be at least attributed to the absence of the Mg_2Si intermetallic phases, which were dissolved during T4 thermal treatment. Based on the microstructural analyses, the DAS and silicon particle size in the fusion zone (ER4043) were finer than those of the base metal, which resulted in an increase in strength of the fusion zone of the filler alloy (4043).
5. The improvement in the strengths of the A356 treated at T5 condition should be at least attributed to the presence of the Mg_2Si intermetallic phase.
6. The insufficient presence of the Mg_2Si intermetallic phase, due to the dissolution of the Mg_2Si phases in T6 heat treatment in A356 cast alloy should be responsible for the reduction in the strengths of the A356 treated at T6 condition.
7. Comparing to the as-cast and T5 (220 ^{o}C) treatment conditions, it indicates that the T6 and T4 treated specimens had the relatively high amount of porosity, which resulted from high temperature treatment. The presence of gas porosity in castings is harmful to the mechanical properties of aluminum die castings. The relatively high porosity level should be responsible for the poor mechanical properties, compared to both filler metal (ER 4043) and wrought alloy 6061.
8. The fracture took place in T4 A356 cast alloy, which indicated that the strengths of the fusion

zone and 6061 wrought alloy was higher than T4 A356 cast alloy. Also, the fractured faces of T4 A356 were shallower and smaller than those in wrought alloy 6061, which meant the T4 A356 cast alloy (Ef:9.48%) was less ductile than 6061wrought alloy (Ef:16.18%).

9. The analyses of fractography indicated that the dimples in the fractured faces of 6061were shallower and smaller than those in T5 A356 cast alloy. Although the wrought alloy 6061 was more ductile than T5-A356 cast alloy, the strengths of T5-A356 cast alloy were higher than 6061 wrought alloy.
10. The fracture took place in T6 A356 cast alloy, which indicated that the strength of the fusion zone and 6061 wrought alloy was stronger than T6 A356 cast alloy. The analyses of fractography indicated that the fractured surfaces of T6 A356 cast alloy contain deeper dimples with dramatic height variation, which fit the high elongation data.

5.2 Future Work

1. Modified vacuum die cast AA365 alloy responds to thermal treatments. Tensile properties were influenced by both thermal treatment temperatures and times. Eutectic silicon morphology and their distribution around the matrix were affected by higher thermal treatment temperature. Intermetallic phases were dissolved at certain thermal treatment schemes. However, the dissolution kinetics, i.e., the exact amount of dissolved intermetallic phases (Mg_2Si) and their morphology change with successive thermal treatment needs to be further studied.
2. Vacuum assistance provides substantial benefit on die casting process in terms of gas porosity. A throughout study on different levels of vacuum should be conducted to determine

the optimum level of vacuum which minimizes the blistering effect and the porosity level increase during thermal treatment on modified A365 alloy.

3. Joining vacuum high pressure die cast A356 alloy with wrought alloy by using MIG welding method is provided in this report. However, by applying different welding methods, such as friction stir method or gas tungsten arc welding (TIG), a different and detail analysis on tensile properties maybe carried out.

CHAPTER 6.

REFERENCES

1. S.C. Jeng and S.W. Chen, "The Solidification Characteristics of 6061 and A356 aluminum alloys and their ceramic particle-reinforced composites", Acta Materialia, Vol 45, December 1997, 4887–4899.
2. P.W. Cleary and H.A Joseph, "Three Dimensional Modeling of High Pressure Die Casting" CSIRO Mathematical and Information Sciences, Vol 6-8, December 2009, 1-2.
3. Aluminum and Aluminum Alloys, ASM Specialty Handbook, ASM International, 2002.
4. K. Ahmmed and H. Hu, "Effect of thermal treatment on tensile properties of vacuum die cast modified aluminum alloy A356", NADCA Transactions, 2010, 10-32.
5. D. Aldum, P, Martin and J. Sun, "Effects of heat treatment on the mechanical properties of SiC p/6061 Al composite", Journal of Materials Engineering and Performance, Vol 1, 2010, 615-624.
6. Z.Y. Ma, S.R. Sharma, R.S. Mishra, and M.W. Mahoney, "Microstructural modification of cast aluminum alloys via friction stir processing", Materials Science Forum, Vol 426-432, 2003, 2891-2896.
7. Y. G. Kim, H. Fujii, T. Tsumura, T. Komazaki, and K. Nakata, "Three defect types in friction stir welding of aluminum die casting alloy", Materials Science and Engineering: A .415, 2006, 250-254.
8. L. Hwang, C. Gung and T.S. Shih, "A study on the qualities of GTA-welded squeeze-cast A356 alloy," Journal of Materials Processing Technology, Vol 116, 2011, 101-113.

9. H Hu, Y. Wang, Y. Chu, P. Cheng, and A. T. Alpas, "Solution Heat Treatment of Vacuum High Pressure Die Cast Aluminum Alloy A380," NADCA Transactions 7, 2005, 61-73.
10. H. Koch, U. Hielscher, H. Sternau and A.J. Franke, "The new low-iron high-pressure die-casting alloy", The Minerals, Metals & Materials Society, 78 1995, 1011-1018.
11. M, William. "Gas Metal Arc Welding", ASM International Handbook Committee, Tinley Park, 2007.
12. Aluminium alloy, http://en.wikipedia.org/wiki/Aluminium_alloy, January 2012.
13. D. Beaulieu, "Characteristics of Structural Aluminum", Metallurgical and Materials Transaction A, Vol 2, October 2005, 25-31.
14. R.D. Howard, Aluminum Heat Treatment Processes- Applications and Equipment, www.industrialheating.com, January 2012.
15. J.R. Davis, Machining of aluminium and its Alloys, ASM International Handbook Committee, September, 2009.
16. B.R Michael, Welding Safety Protection, http://www.statefundca.com/safety meeting/SafetyMeetingArticle.aspx?ArticleID=5, January2012.
17. M.F. Ashby and R.H. Jones, "An Introduction to Microstructures Processing and Design", Engineering Materials 2, Vol 3, 1998, 79-82.
18. G. Mathers, The Welding of Aluminium and its alloys, Woodhead Publishing Ltd and CRC Press LLC, UK, 2002.
19. L.J. Barley, "Gas Tungsten Arc Welding Technical Guide", Hobart Institute of Welding Technology, Vol 2, 1998, 4-5.
20. S.A. Waldon, "Welding Processes", ASM International Handbook, Vol 7, 2006, 131-141.
21. J. Cornu and J. Weston, "TIG and Related Processes", Journal of Material Science, Vol. 3,

2008, 11-19.

22. P.W. Muncaster, “Practical TIG (GTA) Welding”, International Journal of Applied Engineering Research. Vol. 1, 2010, 3-11.
23. A. K. Hussain, A. Lateef, M. Javed and P.Tramesh , MIG Welding - Part 1. Specification for MIG Welding of Aluminium and Aluminium Alloys, British Standards publishing Institution, British, 2006.
24. A. Romeyn, Welding Ai-Zn-Mg (7xxx Series) Alloys, Defence Science and Technology Organization, Melbourne, Victoria, 2006.
25. S. Kou, “Heat Affected Zones on Aluminium Alloys”, Journal of Materials Processing Technology, Vol. 7, 2007, 40-50.
26. J. Cornu, “Fundamentals of Fusion Welding Technology”, Journal of Materials Processing Technology, Vol. 2, 2009, 39-49.
27. J. Gandraa, R. Mirandaa, P. Vilaca, A. Velhinhod and J.P. Teixeiraa, “Functionally graded materials produced by friction stir processing”, Journal of Materials Processing Technology, Vol 4, 2011, 7-29.
28. A. De and T. DebRoy, “Probing Unknown Welding Parameters from Convective Heat Transfer Calculation and Multivariable Optimization”, Journal of Applied Physics, Vol 37, 2008, 14-15.
29. A. Hobbacher, Design of Welded Joints and Components, Scientific Publishing Co, NewYork, 1998.
30. C. Webb and J. Jones, “Laser Welding for Custom Beam”, Handbook of Laser Technology and Applications. Vol. 2, 2004, 14-42.

31. A. Klimpel, A. Rzeźnikiewicz and L. Janik, “Study of Laser Welding of Copper Sheets”, Journal of Achievements in Materials and Manufacturing Engineering, Vol. 20A, 2007, 1-2.
32. R. Rai, S. Kelly, M. Martukanitz and R.P. DebRoy, “A Convective Heat-Transfer Model for Partial and Full Penetration Keyhole Mode Laser Welding of A Structural Steel”. Metallurgical and Materials Transactions A, Vol.39, 2008, 98-112.
33. P.Q, Xu, X.J. Zhao, D.X. Yang and S. Yao, “Studying on Filler Metal During GTAW of Carbon Steel”, Journal of Materials Science, Vol 40, 2005, 59-64.
34. The Key to Metal, Welding of Aluminum Alloys, http://www.keytometals.com/ Article12.htm, January 2012.
35. T. Aizawa, M. Kashani and K. Okagawa, “Application of Magnetic Pulse Welding for Aluminum Alloys”, Journal of Welding Research, Vol.7C, 2009,3-9.
36. S. Shivkumar, S. Ricci, and D. Apelian, “Effect of Solution Treatment Parameters on Tensile Properties of Cast Aluminum Alloys”, Journal of Heat Treating, Vol. 8, 1990, 1-2.
37. L. Backerud, G. Chai and J. Tamminen, “Solidification Characteristics of Aluminum Alloys”, Foundry alloys, Vol.2, 1990, 3-5.
38. I. M. Liftshitz and V. V. Sloyozov, “The Kinetics of Precipitation From Supersatureated Solid Solutions”, Journla of Physical and Chemical Solidification, Vol 4, 1999, 9- 16.
39. F. Rhines, and M. Aballe, “Growth of Silicon Particles in an Aluminum Matrix”, Met. Transactions, 17A, 1986, 2139-2154.
40. S. Shivkumar and S. Ricci, “Influence of Solution Parameters and Simplified Supersaturation Treatments on Tensile Properties of A356 Alloy”, AFS Transactions 97, 1989, 913-922.

41. T. Shin and D. Lee. “Effect of trace elements in super alloys", Metals and- Ceramics Korean Inst, No.10, 1985, 1116-1122.
42. M. Tsukuda, S. Koike, and M. Harada, Journal of Japan Institute of Light Metals, 28(1), 1978, 8-14.
43. A.M. Samuel, J. Gauthier and F.H. Samuel, “Microstructural Aspects of the Dissolution and Melting of Al_2Cu Phase in Al-Si Alloys during Solution Heat Treatment”, Metallurgical and Materials Transactions A, Vol 27A, 1996, 1785-1798.
44. J. Gauthier and F.H. Samuel, “Tensile Properties and Fracture Behavior of Solution-Heat-Treated 319.2 Al Automotive Alloy”, AFS Transactions, Vol.95, 2002, 849-858.
45. W. Schneider and F. J. Feikus, “Heat Treatment of Aluminum Casting Alloys for Vacuum Die Casting”, Light Metal Age, August 1998, 14-29.
46. Internet article: Introduction To High Integrity Die Casting Processes, http:// media.wiley.com/product_data/excerpt/16/04712013/0471201316.pdf, July,2002.
47. G. Drossel, R. Mai, and O. Liesenberg, Giessereitechnik, “The influence of melt treatment on the density of castings made from Al-Si cast alloys”, Giessereitechnik, Vol.27, 1981, 167-70.
48. J.E. Gruzleski, P.M. Thomas, and R.A. Entwistle, Br. Goundryman, “Development of porosity in aluminum-base alloys”, Solidification and Casting of Metals , Vol.71, 1978, 69-78.
49. P. Jonason, “Thermal Fatigue of Cylinder Head Alloys”, AFS Trans., Vol. 100, 1992, 601-607.

APPENDIX I

TENSILE CURVES OF AS-CAST AND SOLUTION TREATED SAMPLES

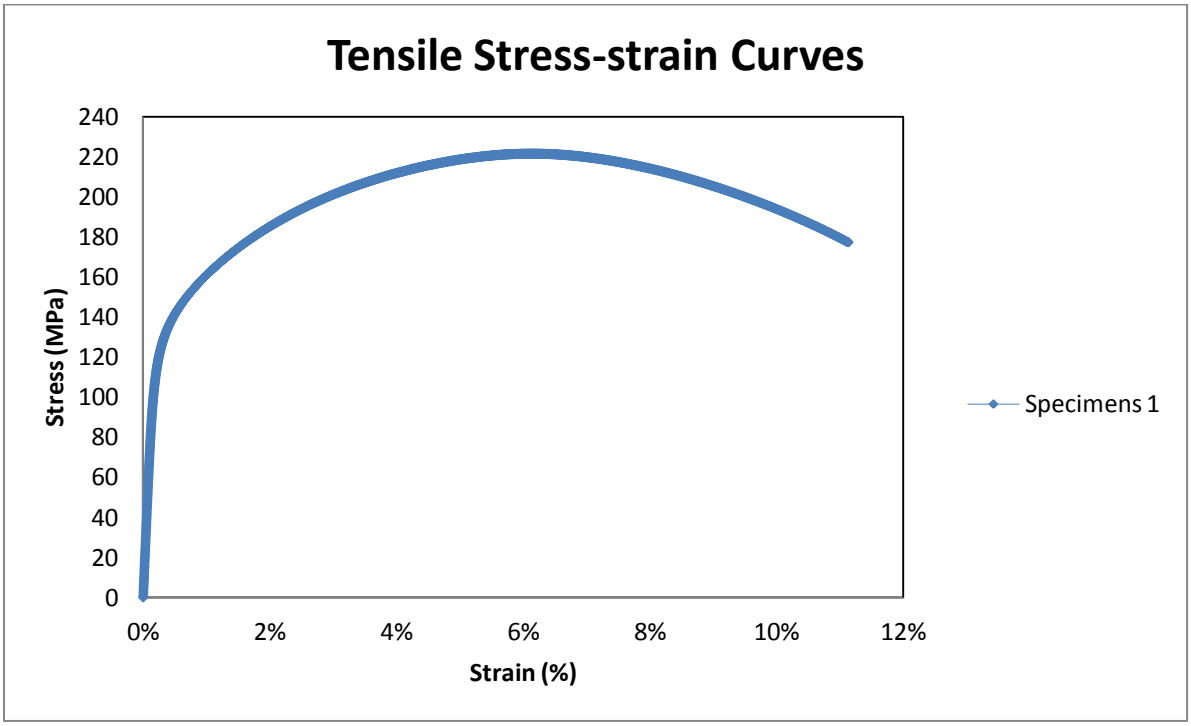

Figure Ap1.1 Tensile curve of as-cast sample A356_Specimens 1

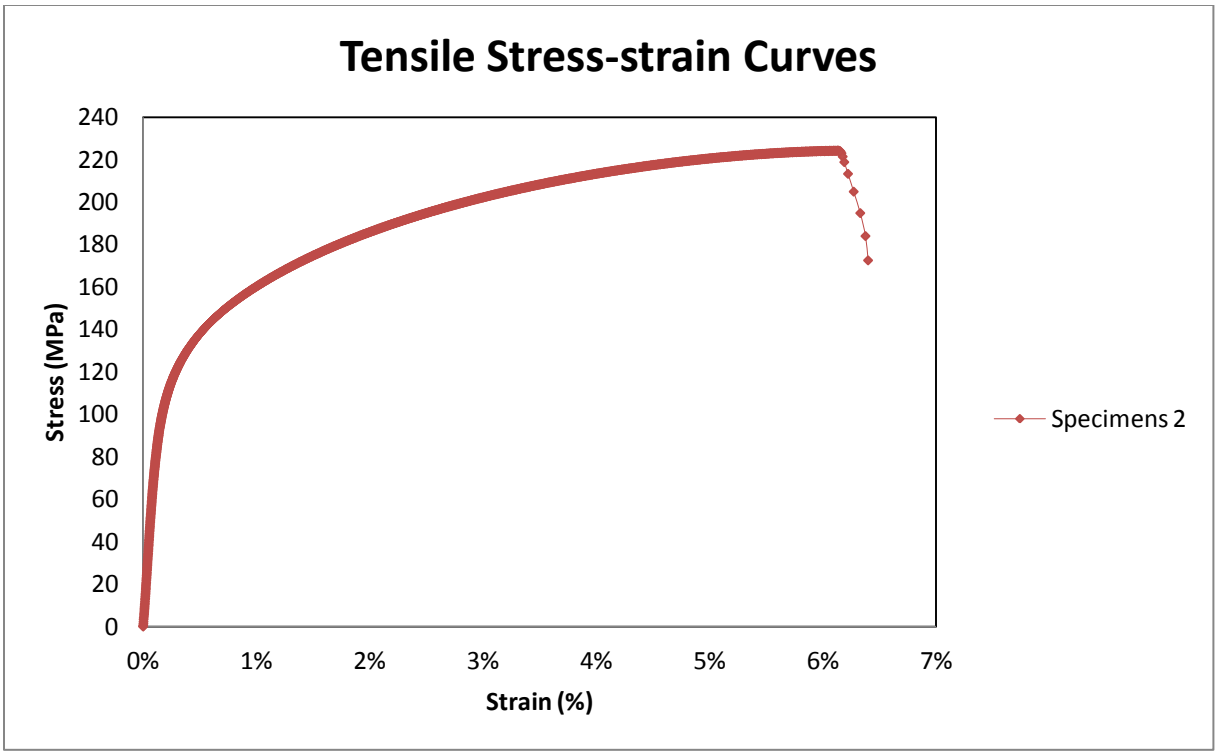

Figure Ap1.2 Tensile curve of as-cast sample A356_Specimens 2

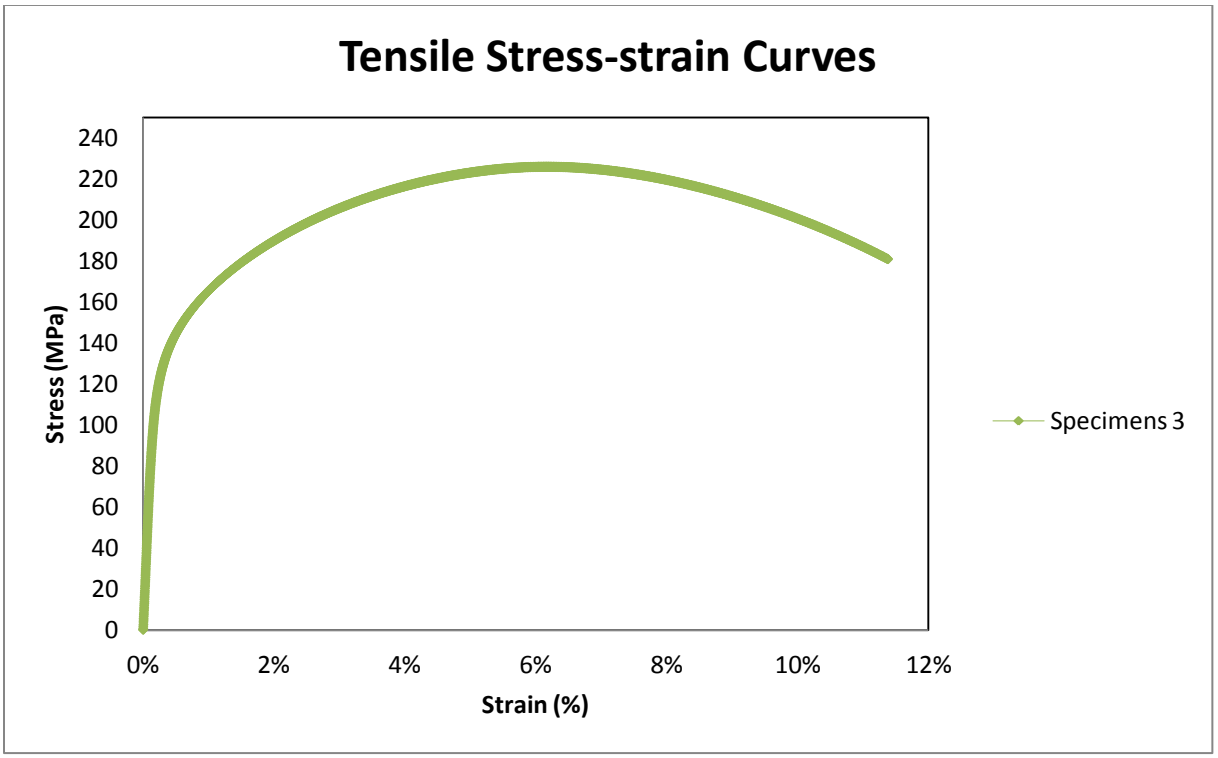

Figure Ap1.3 Tensile curve of as-cast sample A356_Specimens 3

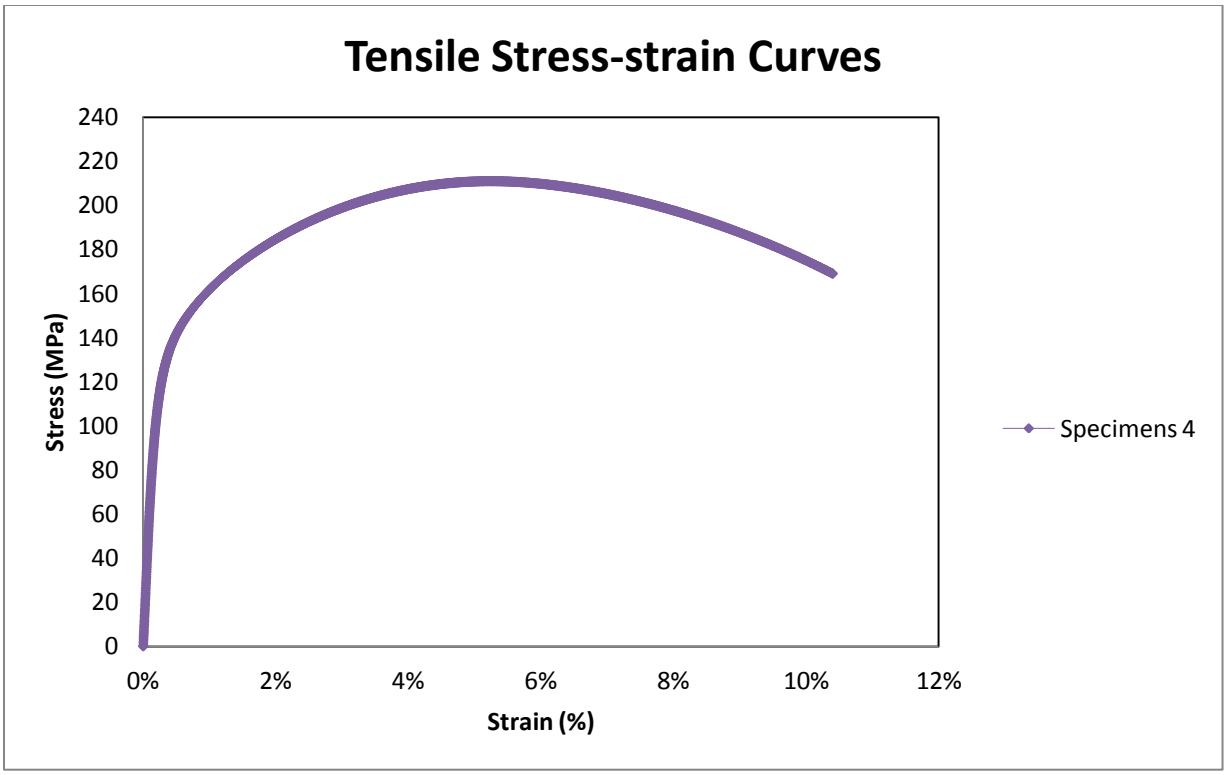

Figure Ap1.4 Tensile curve of as-cast sample A356_Specimens 4

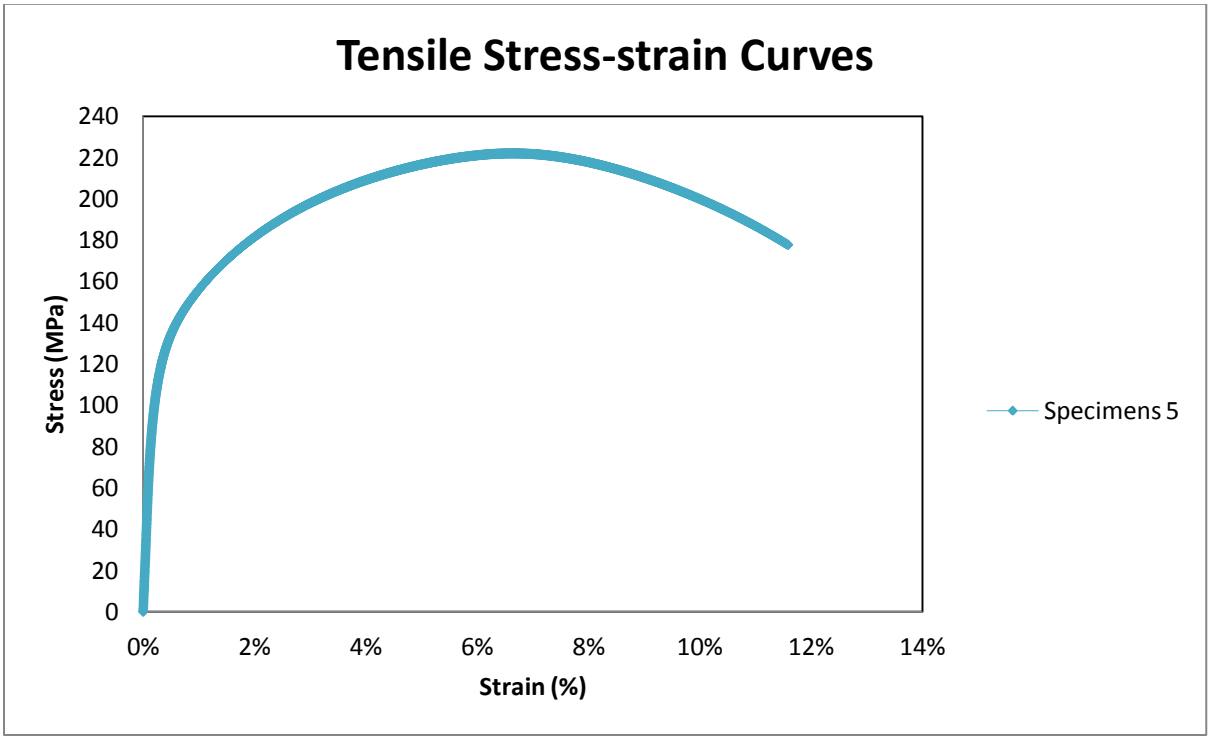

Figure Ap1.5 Tensile curve of as-cast sample A356_Specimens 5

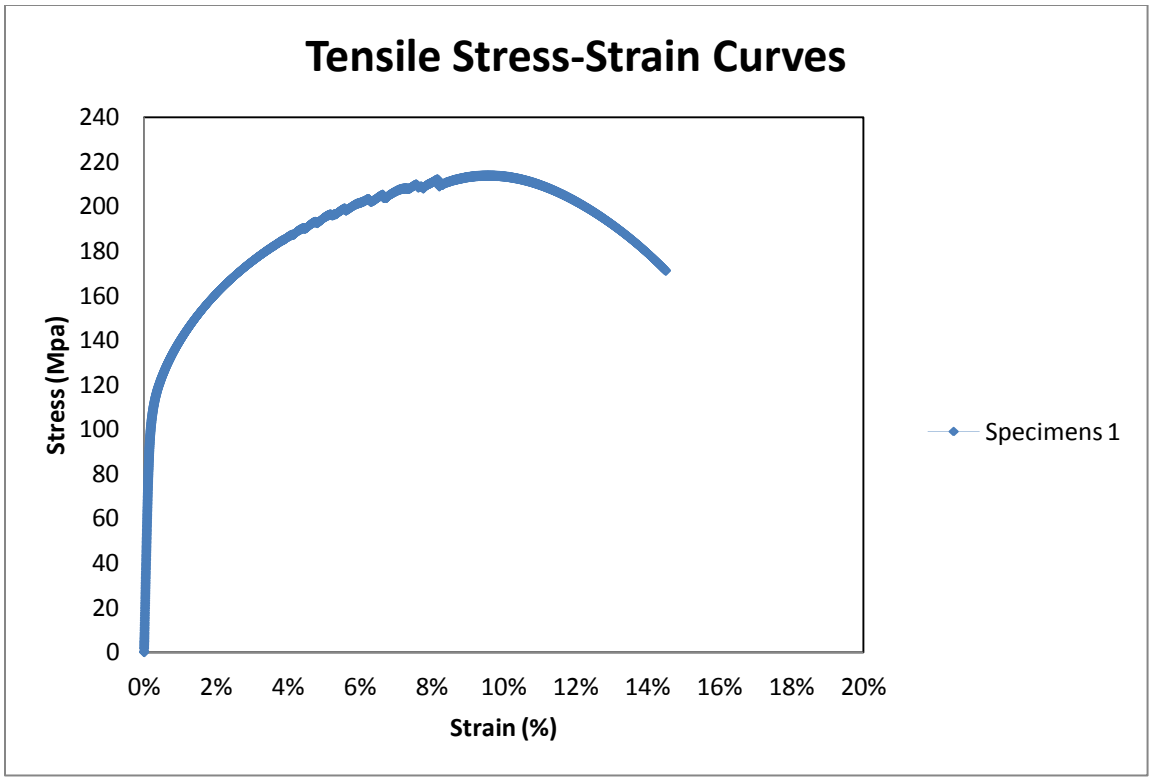

Figure Ap 1.6 Tensile curve of 6061 wrought alloys_Specimens 1

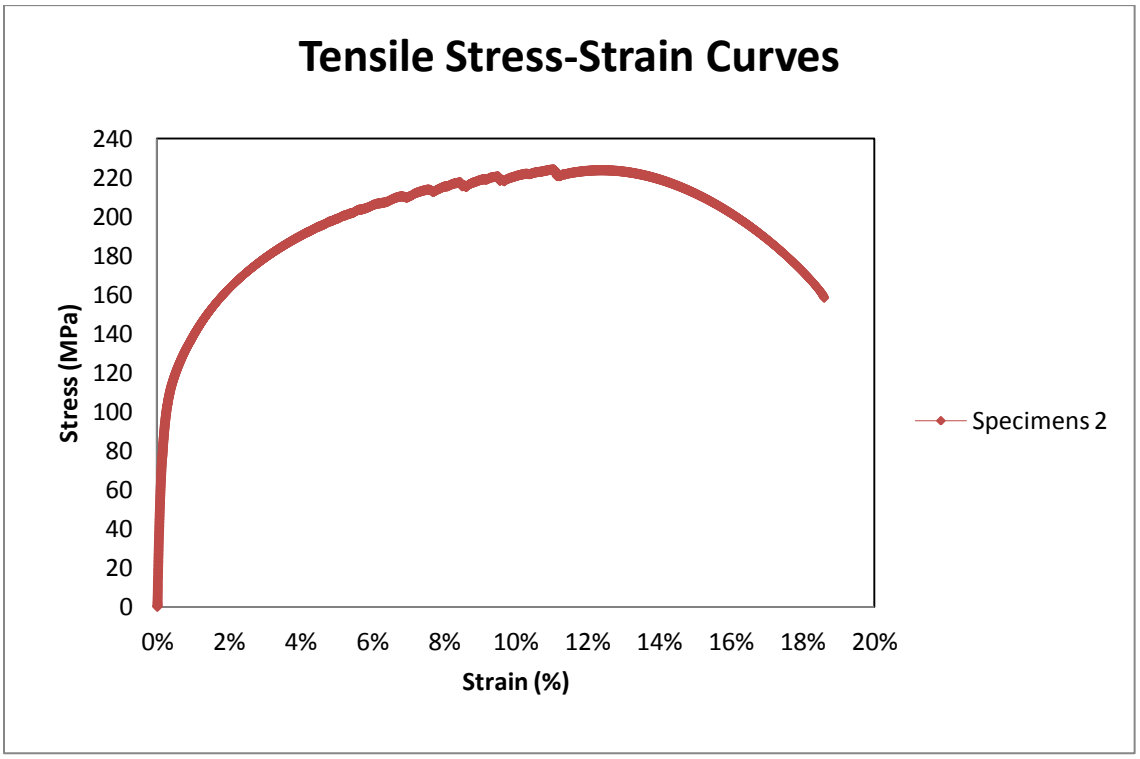

Figure Ap 1.7 Tensile curve of 6061 wrought alloys_Specimens 2

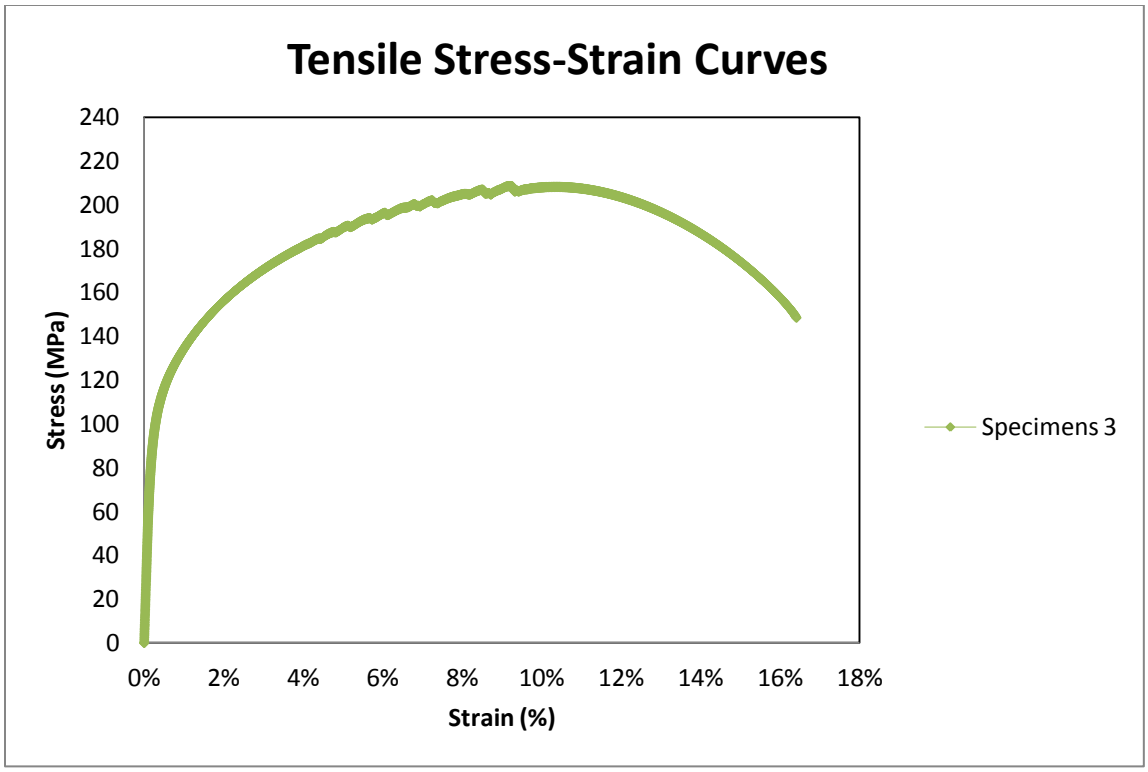

Figure Ap 1.8 Tensile curve of 6061 wrought alloys_Specimens 3

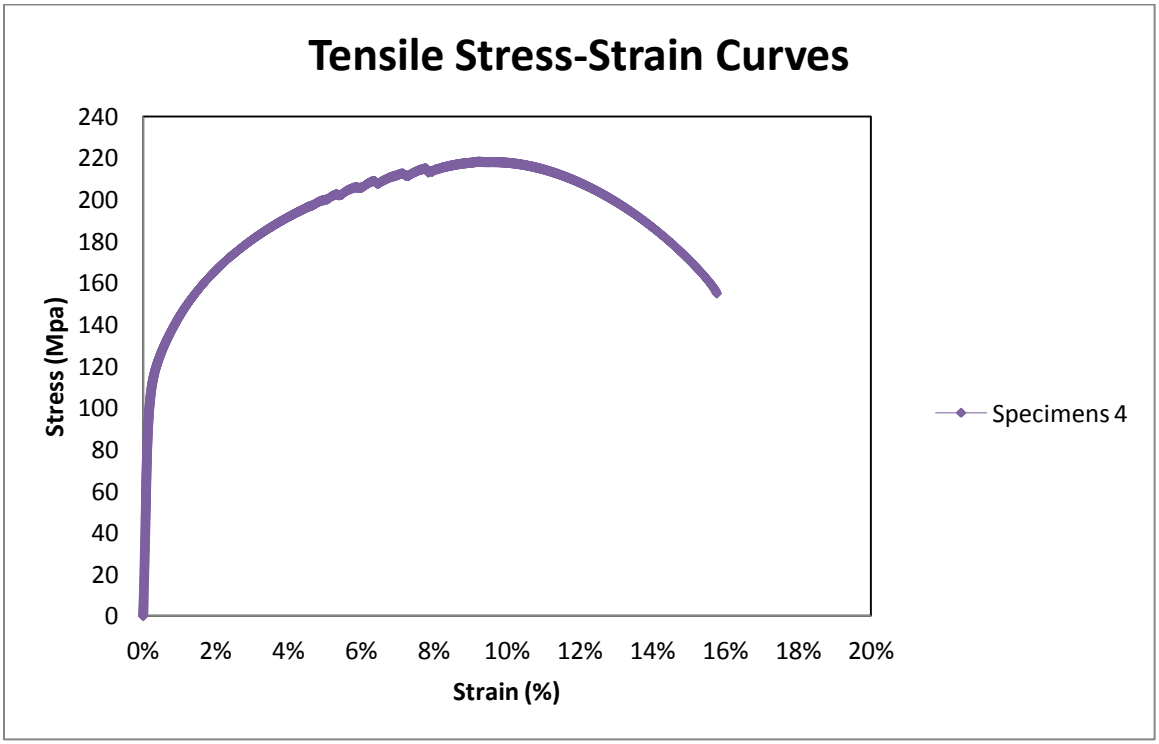

Figure Ap 1.9 Tensile curve of 6061 wrought alloys_Specimens 4

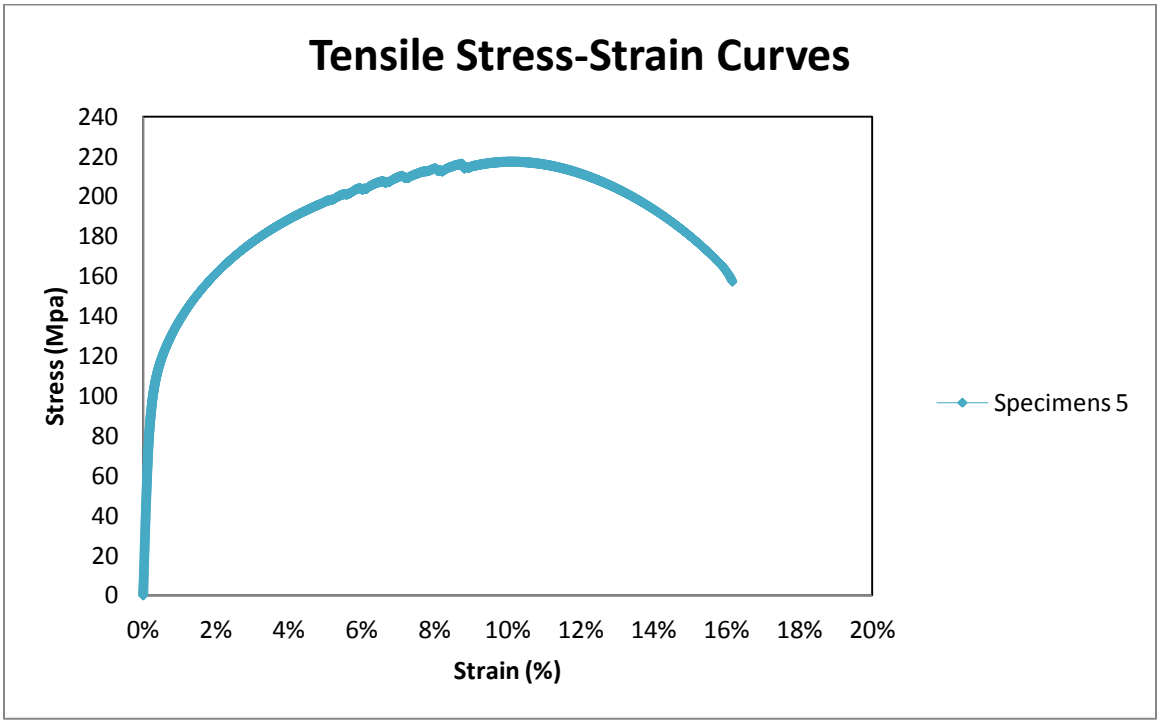

Figure Ap 1.10 Tensile curve of 6061 wrought alloys _Specimens 5

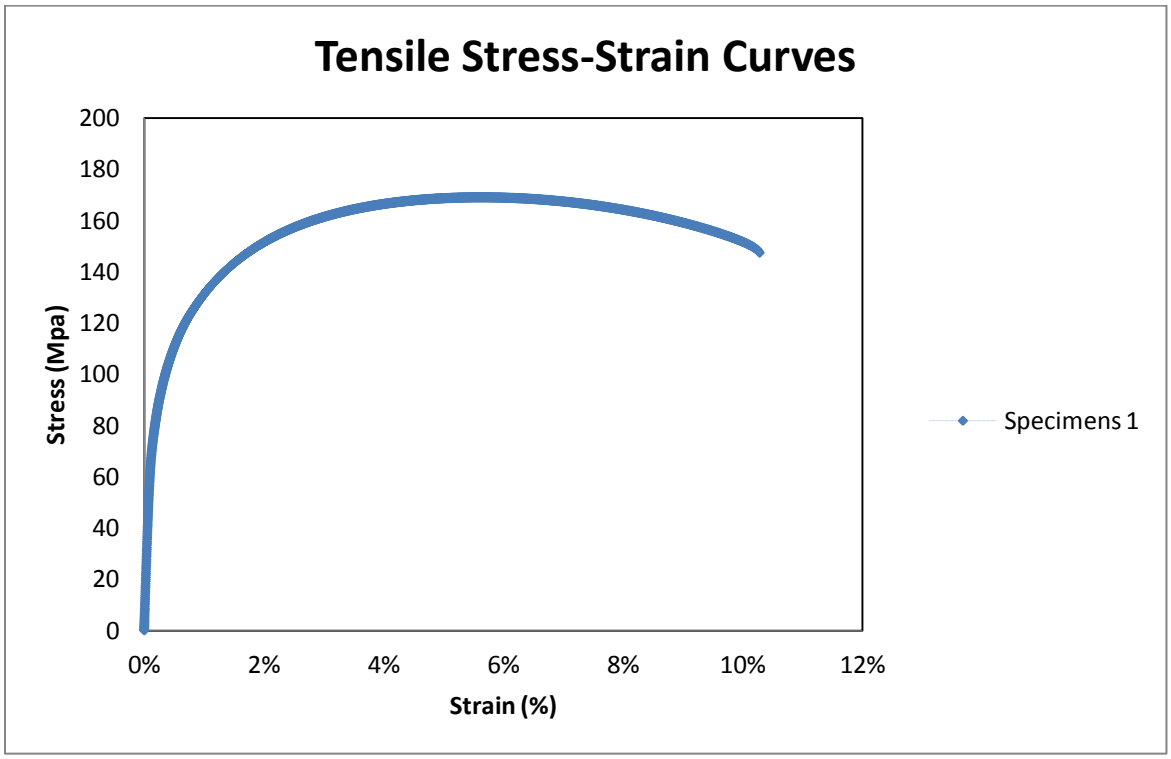

Figure Ap 1.11 Tensile curve of T4 sample A356_Specimens 1

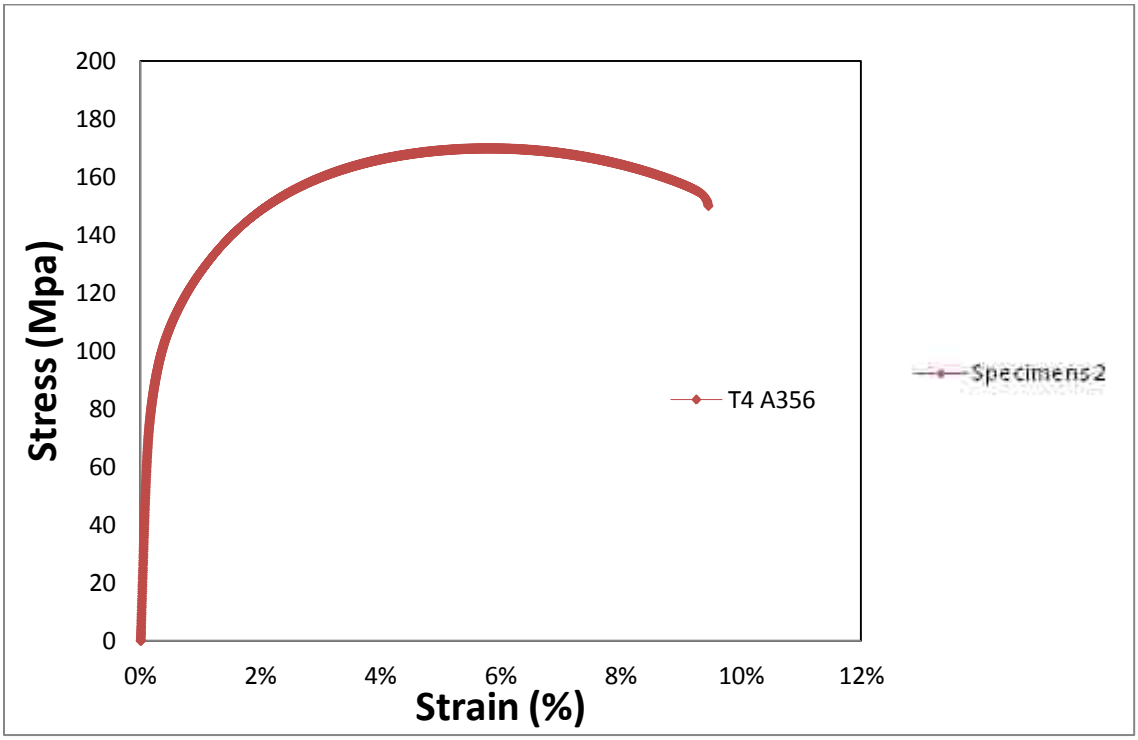

Figure Ap 1.12 Tensile curve of T4 sample A356_Specimens 2

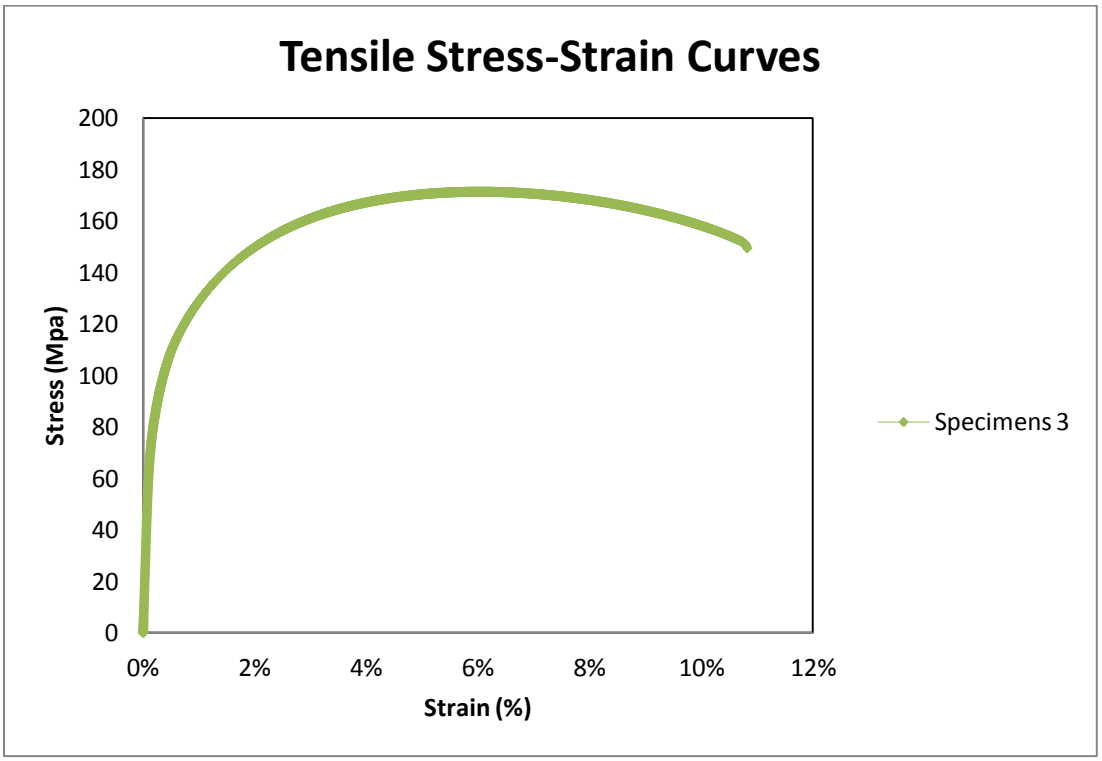

Figure Ap 1.13 Tensile curve of T4 sample A356_Specimens 3

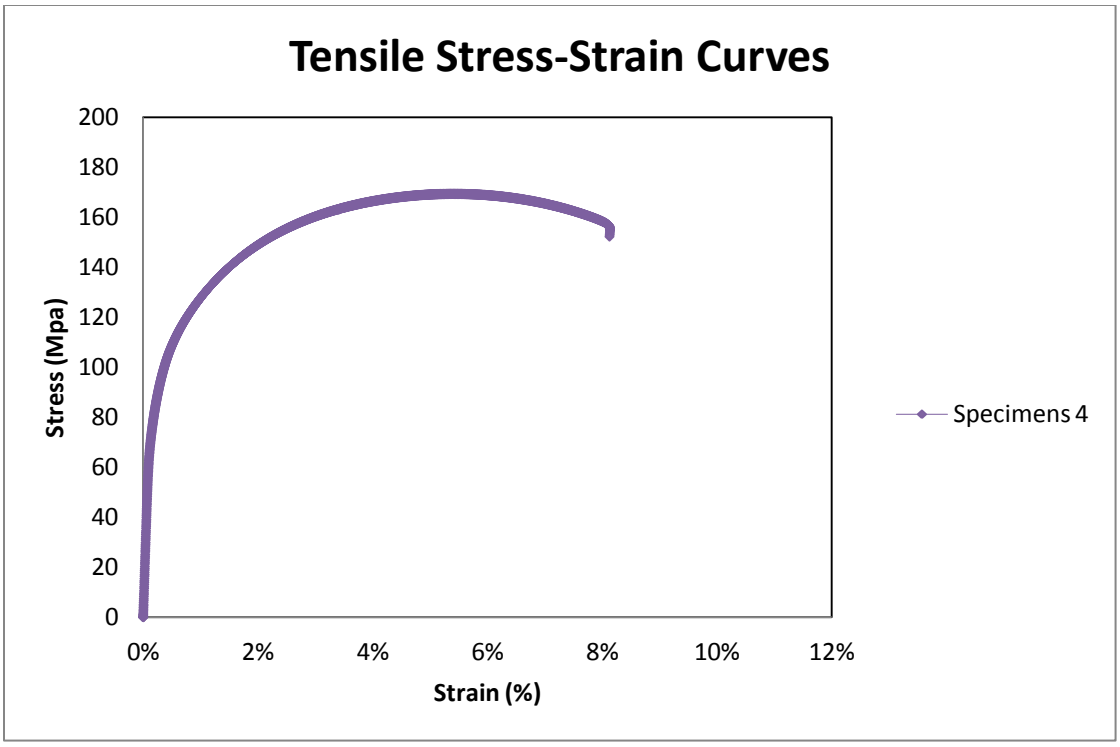

Figure Ap 1.14 Tensile curve of T4 sample A356_Specimens 4

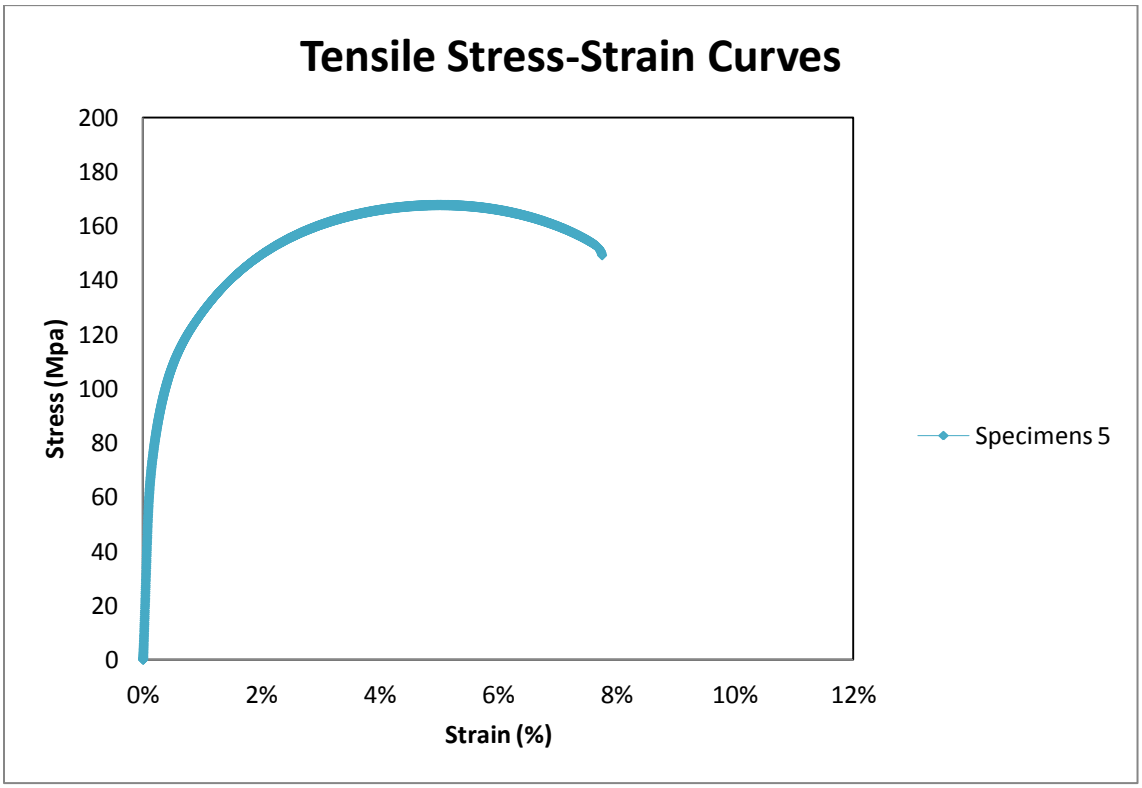

Figure Ap 1.15 Tensile curve of T4 sample A356_Specimens 5

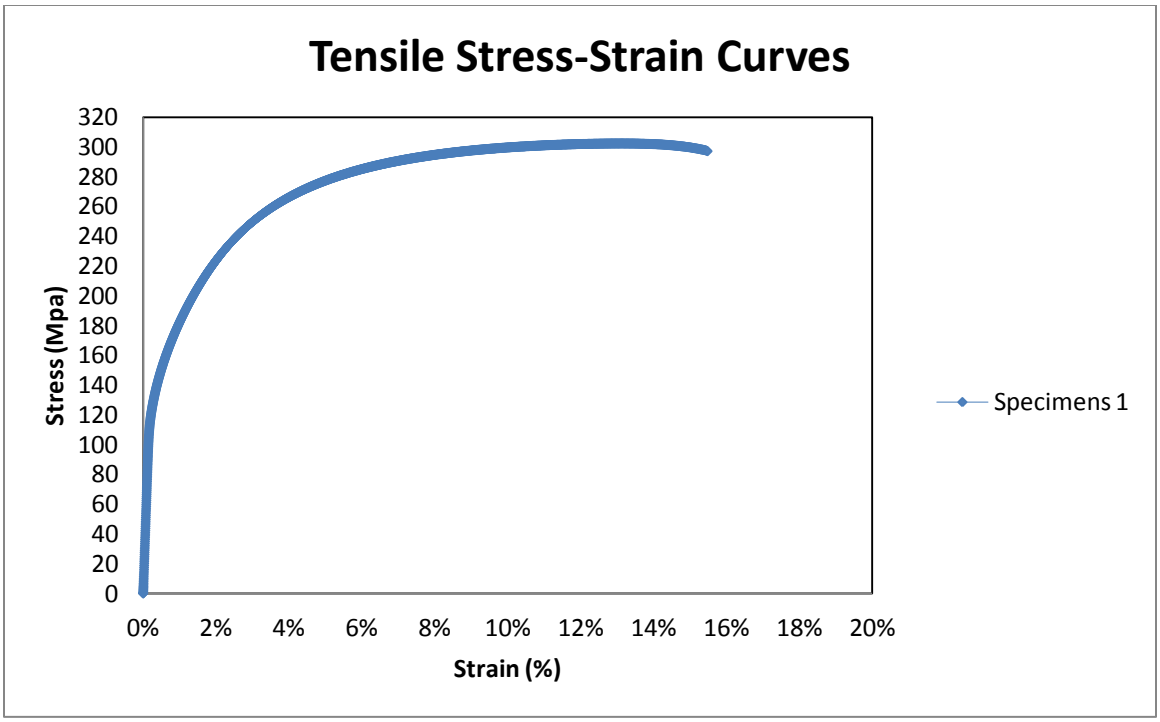

Figure Ap 1.16 Tensile curve of T5 sample A356_Specimens 1

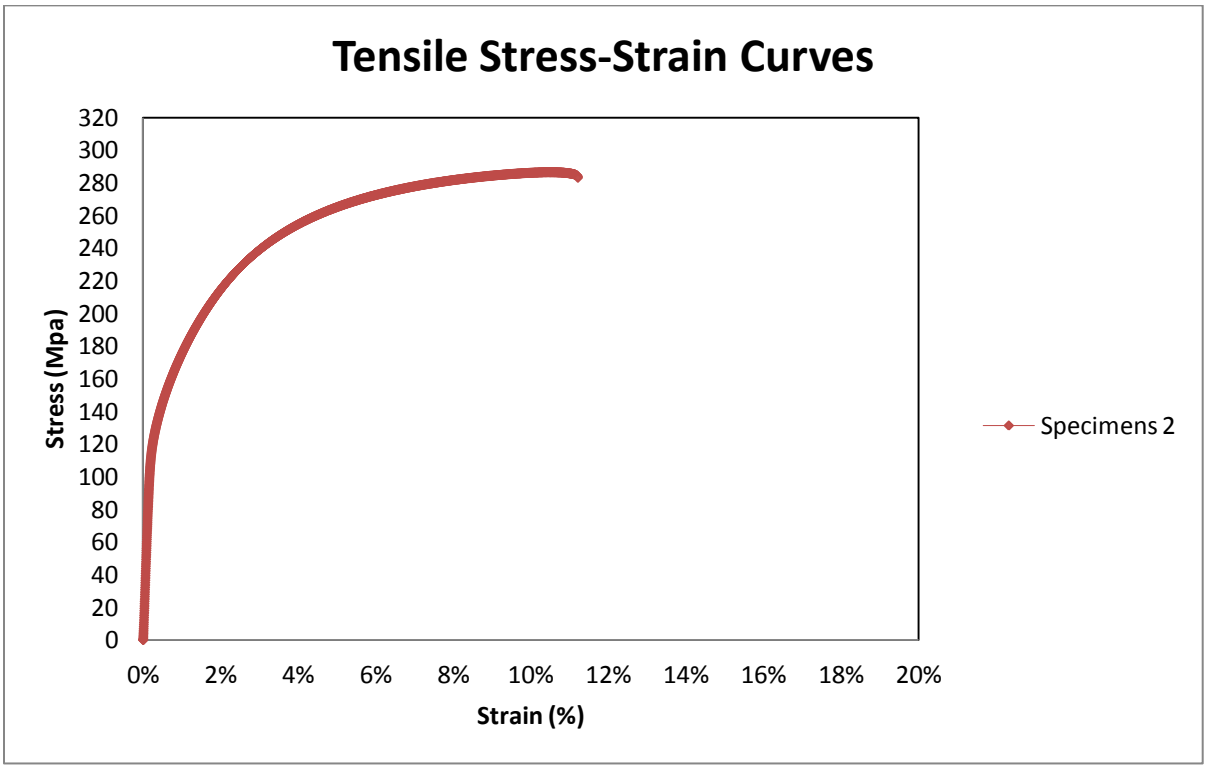

Figure Ap 1.17 Tensile curve of T5 sample A356_Specimens 2

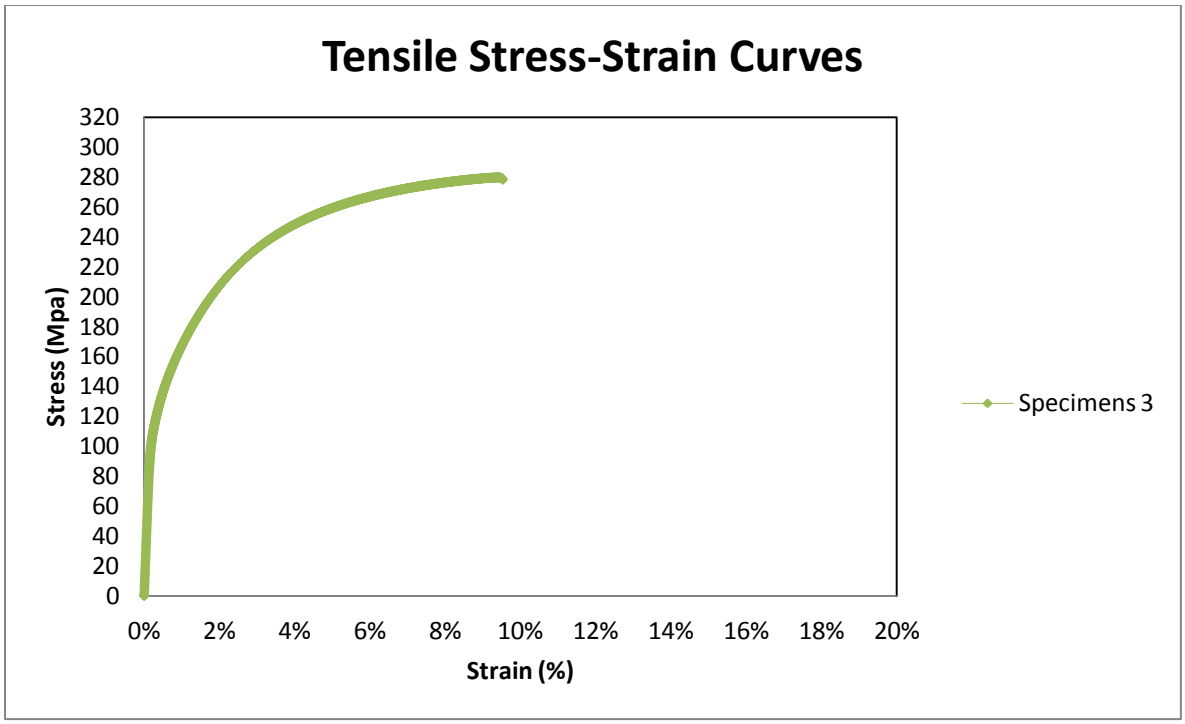

Figure Ap 1.18 Tensile curve of T5 sample A356_Specimens 3

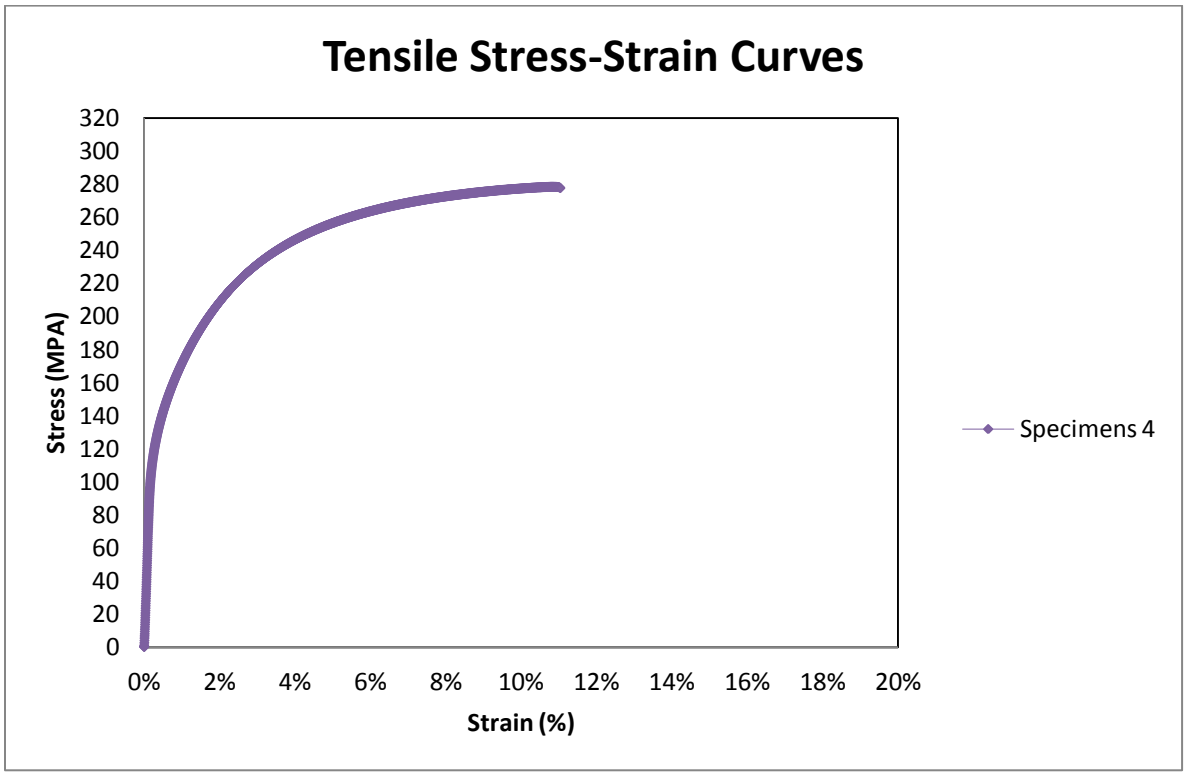

Figure Ap 1.19 Tensile curve of T5 sample A356_Specimens 4

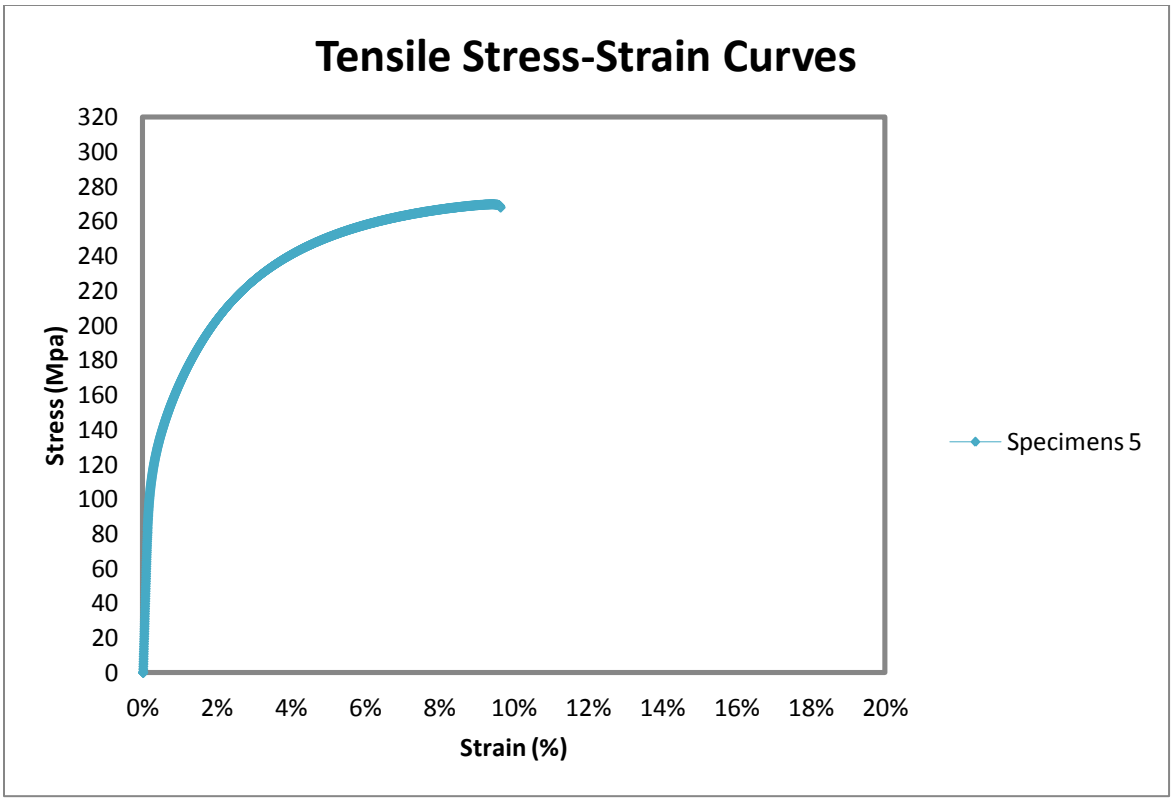

Figure Ap 1.20 Tensile curve of T5 sample A356_Specimens 5

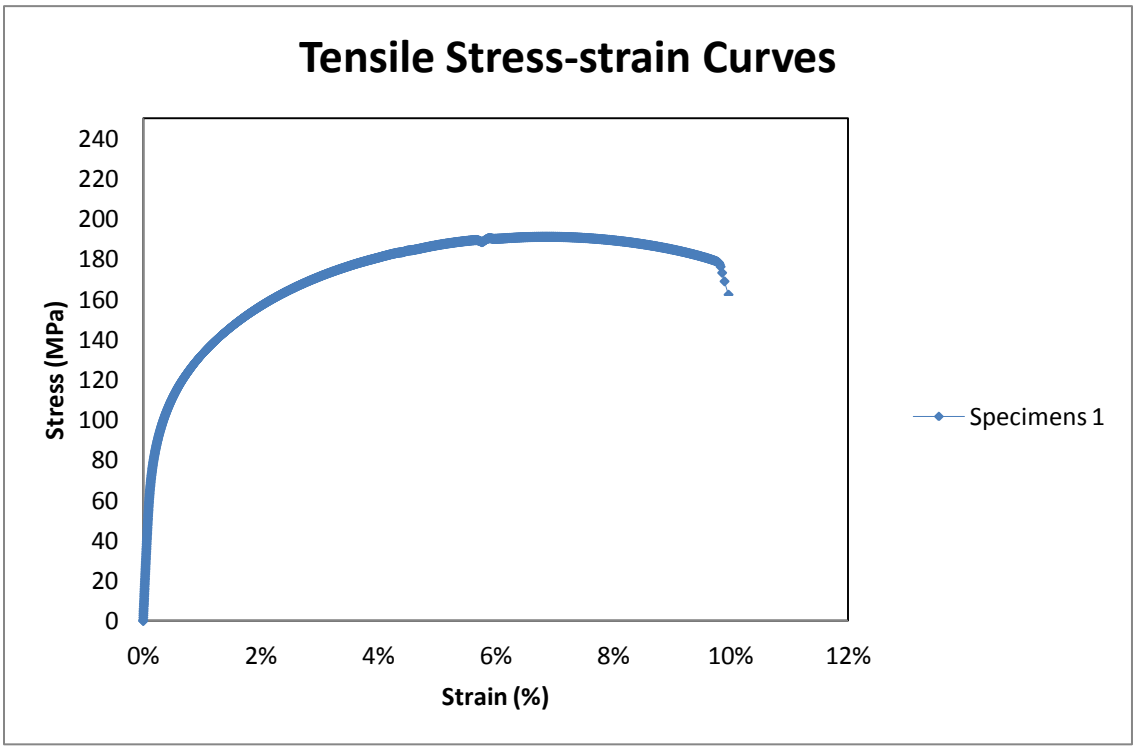

Figure Ap 1.21 Tensile curve of T6 sample A356_Specimens 1

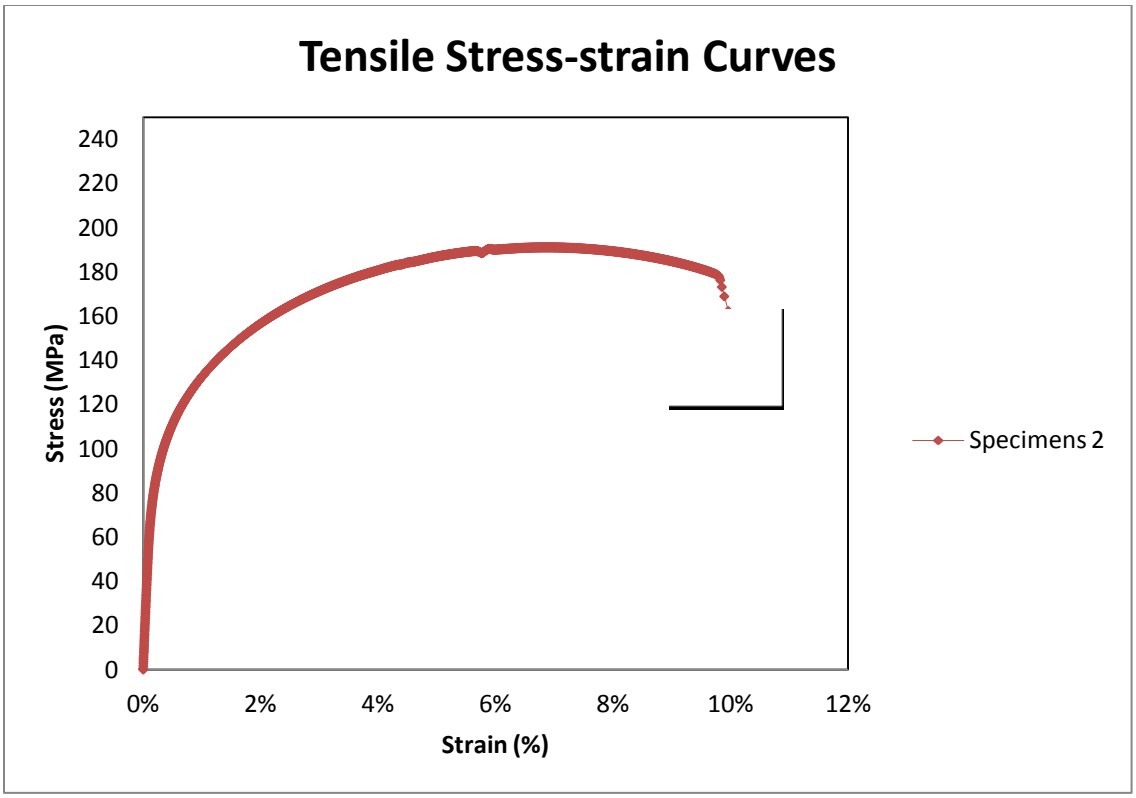

Figure Ap 1.22 Tensile curve of T6 sample A356_Specimens 2

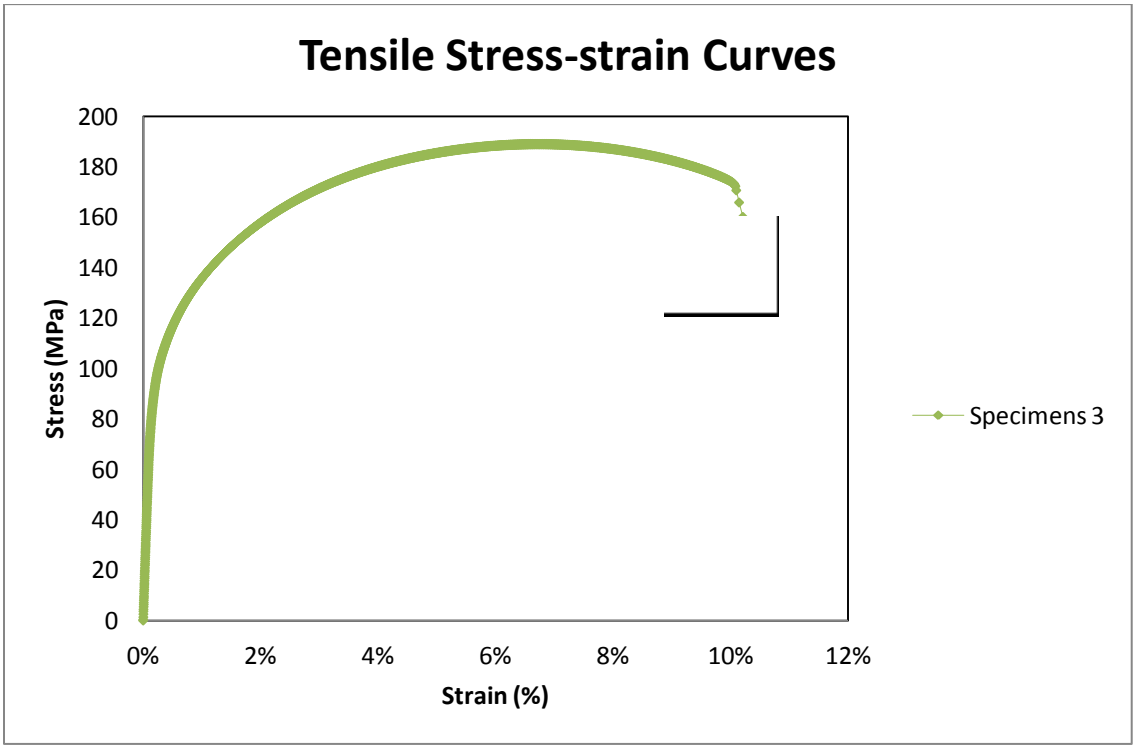

Figure Ap 1.23 Tensile curve of T6 sample A356_Specimens 3

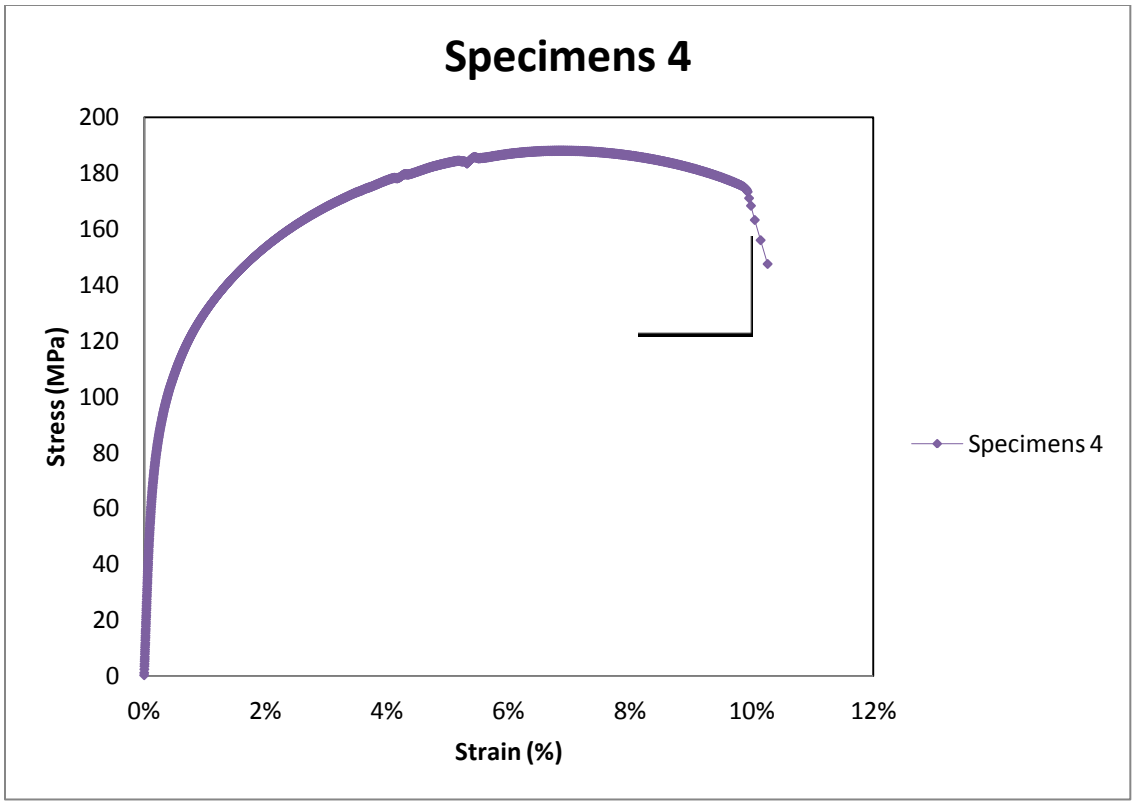

Figure Ap 1.24 Tensile curve of T6 sample A356_Specimens 4

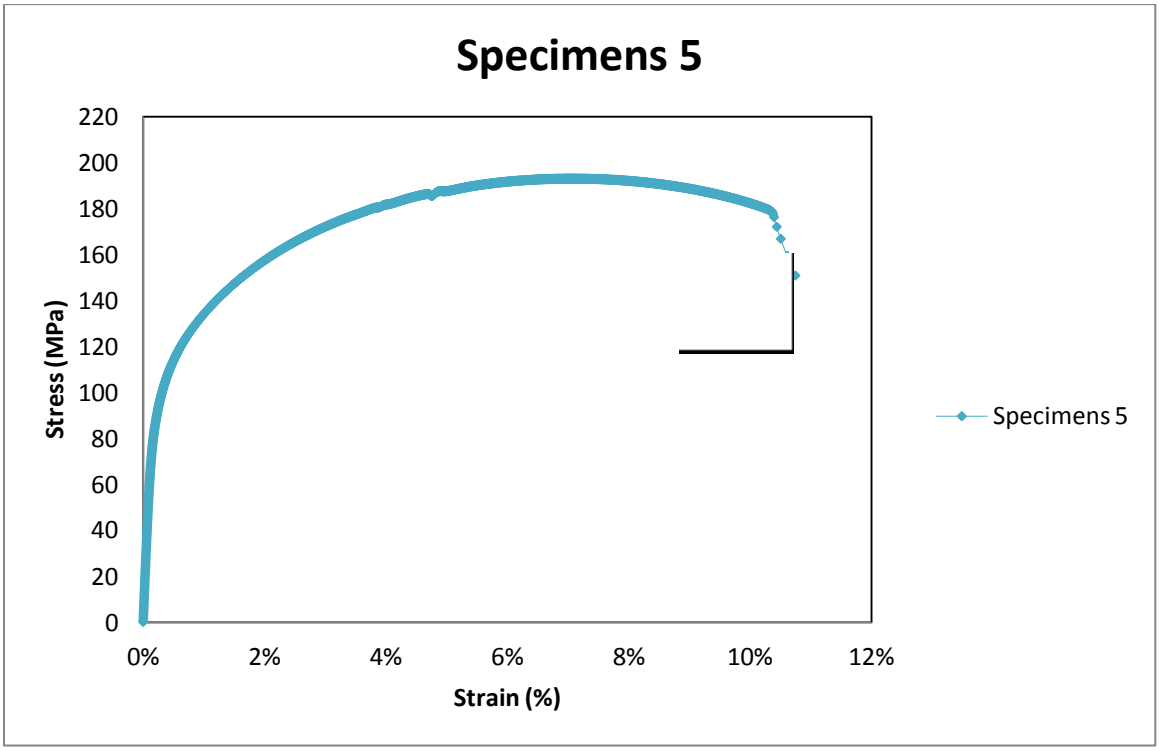

Figure Ap 1.25 Tensile curve of T6 sample A356_Specimens 5

APPENDIX II

OPTICAL IMAGES OF AS CAST AND DIFFERENT SOLUTION HEAT TREATMENT (T4 T5 T6) CONDITIONS IN THREE WELDING ZONES

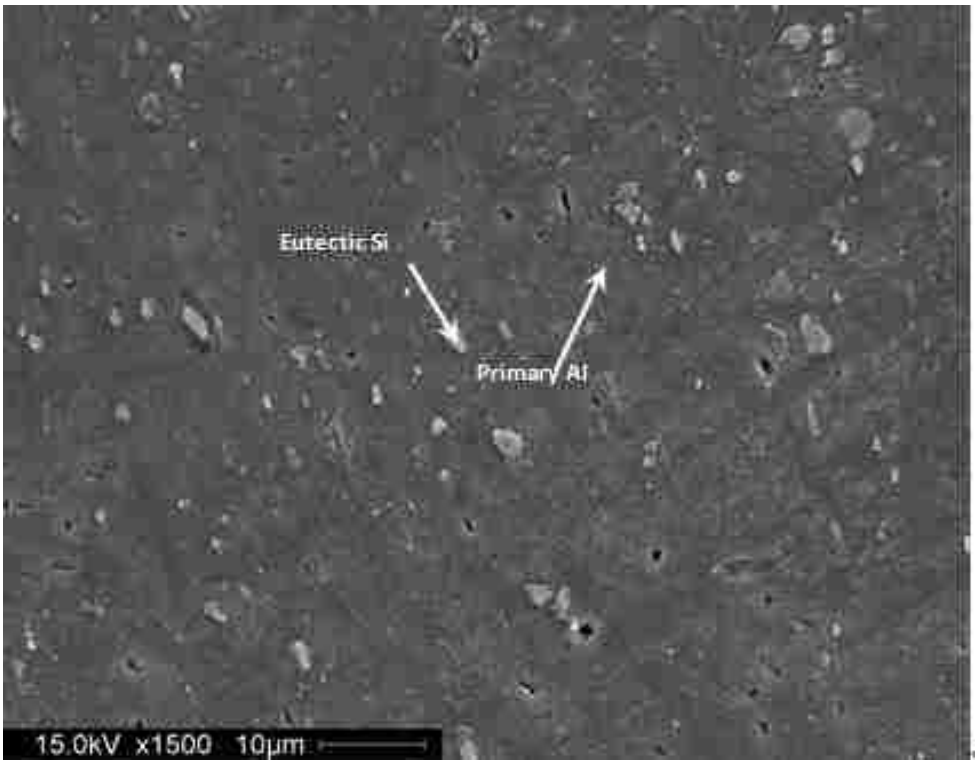

Figure Ap 1.26 SEM micrograph showing primary and secondary phases in the Base Metal of 6061 wrought alloy.

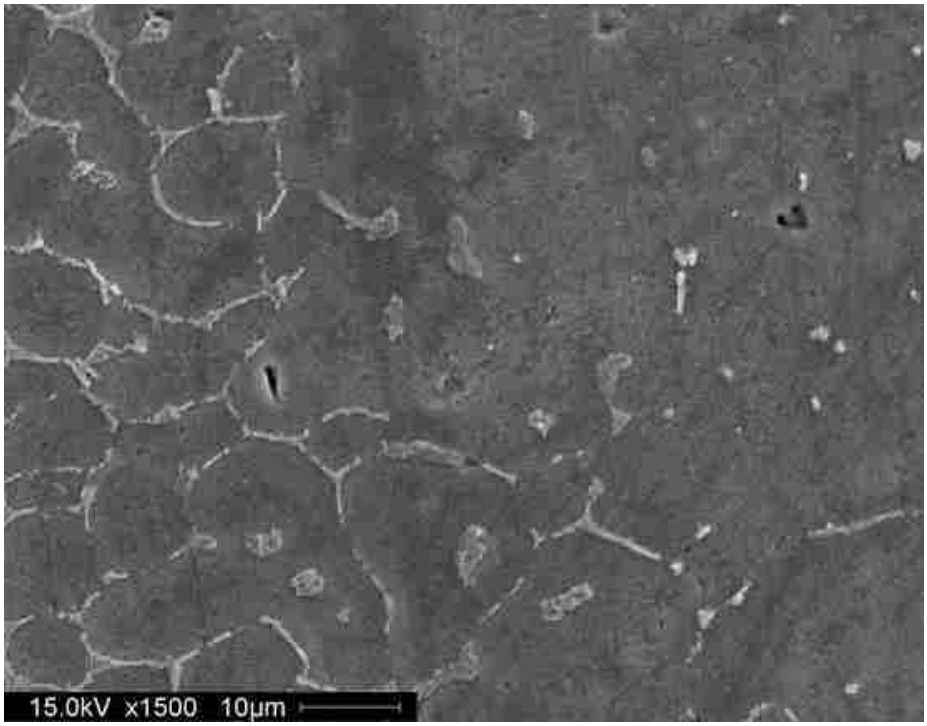

Figure Ap 1.27 SEM micrograph showing primary and secondary phases at Fusion line, HAZ and weld boundary of 6061 wrought alloy.

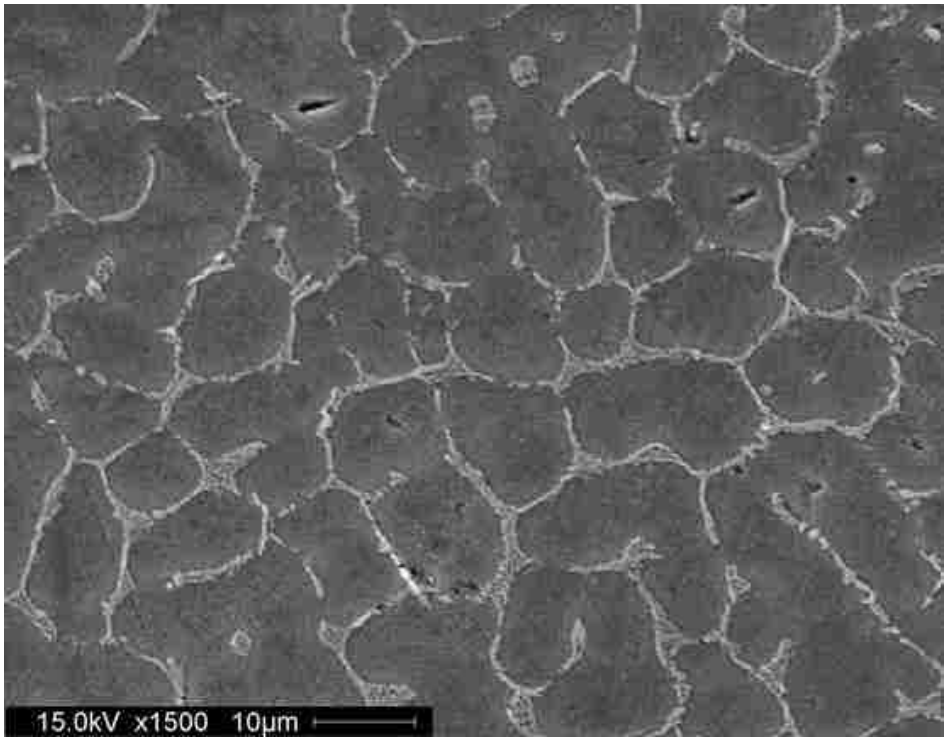

Figure Ap 1.28 SEM micrograph showing primary and secondary phases at Fusion Zone of 6061 wrought alloy

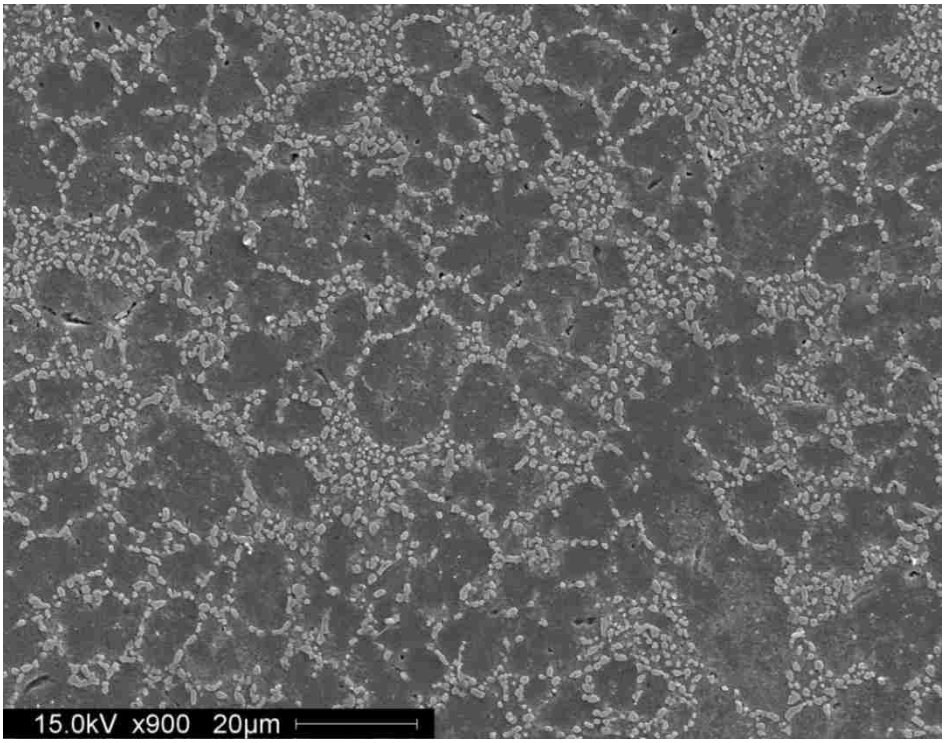

Figure Ap 1.29 SEM micrograph showing the microstructure of Base Metal of T4 A356 cast alloy.

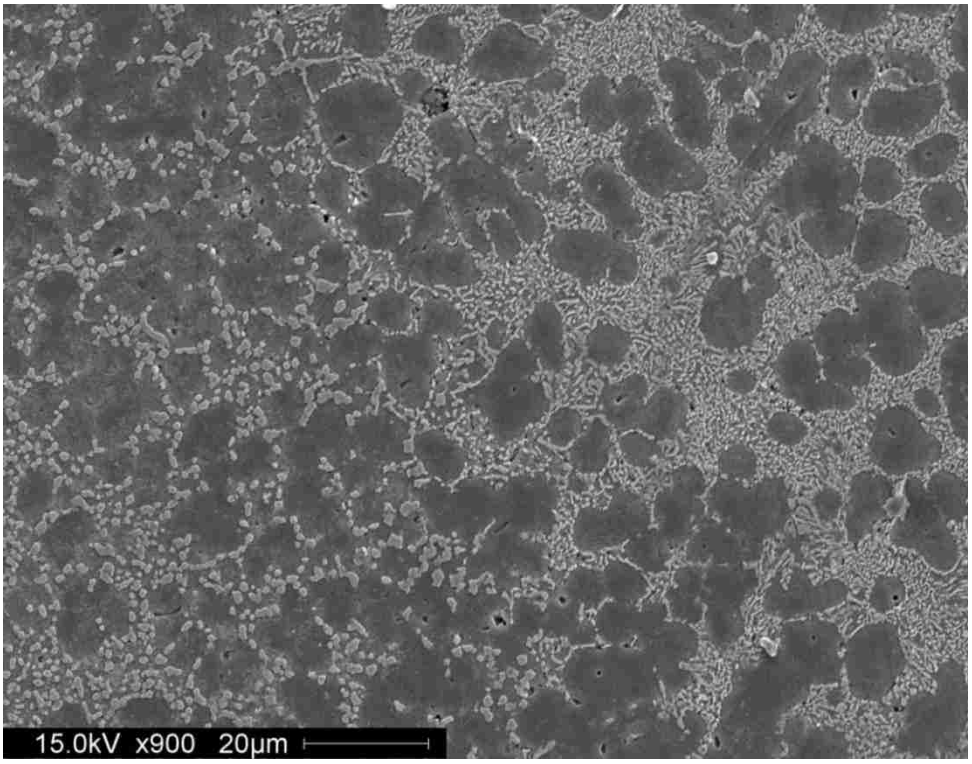

Figure Ap 1.30 SEM micrograph showing the microstructure of weld Boundary of T4 A356 cast alloy.

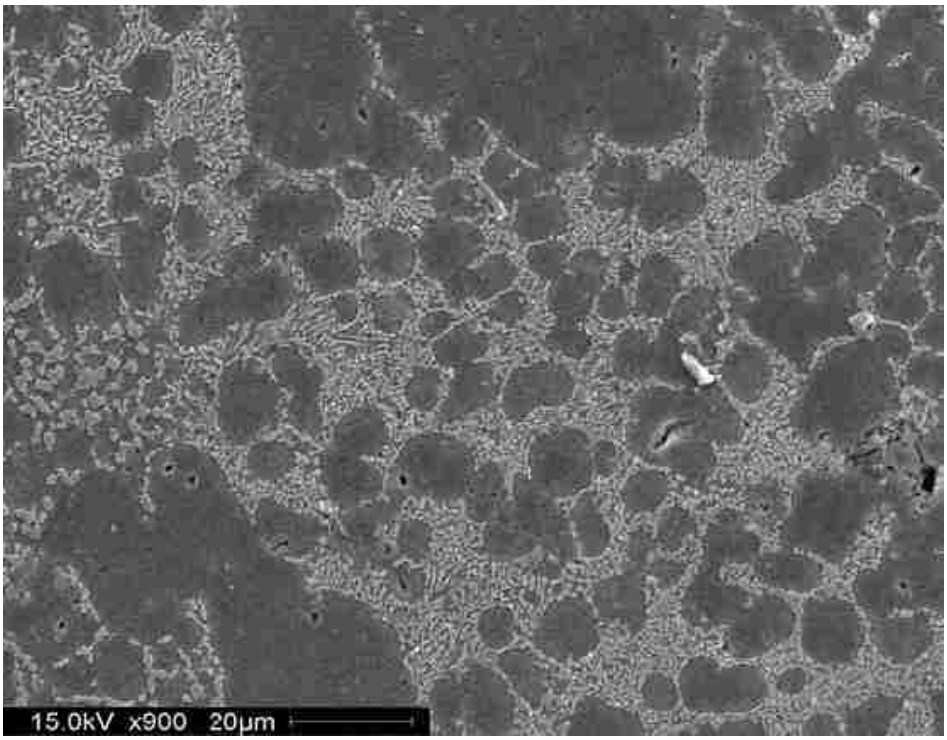

Figure Ap 1.31 SEM micrograph showing the microstructure of the Heat Affected Zone(HAZ) of T4 A356 cast alloy.

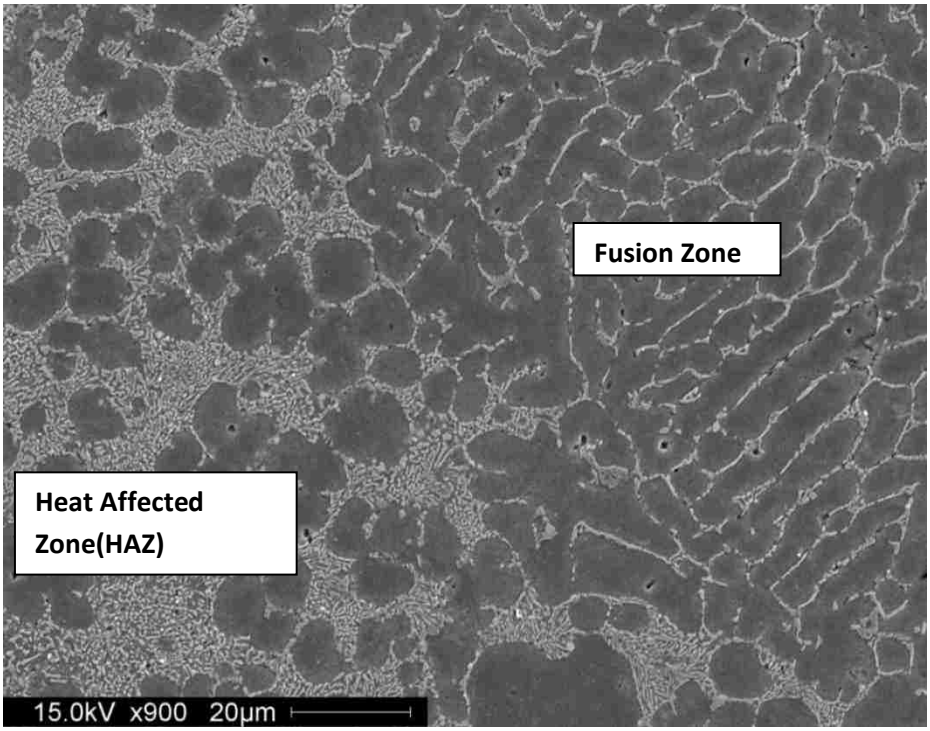

Figure Ap 1.32 SEM micrograph showing the microstructure of Fusion Line of T4 A356 cast alloy.

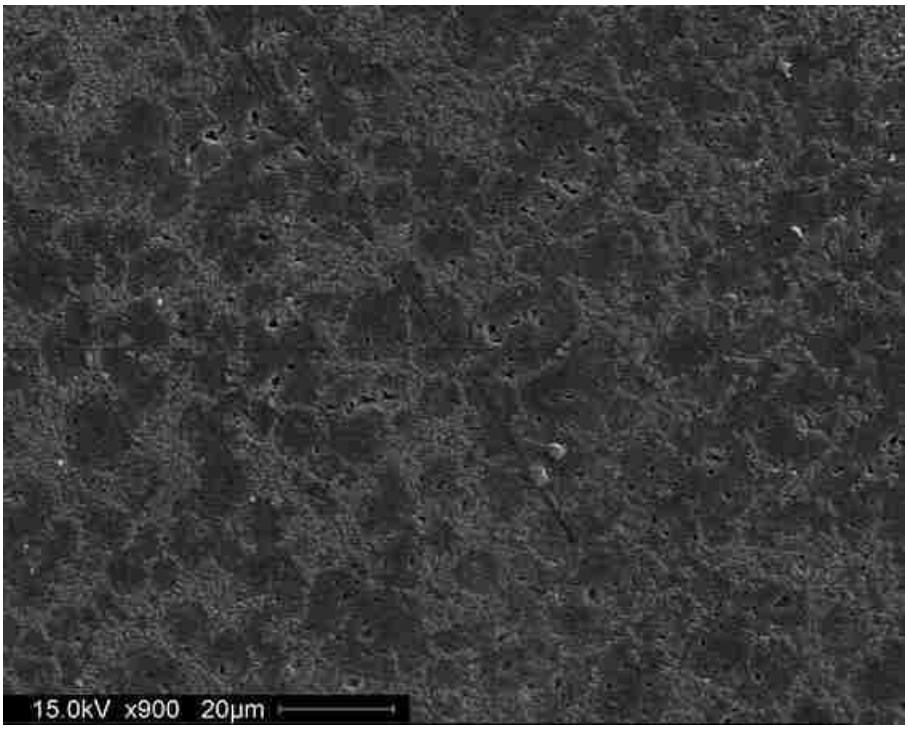

Figure Ap 1.33 SEM micrograph showing the microstructure of theBase Metal of T5 A356 cast alloy.

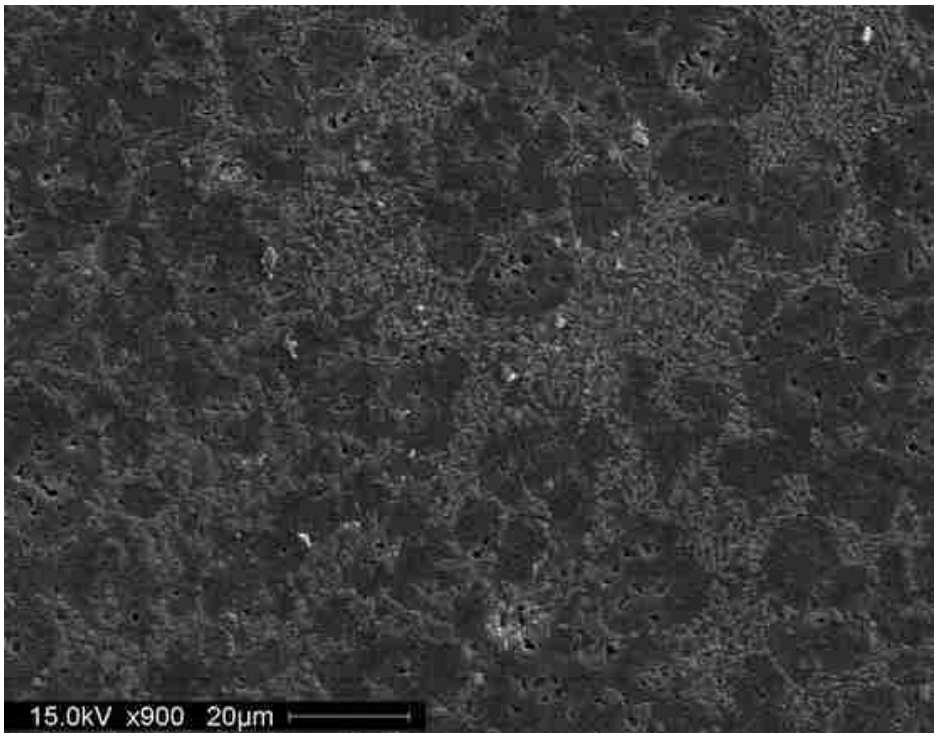

Figure Ap 1.34 SEM micrograph showing the microstructure of weld Boundary of T5 A356 cast alloy.

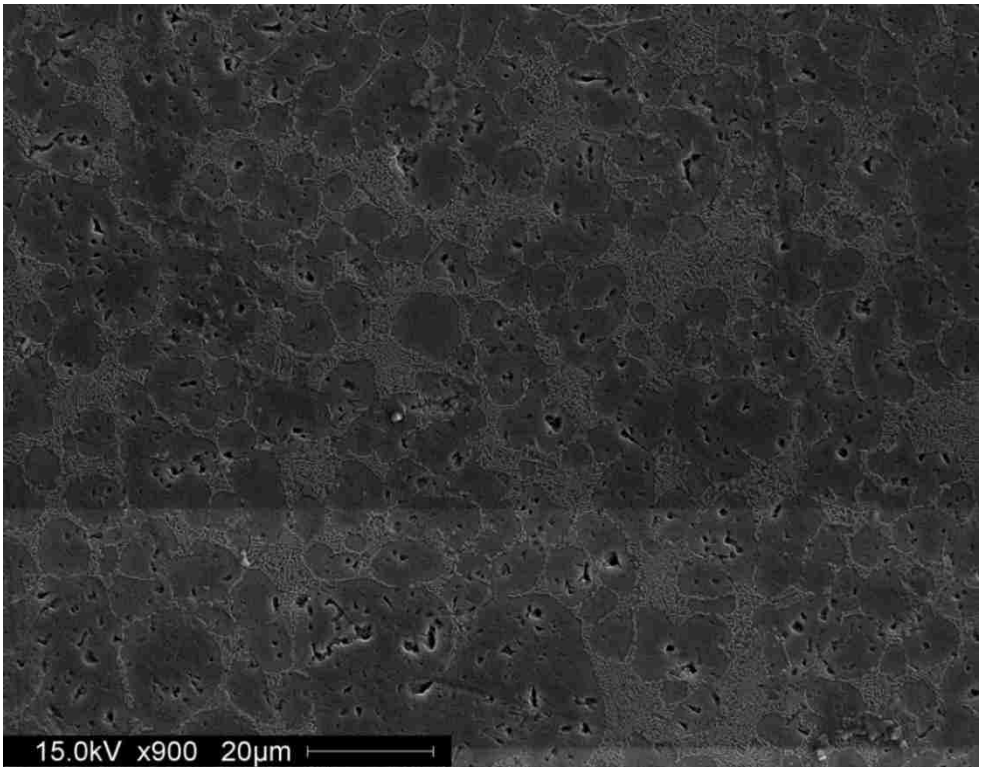

Figure Ap 1.35 SEM micrograph showing the microstructure of the HAZ of T5 A356 cast alloy.

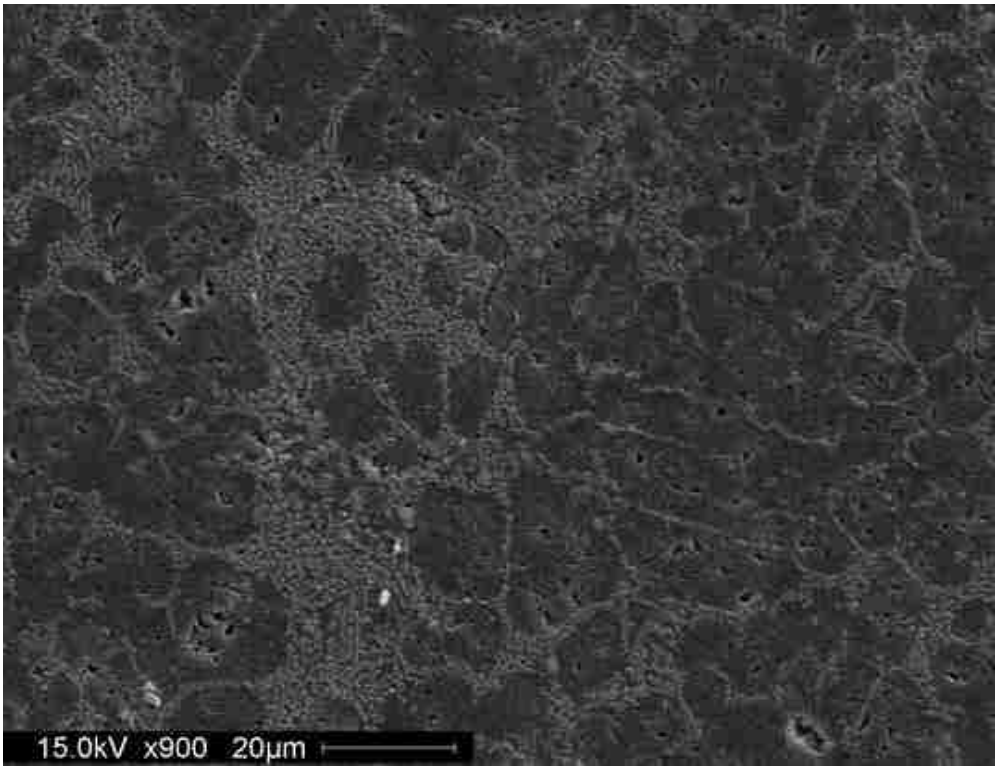

Figure Ap 1.36 SEM micrograph showing the microstructure of the Fusion Line of T5 A356 cast alloy.

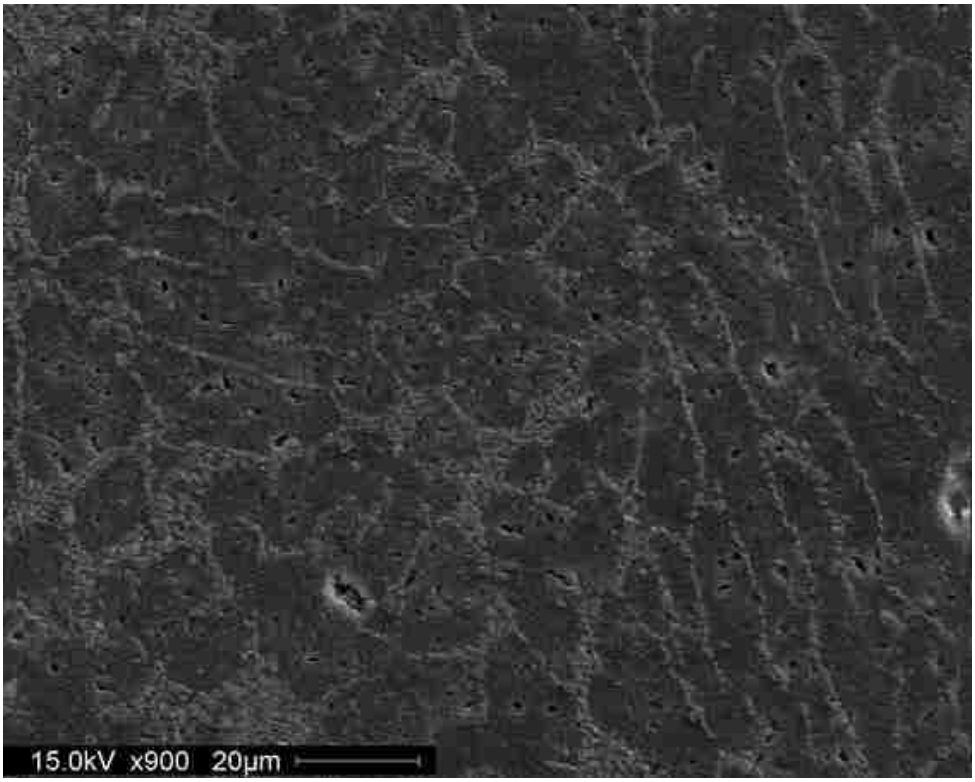

Figure Ap 1.37 SEM micrograph showing the microstructure of the Fusion Zone of T5 A356 cast alloy.

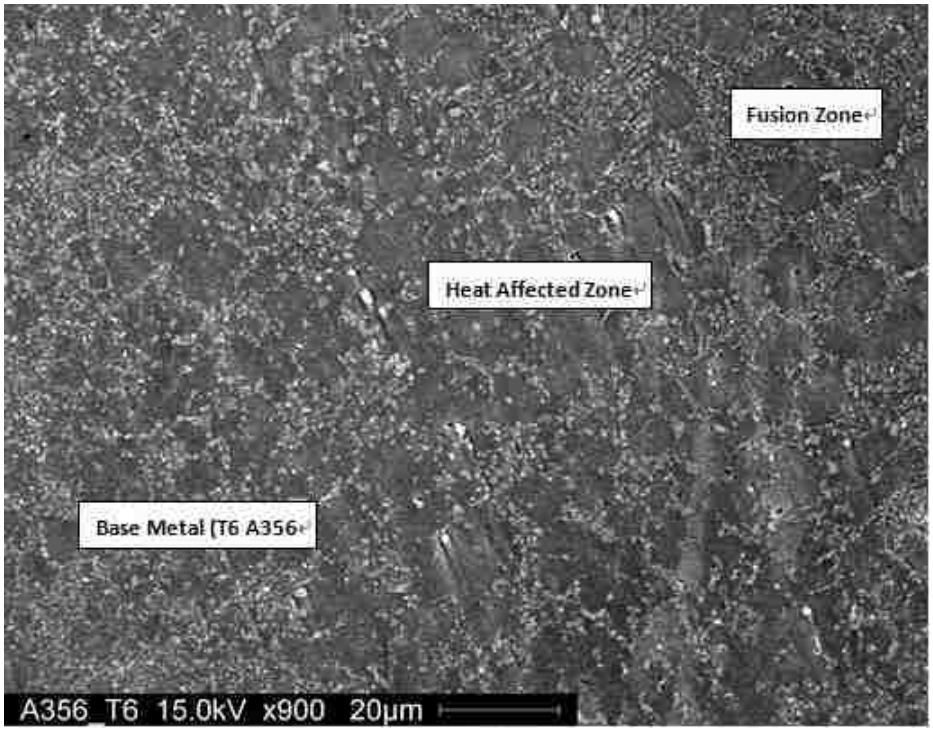

Figure Ap 1.38SEM micrograph showing the microstructure of the joined part of T6 A356 cast alloy.

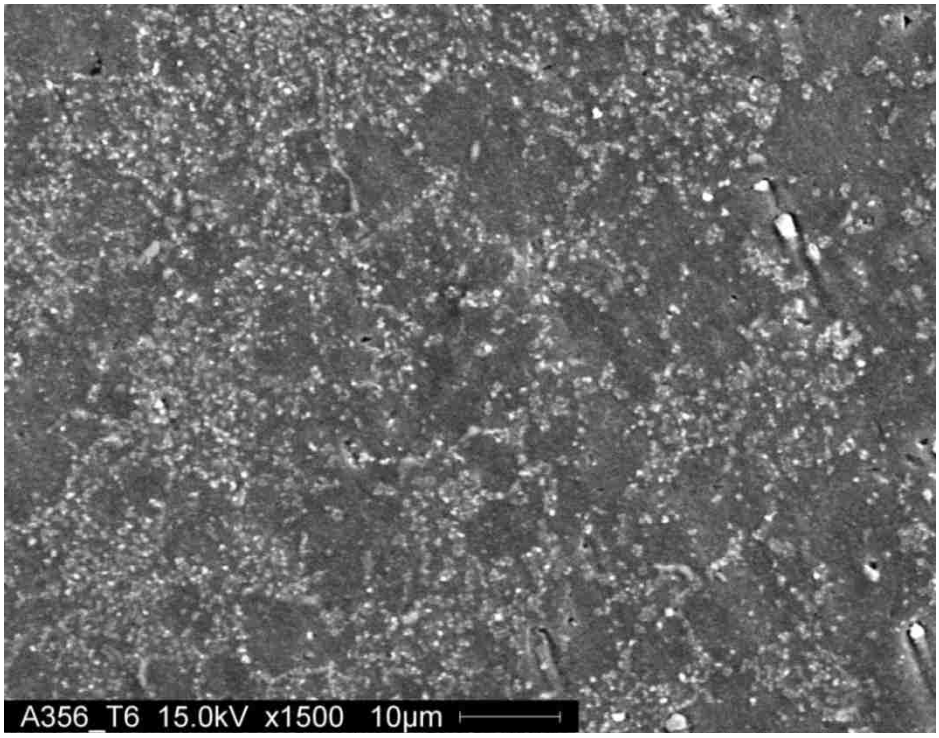

Figure Ap 1.39 SEM micrograph showing the microstructure of the Base Metal of welded T6 A356 cast alloy.

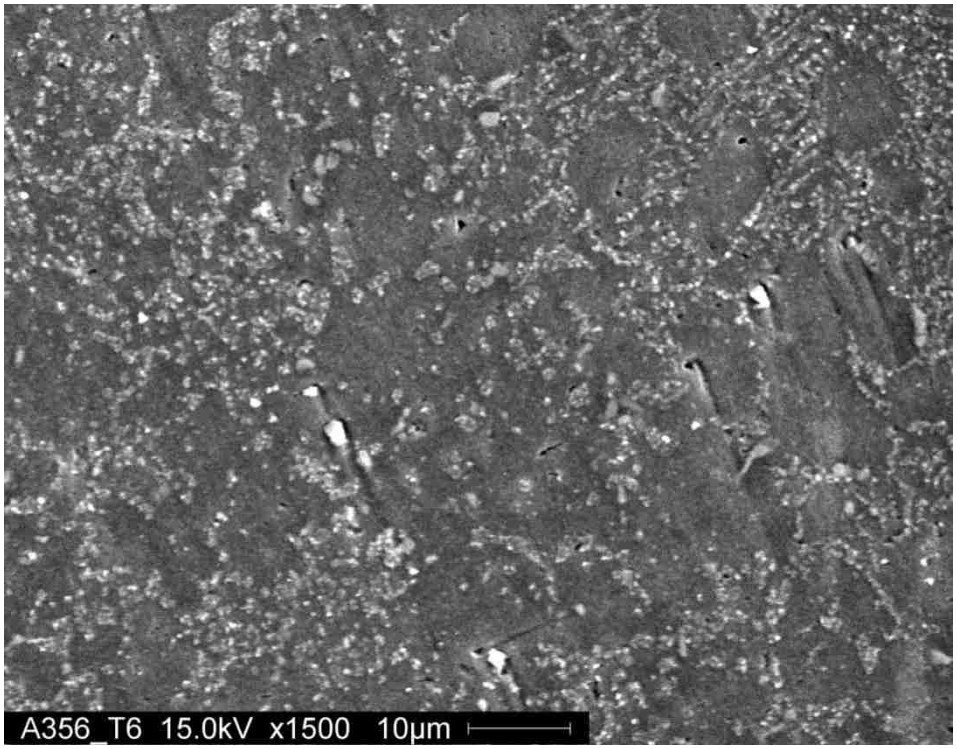

Figure Ap 1.40 SEM micrograph showing the microstructure of the HAZ of T6 A356 cast alloy.

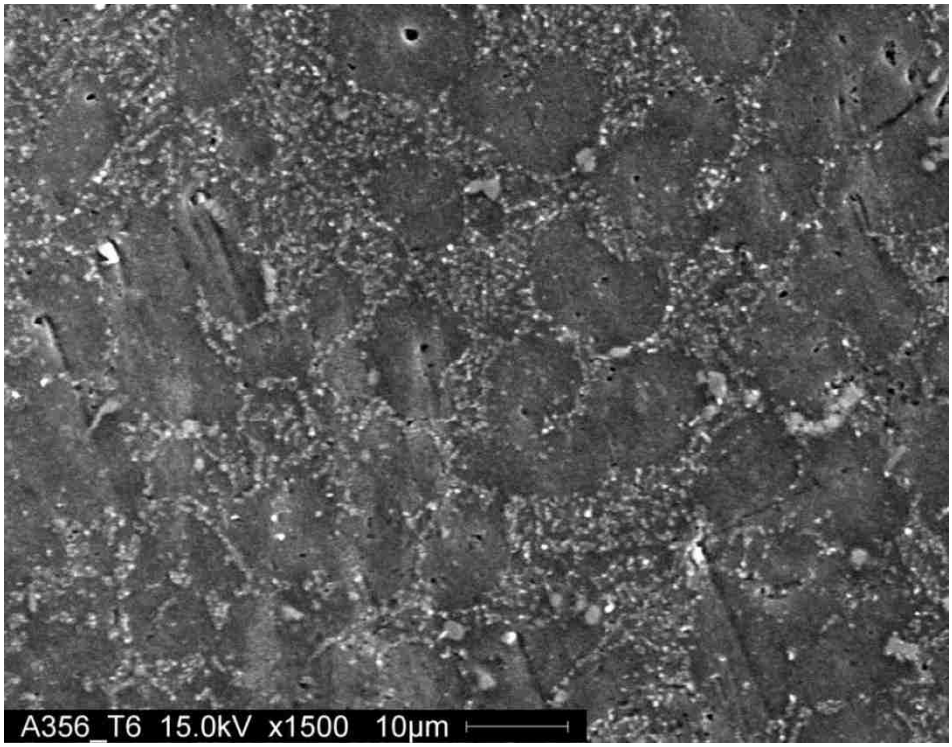

Figure Ap 1.42 SEM micrograph showing the microstructure of Fusion Line of the T6 A356 cast alloy.

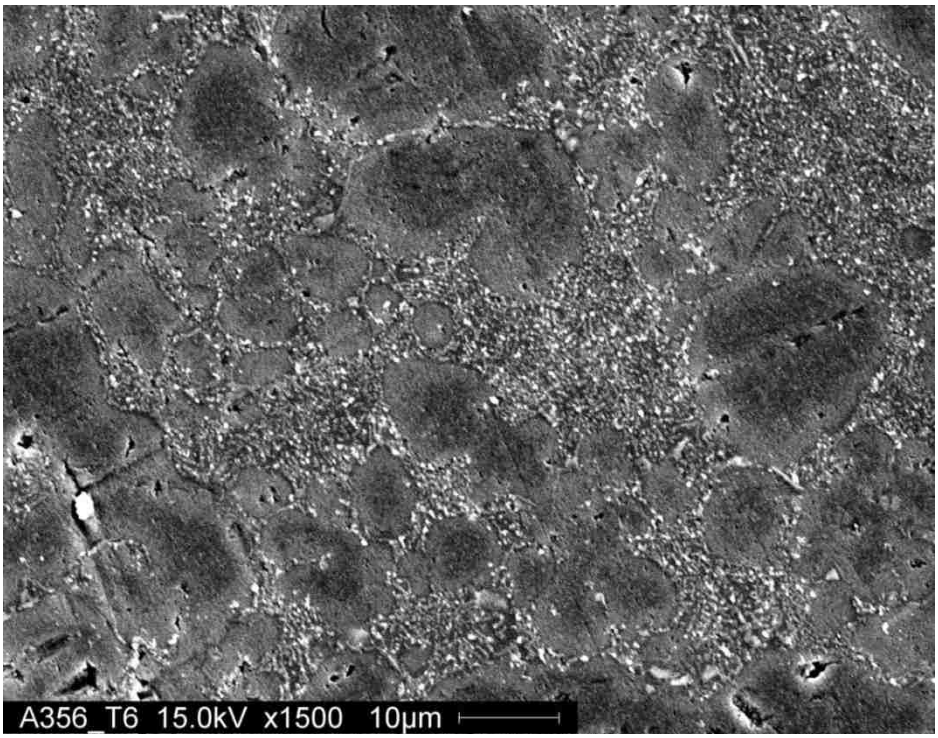

Figure Ap 1.43 SEM micrograph showing the microstructure of the Fusion Zone of T6 A356 cast alloy.

APPENDIX III

SEM IMAGES OF FRACTURE BEHAVIOURS FOR AS CAST,T4, T5 AND T6 SOLUTION HEAT TREATMENT CONDITIONS AND WROUGHT ALLOY 6061

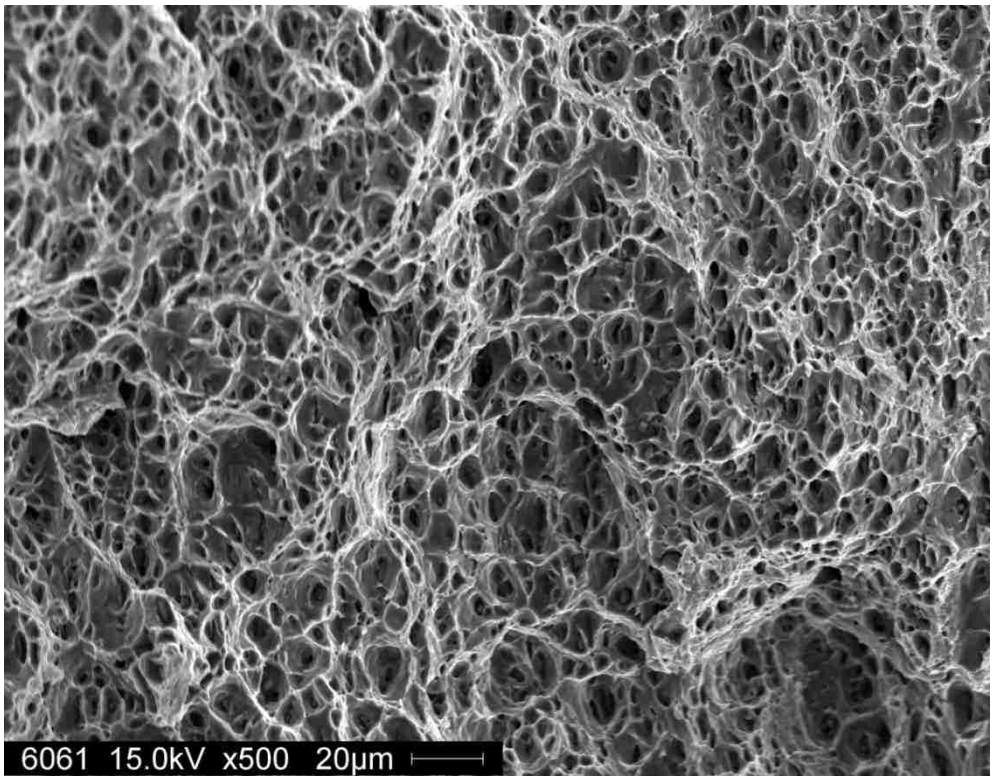

Figure Ap 1.44 Fractograph of the tensile specimen of welded wrought alloy 6061.

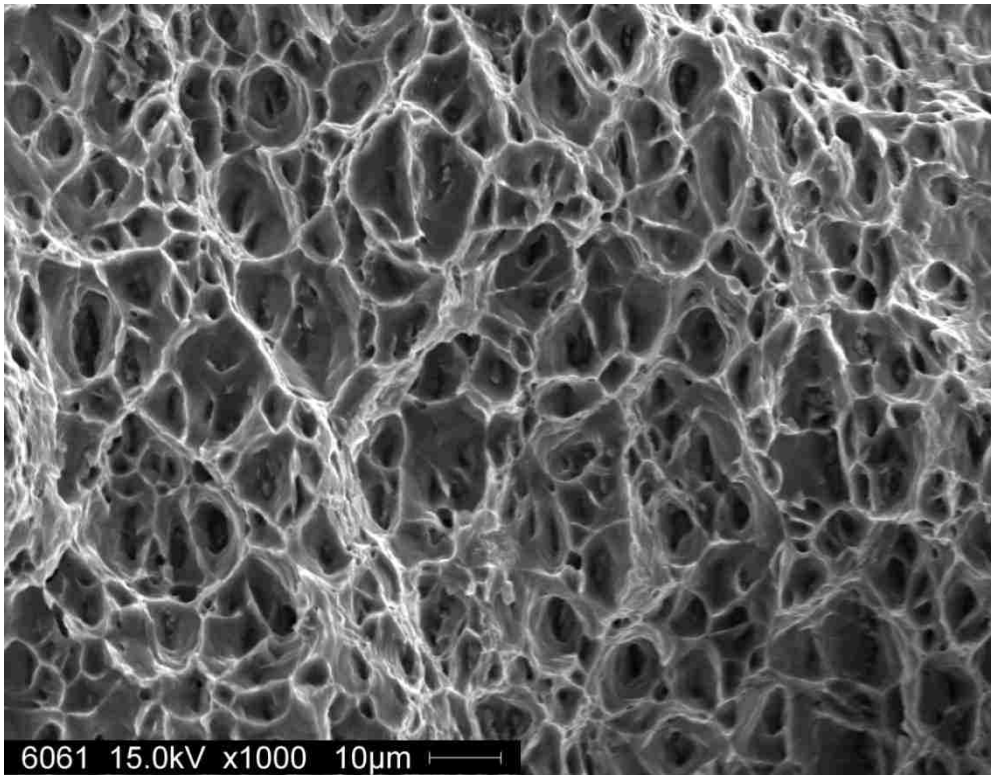

Figure Ap 1.45 Fractograph of the tensile specimen of welded wrought alloy 6061.

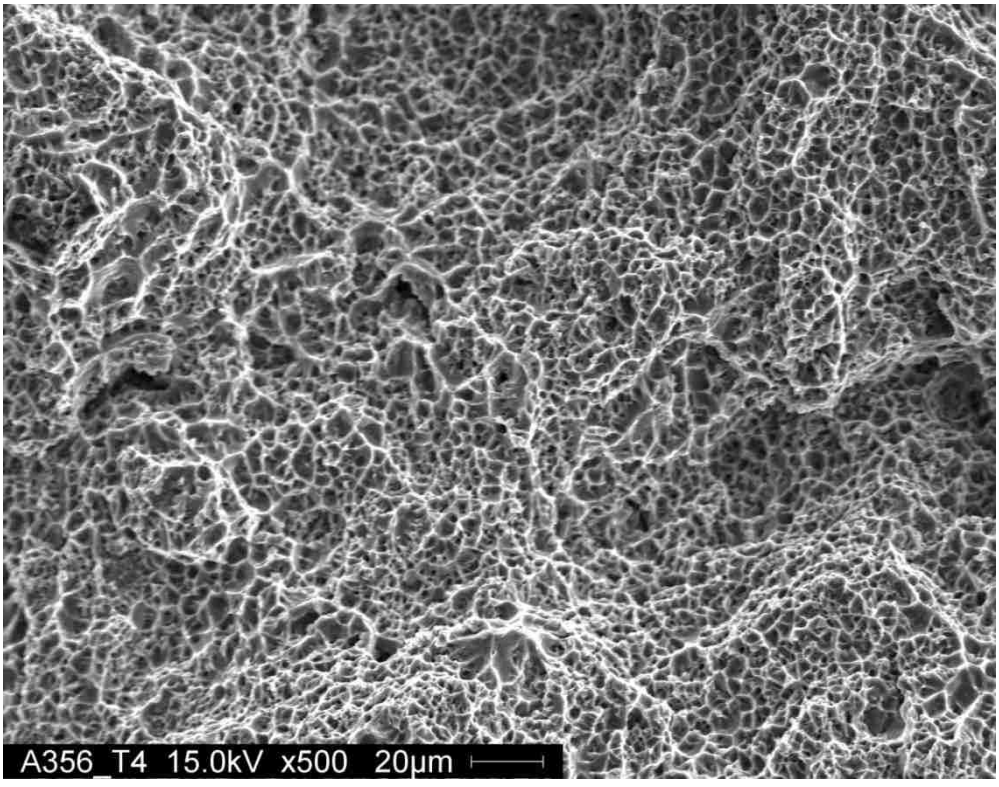

Figure Ap 1.46 Fractograph of the tensile specimen of T4 welded cast alloy A356.

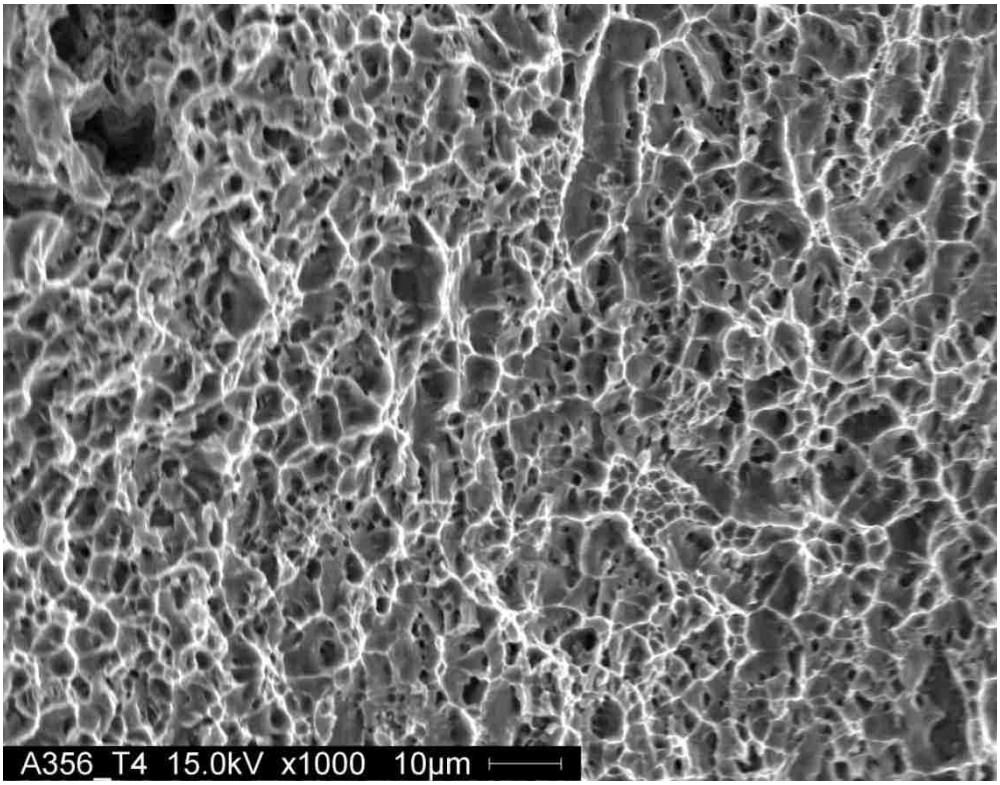

Figure Ap 1.47 Fractograph of the tensile specimen of welded T4 cast alloy A356.

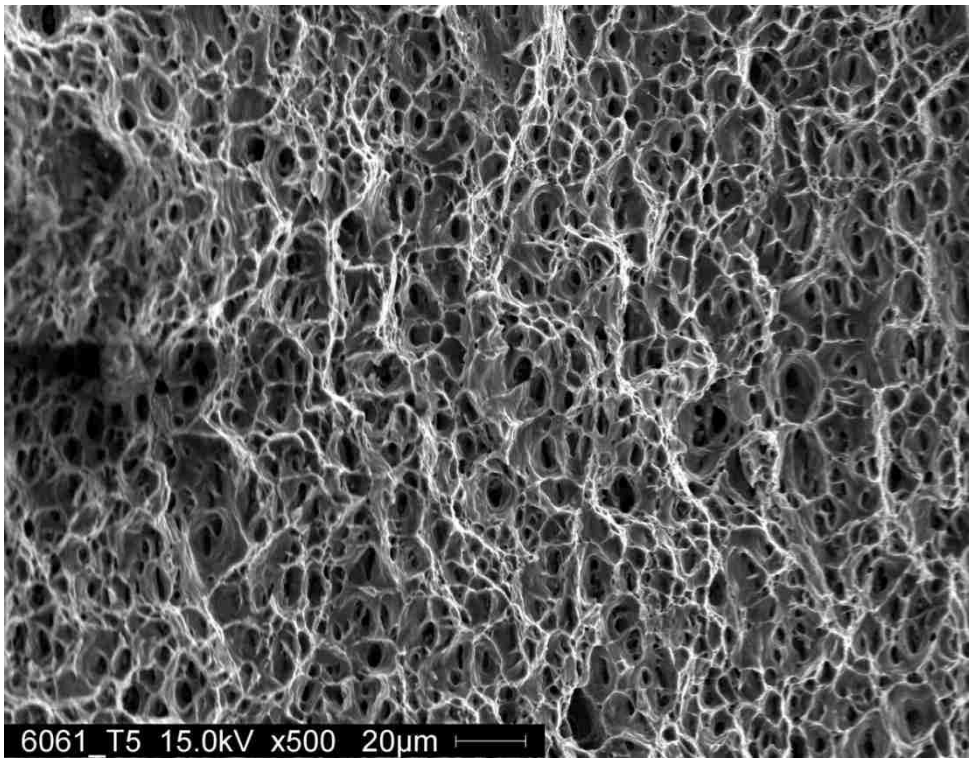

Figure Ap 1.48 Fractograph of the tensile specimen of T5 welded cast alloy A356.

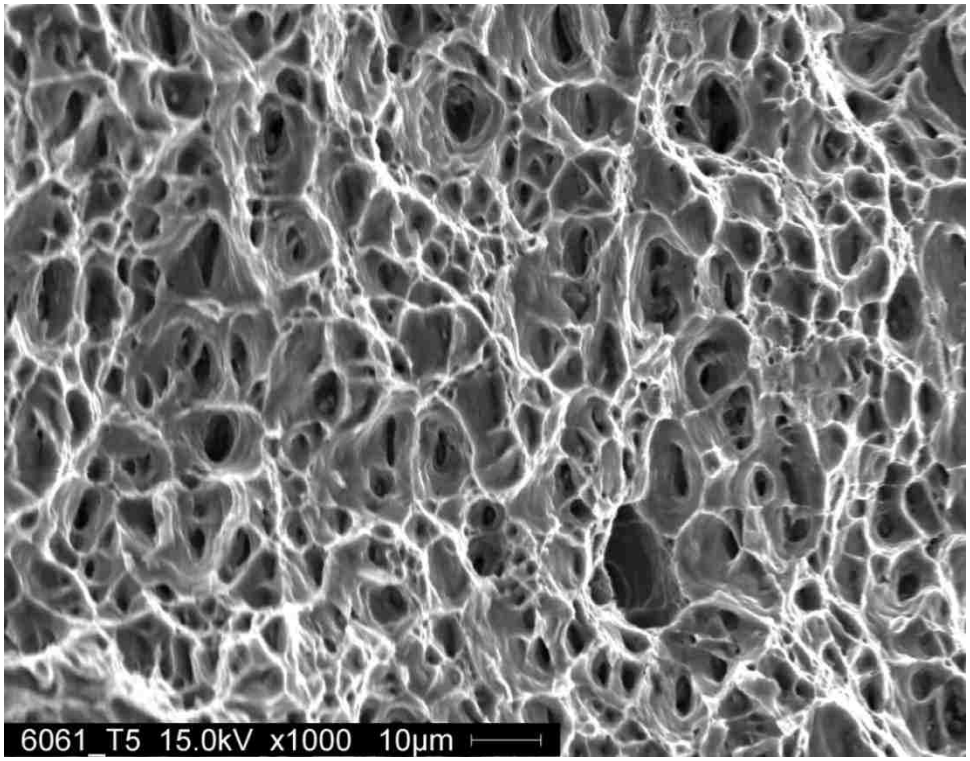

Figure Ap 1.49 Fractograph of the tensile specimen of T5 welded cast alloy A356**.**

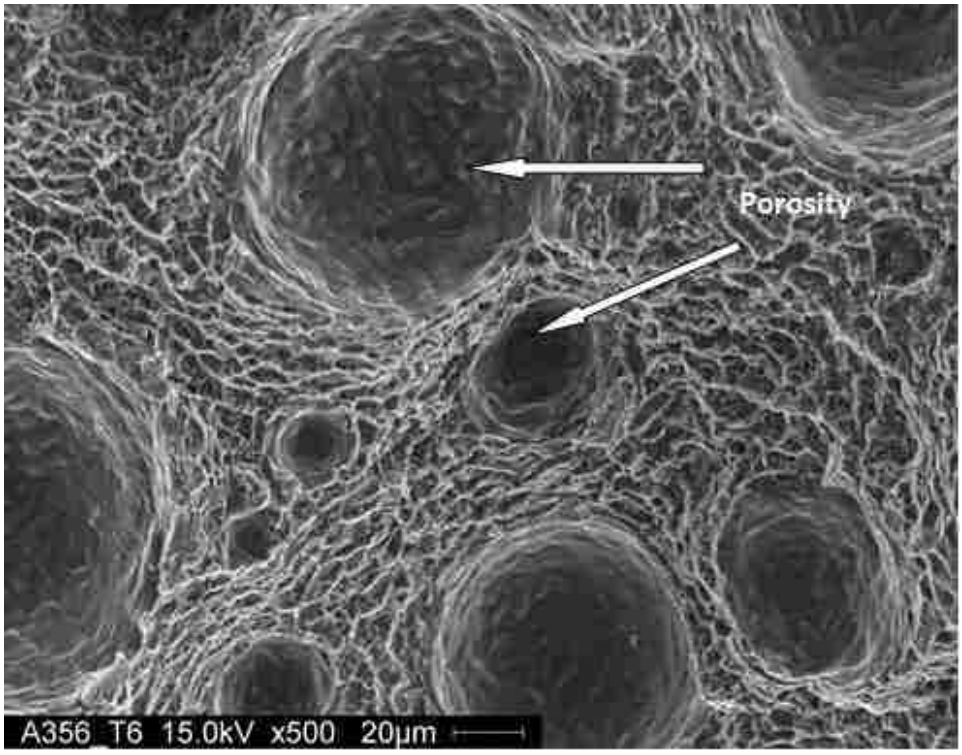

Figure Ap 1.50 Fractograph of the tensile specimen of welded T6 cast alloy A356.

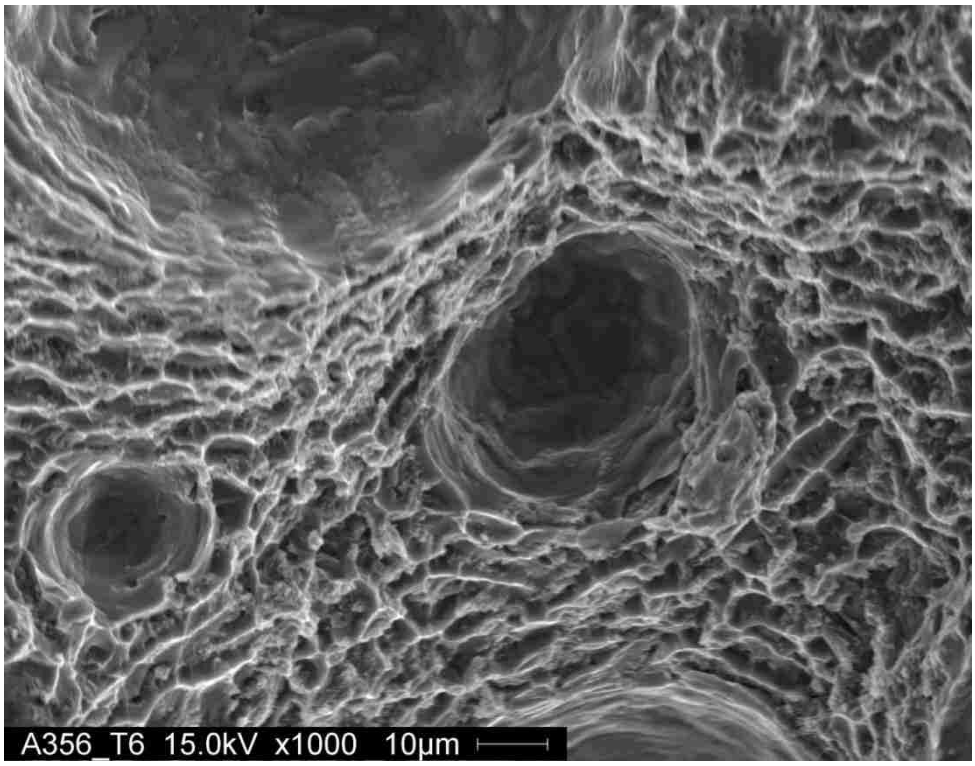

Figure Ap 1.51 Fractograph of the tensile specimen of welded T6 cast alloy A356.

VITA AUCTORIS

NAME: MENG WANG

PLACE OF BIRTH: DALIAN, P. R. CHINA

YEAR OF BIRTH: 1988

EDUCATION:

2011 – 2013 **MAS.c. in Materials Engineering**

University of Windsor, Windsor, ON, Canada

2007 –2011 **B. Sc. in General Mechanical Engineering**

University of Windsor, Windsor, ON, Canada